

**INDOOR AND OUTDOOR RADON AND  
THORON MONITORING IN MIZORAM WITH  
SPECIAL REFERENCE TO LUNGLEI,  
SERCHHIP AND MAMIT DISTRICTS**

**Thesis submitted in fulfillment of the  
requirements for the degree of  
Doctor of Philosophy  
in Physics**

**By**

**P.C. Rohmingliana**

**To**



**Department of Physics  
Mizoram University, Aizawl  
Mizoram, India  
March 2015**

**INDOOR AND OUTDOOR RADON AND  
THORON MONITORING IN MIZORAM  
WITH SPECIAL REFERENCE TO LUNGLEI,  
SERCHHIP AND MAMIT DISTRICTS**

**Thesis submitted in fulfillment of the  
requirements for the degree of  
Doctor of Philosophy  
in Physics**

**By**

**P.C. Rohmingliana**

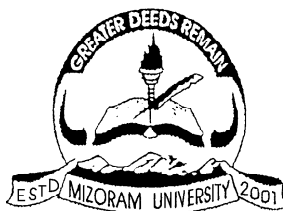
**Registration No and Date: MZU/Ph. D/ 330/10.06.2010**

**To**



**Department of Physics  
Mizoram University, Aizawl  
Mizoram, India  
March 2015**

Ê´É·ÉÊ´ÉtÉ±ÉªÉ  
|ÉÉèÊiÉÉò Ê´ÉYÉÉxÉ  
Ê´ÉtÉ±ÉªÉ  
+É<VÉÉä±É 796004 Ê´ÉWÉÉä@ú´É  
→ñ±-ñ ±.0000



**MIZORAM UNIVERSITY**  
**PHYSICS DEPARTMENT**  
**SCHOOL OF PHYSICAL SCIENCES**  
**AIZAWL 796 004 MIZORAM**  
Phones : 0389 - 2328044(R), 9436140523(M)  
FAX : 0389 - 2330522  
E-mail : r.k.thapa@gmail.com  
**Prof. R. K. Thapa**

---

No. MZU/Acad-12/SPS/

Date: 26<sup>th</sup> March, 2015

## Certificate

This is to certify that the thesis entitled '*Indoor and Outdoor Radon and Thoron Monitoring in Mizoram with special reference to Lunglei, Serchhip and Mamit Districts*' submitted by Shri P.C. Rohmingliana, for the degree of Doctor of Philosophy of the Mizoram University, Aizawl, embodies the record of original investigations carried out by him under my supervision. He has been duly registered and the thesis presented is worthy of being considered for the award of the Ph. D. degree. This work has not been submitted for any degree of any other university.

(Prof. R.K.Thapa)

Supervisor

**Department of Physics,  
Govt. Zirtiri Residential Science  
College, Aizawl.**



Phones : 0389 – 2335338 (R)  
9436140347 (M)

**Prof. B. Zoliana**

E – mail : bzoliana@rediffmail.com

---

No. GZRSC /DAE/BZ/62

Dated: 25<sup>th</sup> March, 2015

## **Certificate**

This is to certify that the thesis entitled '*Indoor and Outdoor Radon and Thoron Monitoring in Mizoram with special reference to Lunglei, Serchhip and Mamit Districts*' submitted by Shri P.C. Rohmingliana, for the degree of Doctor of Philosophy of the Mizoram University, Aizawl, embodies the record of original investigations carried out by him under my supervision. He has done his training at BARC, Mumbai for 4 weeks during 7<sup>th</sup> – 11<sup>th</sup> July, 2008 and 28<sup>th</sup> – 31<sup>st</sup> July, 2009 as a JRF under the coordinated Research Project of Govt. Zirtiri Residential Science College, Aizawl and BARC, Mumbai. The thesis presented is worthy of being considered for the award of the Ph. D. degree. This work has not been submitted for any degree of any other university.

(Prof. B. Zoliana)

Jt. Supervisor

# **Declaration**

**Mizoram University**

**March, 2015**

*I, P.C. Rohmingliana, hereby declare that the subject matter of this thesis is the record of work done by me, that the contents of this thesis did not form basis of the award of any previous degree to me or to do the best of my knowledge to anybody else, and that the thesis has not been submitted by me for any research degree in any other University or Institute.*

*This is being submitted to the Mizoram University for the degree of Doctor of Philosophy in Physics.*

**(P.C. ROHMINGLIANA)**  
**Candidate**

**(Prof. ZAITHANZAUVA PACHUAU)**  
**Head**

**(Prof. R.K. THAPA)**  
**Supervisor**

**(Prof. B. ZOLIANA)**  
**Jt. Supervisor**



# Acknowledgement

I wish to express my sincere gratitude to my supervisor Prof. R. K. Thapa, for his supervision, advice, and guidance from the beginning of this research as well as giving me extraordinary experiences throughout the work. His encouragement and support in various ways has made me inspire and enrich my growth as a student.

I am very much grateful to Prof. B. Zoliana, my Joint Supervisor, under whose guidance this study was initiated. Since then, he has been a constant inspiration to me till the completion of this work.

I wish to express my sincere gratitude the cooperation and support received from staff of RP&AD, BARC, Mumbai, especially to Dr. Y.S. Mayya, Dr. B.K. Sahoo, Dr. Rosaline Mishra and other members of radon group and Dr. Anil Kumar, RSSD, BARC, Mumbai, who always provide technical support and spared their valuable times throughout the entire course of my study.

I would like to acknowledge Board of Research in Nuclear Sciences (BRNS), Department of Atomic Energy (DAE) that provided the necessary financial support for this research.

I am thankful to the Principal, Govt. Zirtiri Residential Science College, Aizawl, Mizoram for showing enthusiasm and unflinching support given to me during the work.

I am most grateful to Dr. Lalmuanpuia Vanchhawng and David Saidingliana Sailo, Field Assistant, my colleagues and friends in the group, with whom I gained lots of fruitful knowledge through discussion and valuable work experience during the study period.

My heartfelt thanks go especially to Prof. R. C. Tiwari, Dean, School of Physical Sciences, M.Z.U. and Prof. Zaithanzauva Pachuau, Head, Department of Physics, M.Z.U. for their advice, support and giving useful suggestions. I deeply acknowledge to all the teaching faculty of the Department of Physics, Mizoram University, Aizawl for their encouragement during the course of this Ph. D. work. I would also like to thank all the non-teaching staff members of Department of Physics, Mizoram University, Aizawl for their co-operation.

I sincerely acknowledge the most valuable help receive from my family members, especially my parents, P.C. Neihkima and Vanlalthuami, for their gentle love

## *Acknowledgement*

and caring. I would like to thank all my brothers and sisters for their support and great patience at all times. It would not have been possible to write this doctoral thesis without their help and support.

I really thank all the members of my fellow Kristian Thalai Pawl, Mualpui Branch, Chhingchhip for their love and prayer support.

I wish to place on record my sincere thanks to my friends from Chhingchhip, C. Lalnunmawia and K. Lalbiakzuala, for their encouragement and support during the study.

I would like to thank Rev. V. Laltlanzuala and his family, Mamit, Vanlalhluna and his family, Serchhip, H. Biakdawla and his family, Lunglei and Sainguri Sailo for their loving care and support.

I would like to thank all the residents of the study area who have helped in carrying out the study. Also I really thank to the people who was important to the successful realization of this thesis.

Finally, I thank God for keeping me in good health and showering me with blessings throughout the study

Dated: 25<sup>th</sup> March, 2015

Department of Physics,

Mizoram University, Aizawl.

**(P.C. Rohmingliana)**



# CONTENTS

	<b>Pages</b>
<b>Title of the Thesis</b>	i
<b>Certificates</b>	ii
<b>Declaration</b>	iv
<b>Acknowledgment</b>	v
<b>Contents</b>	vii
<b>List of Figures</b>	xi
<b>List of Tables</b>	xiii
<b>Dedication</b>	xiv
<b>Chapter 1</b> : <b>Introduction</b>	1
1.1 : Radon, thoron and their progeny	2
1.2 : Indoor radon and thoron	8
1.3 : Radon measurement	9
1.3.1 : Equilibrium Equivalent Concentration	13
1.3.2 : Equilibrium factor	13
<b>Chapter 2</b> : <b>Theoretical Formalism and Methodology</b>	16
2.1 : Measurement of radon and thoron concentrations	16
2.1.1 : Twin Cup Dosimeter	16
2.1.2 : Standardization of bulk etching rate	18
2.1.3 : Calibration Factor	19
2.1.4 : Spark counter for track counting	20
2.1.5 : Operating voltage of a spark counter	22

2.1.6	:	Formulae used for calculations of concentration of radon and thoron	23
2.2	:	Radon and thoron progeny concentrations	24
2.2.1	:	Equilibrium Equivalent Concentration (EEC)	24
2.2.2	:	Equilibrium factor (F) for radon and thoron	25
2.2.3	:	Inhalation Dose Rate (D) of radon and thoron	26
2.3	:	Radon in Soil (Surface Radon Flux)	27
2.3.1	:	RAD7	30
2.4	:	Background Gamma radiation survey	31
2.5	:	Radioactivity content in soil and building materials	31
2.6	:	Classification of parameters for measurements	33
2.6.1	:	Geographical classification and seasonal variation of concentration of gases	33
2.6.2	:	Geological conditions	34
2.6.3	:	Selection of Types of houses	34
<b>Chapter 3</b>	:	<b>Experimental determination of indoor radon, thoron and their progeny concentrations in Lunglei, Serchhip and Mamit Districts</b>	<b>36</b>
3.1	:	Indoor radon and thoron measurements	37
3.1.1	:	Calibration of dosimeter	38
3.1.2	:	Experimental Standardization of etching rate	39
3.1.3	:	Determination of Operating voltage of a spark counter	40
3.1.4	:	Results and discussions	41

3.2	:	Progeny concentrations measurements	57
3.2.1	:	Results and discussions	58
3.3	:	Determination of Equilibrium factors for radon ( $F_R$ ) and thoron ( $F_T$ )	61
3.3.1	:	Results and discussions	62
3.4	:	Estimation of annual inhalation dose for radon and thoron	65
<b>Chapter 4</b>	:	<b>Experimental determination of surface flux, radioactivity content and radon content in soil gas</b>	69
4.1	:	Measurement of Surface radon flux	69
4.1.1	:	Results and discussions	70
4.2	:	Radioactivity content in soil samples and building materials	74
4.2.1	:	Results and discussions	75
4.3	:	Radon content in soil gas	80
4.3.1	:	Results and discussions	80
4.4	:	Background gamma radiation	82
4.4.1	:	Results and discussions	83
<b>Chapter 5</b>	:	<b>Conclusion</b>	84
<b>References</b>	:		93
<b>Appendices</b>	:	Appendix – I (a)	104
		Appendix – I (b)	109
		Appendix – II	111

Appendix – III	114
Appendix – IV (a)	118
Appendix – IV (b)	125
Appendix – IV (c)	129
<b>Lists of Research Publications</b> :	137
<b>Brief bio-data of the author</b> :	142
<b>Reprint of published papers</b> :	144

## Lists of Figures

Figure Nos.	Titles of the figures	Page
1.1	Decay diagram of $^{238}\text{U}$ series with the half-life of each radionuclide.	3
1.2	Decay diagram of $^{232}\text{Th}$ series with the half-life of each radionuclide	7
1.3	Typical radon sources and entry routes	9
2.1 (a)	Schematic diagram of twin-cup dosimeter	18
2.1 (b)	BARC type twin cup dosimeter	18
2.2	Schematic diagram of a spark counter	21
2.3	Applied Voltage vrs Count showing the plateau region.	22
2.4	Diagram of the detector element (Direct Progeny Sensor (DPS))	24
2.5	Building up of radon concentrations with time inside the accumulator	29
3.1	A map of Mizoram showing the sampling sites covering Lunglei, Serchhip and Mamit Districts	36
3.2	Block diagram of the calibration chamber for calibrating twin cup dosimeter	38
3.3	Operating voltage of the spark counter used in the present study	40
3.4	Indoor radon concentrations in each district along with the combined study area for different seasons including the annual average	49
3.5	Indoor thoron concentrations in each district along with the combined study area for different seasons including the annual average	50
3.6	Indoor radon and thoron concentrations of different types of buildings in Lunglei District	53
3.7	Indoor radon and thoron concentrations of different types of buildings in Serchhip District	53
3.8	Indoor radon and thoron concentrations of different types of buildings in Mamit District	54
3.9	Indoor radon and thoron concentrations of different types of buildings in the combined study area	55
3.10	Annual average concentration of indoor radon in geological areas	56
3.11	Annual average concentration of indoor thoron in geological areas	56

3.12	Annual average value of Equivalent Equilibrium Concentration of Radon	61
3.13	Annual average value of Equivalent Equilibrium Concentration of Thoron	61
3.14	Annual average value of equilibrium factor of radon	65
3.15	Annual average value of equilibrium factor of thoron	65
3.16	Annual average of inhalation dose for Radon	66
3.17	Annual average of inhalation dose for Thoron	67
4.1	Radon flux at each sampling sites in Lunglei District	71
4.2	Radon flux at each sampling sites in Serchhip District	71
4.3	Radon flux at each sampling sites in Mamit District	72
4.4	Radon flux at different geographical locations	73
4.5	Correlation of radon flux obtained and indoor radon concentration	73
4.6	Radioactivity content in Soil samples	76
4.7	Radioactivity content in Building materials	77
4.8	Relation of $^{238}\text{U}$ content of the building materials with indoor radon concentrations	78
4.9	Relation of $^{232}\text{Th}$ content of the building materials with indoor radon concentrations	79
4.10	Radon content in soil gas in Lunglei District	81
4.11	Radon content in soil gas in Serchhip District	81
4.12	Radon content in soil gas in Mamit District	82
4.13	Comparision of radon content in soil gas	82

# LISTS OF TABLES

Table	Title of the table	Page
1.1	Physical properties of radon	4
2.1	Global averaged radon and thoron inhalation dose	27
3.1	Concentrations of radon and thoron in Lunglei District.	42
3.2	Concentrations of radon and thoron in Serchhip District.	43
3.3	Concentrations of radon and thoron in Mamit District.	44
3.4	Annual average concentration of radon in Lunglei, Serchhip and Mamit Districts	45
3.5	Annual average concentration of thoron in Lunglei, Serchhip and Mamit Districts	45
3.6	Annual average indoor radon and thoron concentrations for different house types in the three districts along with the whole study area	52
3.7	Detail values of EERC and EETC in the study area.	59
3.8	The EEC values of radon and thoron in Lunglei District	59
3.9	The EEC values of radon and thoron in Serchhip District	60
3.10	The EEC values of radon and thoron in Mamit District	60
3.11	Detail values of Equilibrium factors in the study area.	63
3.12	Annual inhalation dose rate of radon and thoron in Lunglei District.	66
3.13	Annual inhalation dose rate of radon and thoron in Serchhip District.	66
3.14	Annual inhalation dose rate of radon and thoron in Mamit District.	66
3.15	Detail values of inhalation dose rate in the study areas.	68
4.1	Measured values of surface radon flux in the study areas.	70
4.2	Radioactivity content of soil sample (in Bq/kg) collected from the study areas.	75
4.3	Activity content of Building materials (in Bq/kg)	76
4.4	Measured values of radon content in soil gas from the study areas.	80

**This thesis is dedicated**

**to**

*My late Grandmother,*

*Saidawli*

*Her love and support meant the world to me.*



# Chapter 1

## Introduction

Human beings have been continuously exposed to radiation. This radiation can be classified into ionizing and non-ionizing radiation. The high energy radiation which can strip off electrons from atoms or molecules through which they travel, leaving them charged and reactive are called ionizing radiations and the lower energy sufficient only to change the rotational, vibrational or electron valence configurations of atoms are termed as non-ionizing radiations.

The ionizing radiations are again divided into two types, natural and artificial radiation. The radiation from man-made or induced unstable nuclei is called artificial radiation and the main sources are medical sources, industrial sources, nuclear sources, occupational sources and consumer products, etc. The radiation coming from naturally occurring nuclei is called natural radiation and the main sources are cosmic rays and terrestrial radiation. Although high levels of radiation are definitely harmful to organisms, some environmental radiation is of importance to life. Hence, it is clear that contemporary life have adjusted or are doing so to all features and limitations of the environment, including the natural background radiation. The term cosmic rays or cosmic radiation refers to primary energetic particles of extraterrestrial origin that enter the earth's atmosphere, and to the secondary radiations produced by their interactions with the atmosphere. Primary cosmic radiation consists mostly of very high-energy protons: up to  $10^{18}$  eV. Most of it comes from outside our solar system and some of the primary cosmic radiation is from our sun, produced during solar flares and little of it penetrates to the earth's surface; the vast

majority of it interacts with the atmosphere. When it does interact, it produces the secondary cosmic radiation.

Terrestrial radiation includes radiation emanating from the earth itself and not from outer space. Radionuclides, which appeared on the Earth at the time of formation of the Earth, are termed "primordial". Of the primordial radionuclides, three are of overwhelming significance, these are Potassium-40, Uranium-238 and Thorium-232. Among the radionuclides in the decay chain of U-238 and Th-232, the concentration of Radon ( $^{222}\text{Rn}$ ) and Thoron ( $^{220}\text{Rn}$ ) and their progeny will be dealt in the present study.

### 1.1 Radon, thoron and their progeny

Radon, thoron and their progeny, which is a topic of public health concern, has been found to be a ubiquitous indoor air pollutants in homes to which all persons are exposed. Annual exposure due to these nuclei imparts the major contribution to the inhalation dose. Therefore, it is fundamental and justified to make a quantitative assessment of their concentrations in dwellings. In view of the fact that radon, thoron and their progeny concentrations contribute the most to the natural radiation dose to general populations, large scale and long-term measurement of radon, thoron and their progeny concentrations has been receiving considerable attention (Mayya *et al.*, 1998).

Radon and Thoron are originated from the radioactive decay of radium isotopes; they are the products of natural  $^{238}\text{U}$  and  $^{232}\text{Th}$  decay series in the earth's crust and the sequence ends with the formation of  $^{206}\text{Pb}$  which is stable and non-radioactive. More than 25 isotopes of radon have been identified in which  $^{222}\text{Rn}$  (radon),  $^{220}\text{Rn}$  (thoron) and  $^{219}\text{Rn}$  (actinon) occur in nature as members of uranium, thorium and actinium series respectively. Figure 1.1 shows the decay series of uranium. Because of its short half life (4 sec) and relatively low abundance of its major source  $^{235}\text{U}$ , actinon series is of minor importance.

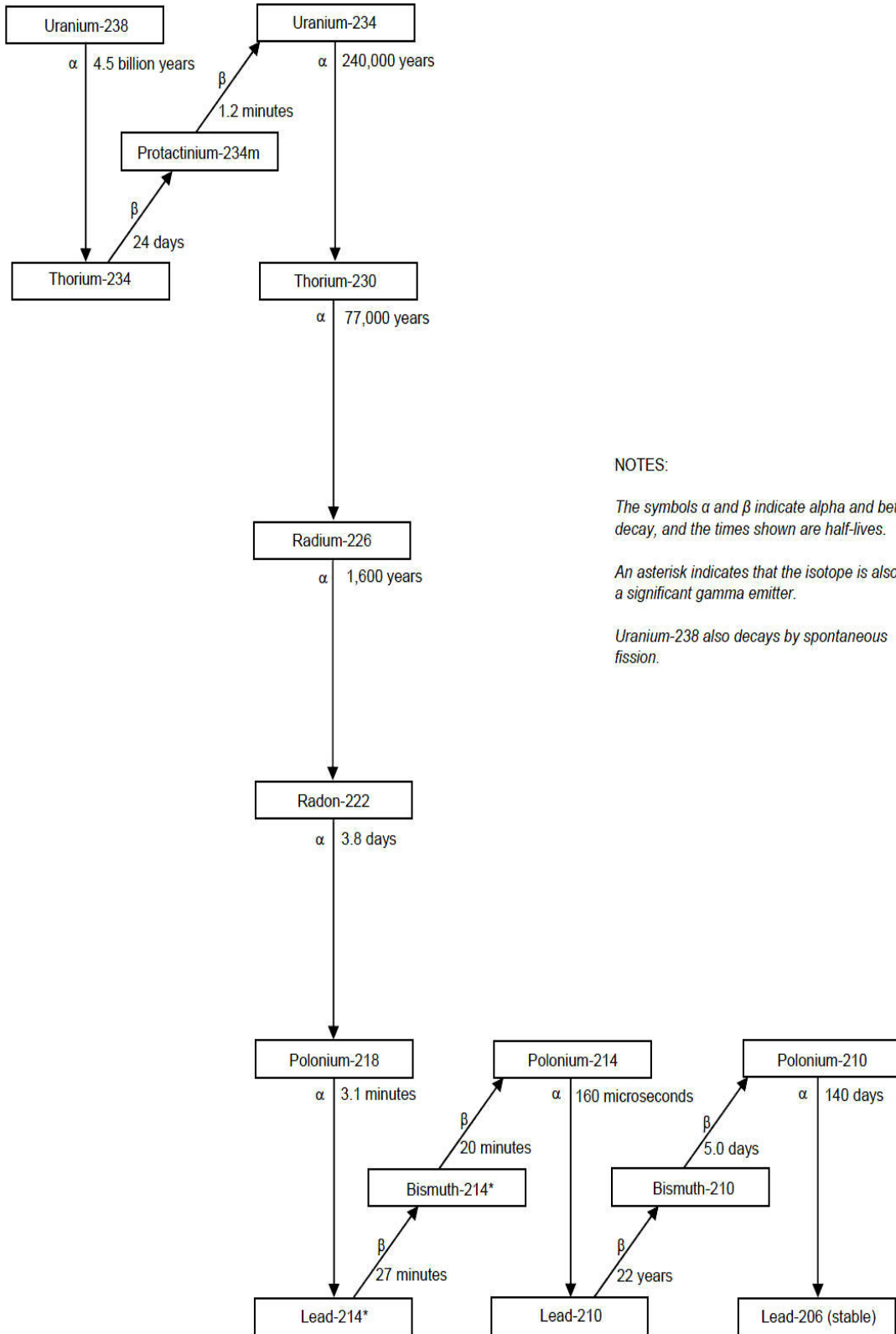


**Figure 1.1** Decay diagram of  $^{238}\text{U}$  series with the half-life of each radionuclide.

Radon (Rn) was originally named niton, from Latin nitens, which means shining. It was first discovered by Fredrich Ernst Dorn in Germany in 1898. Ramsay and Grey in 1908 were the ones to name it niton and isolate it and determine its density. In 1923, it was officially named radon. Radon with an atomic number of 86, is a colourless, odourless, tasteless and radioactive noble gas which disperses widely in the environment and is readily soluble in water. It is mainly found in soil and sea water. When cooled below its freezing point, it exhibits brilliant phosphorescence that becomes yellow at lower temperatures and orange-red at the temperature of the liquid air. It has the highest density among gases, making it the heaviest gas presently known. A detail list of the physical properties of radon is given in Table 1.1.

**Table 1.1** Physical properties of radon

Density at 1 atm pressure and 0°C	9.73 g/L
Boiling point at 1 atm pressure	-62°C
Density of liquid at normal boiling point	4.4g/cm <sup>3</sup>
Diffusion coefficient in air	0.1cm <sup>2</sup> /s
Diffusion coefficient in water	10 <sup>-5</sup> cm <sup>2</sup> /s
Viscosity at 1 atm pressure and 20°C	0.229 poise
Solubility in water at 1 atm pressure and 20°C	230cm <sup>3</sup> /kg
Solubility in various liquids at 1 atm pressure and 18°C	
Glycerine	0.2cm <sup>3</sup> /kg
Ethyl alcohol	7.4cm <sup>3</sup> /kg
Petroleum (liquid paraffin)	9.2cm <sup>3</sup> /kg
Toluene	13.2cm <sup>3</sup> /kg
Carbon disulfide	23.1cm <sup>3</sup> /kg
Olive oil	29.0cm <sup>3</sup> /kg

Being an inert gas, their behaviour is not affected by chemical processes (Nazarof, 1988). It decays by the emission of energetic alpha particles. Radon being a gaseous element in the natural radioactive series gets diffused into the atmosphere from the earth's crust. This mobile radon isotope 222 has a half-life of 3.8 days, which is long enough to diffuse into the atmosphere through the solid rock or soil in which it is formed. The

presence of radon in the free atmosphere was first noted by Elster and Geitel around 1901 (Elster *et al.*, 1901).

Radon is continually being formed in soil and released to the air. Atmospheric radon is not an issue of health concern because radon is rapidly diluted to low levels by circulations throughout outdoor air. It becomes environmental hazards when it remains concentrated in enclosed places such as houses, caves and mines. As radon is a product of uranium, uranium mines may have high concentrations of radon and its highly radioactive daughter products. In spite of their short half life, these radioactive gases are considered hazardous which is mainly due to the progenies produced during the chain decay (Majumdar, 2000). The first major studies of the health concern occurred in the context of uranium mining, first in the Joachimstal region of Bohemia and then in the Southwestern United States during the early Cold War. Due to the result of high levels of exposure to radon in the mid-1950s, many uranium miners in the Four Corners region contracted lung cancer and other pathologies. The danger of radon exposure in dwellings was discovered in 1984 with the case of Stanley Watras, an employee at the Limerick nuclear power plant in Pennsylvania (Nazarof, 1988).

Radon and thoron decay with the emission of alpha particles and produce daughter nuclei – polonium, lead and bismuth. These elements exist as ions and / or free atoms before forming molecules in condensed phase or attached to airborne dust particles and may be inhaled and deposited in the respiratory tract, in which they release all their alpha emissions. These daughter nuclei emit alpha or beta particles. Radon decay products are divided into two groups, namely, the short-lived radon daughters  $^{218}\text{Po}$  (RaA; 3.05 min),  $^{214}\text{Pb}$  (RaB; 26.8 min),  $^{214}\text{Bi}$  (RaC; 19.7 min), and  $^{214}\text{Po}$  (RaC'; 164  $\mu\text{s}$ ) with half-lives below 30 min; and the long-lived radon daughters  $^{210}\text{Pb}$  (RaD; 22.3 yr),  $^{210}\text{Bi}$  (RaE; 5.01 days), and  $^{210}\text{Po}$  (RaF; 138.4 days). In the short-lived daughters, the whole sequence of decays can be completed before the human clearance processes can sweep them away

because even the longest-lived element has a half life of less than 27 min. The long-lived radon progeny contributes relatively little to lung exposure because they are utterly removed from the body before decaying (Amgarou *et al.*, 2001).

Thoron ( $^{220}\text{Rn}$ ) is an isotope of radon having  $^{232}\text{Th}$  as major natural source. It has a half life of just 55 sec (Pillai and Paul, 1999). As the half life of  $^{220}\text{Rn}$  is less than one minute, much of the atoms decay before reaching the earth's surface and its mean diffusion length is lower to that of  $^{222}\text{Rn}$ . The contribution made by thoron to the human exposures in indoor environments is usually small compared with that due to radon, due to the much shorter half-life (55 seconds vs 3.82 days). Radon and thoron are present in the atmosphere, and the presence of thoron has not been well studied in the past studies over a long time because of its short half-life and it was often considered that the concentration of thoron was much less than the concentration of radon. There are also some difficulties in measurement and calibration. In addition, there have been no epidemiological data on thoron exposure so far (Tokonami, 2005; Guo *et al.*, 1992). But it may not be negligible where high amount of thorium bearing regions exist, which are of High Background Radiation Areas (HBRAs). Examples of such places are monazite-bearing sands in Kerala, India and regions of Yangjiang in China. In these areas, excess quantity of thoron along with its decay products is found.

Figure 1.2 shows the decay series of thorium. In this decay chain, there are no long-lived groups in its daughter nuclei.  $^{212}\text{Pb}$  is the most important radionuclide in its decay chain. It has a relatively long half life of 10.64 h. However, a considerable fraction of this radionuclide deposited in the bronchial epithelium can be absorbed into blood; so that it may be carried to other organs and may produce a large biological impact (Amgarou *et al.*, 2001; Vanchhawng, 2012). Among all the other progenies of radon as well as thoron, these short lived progenies are under consideration.

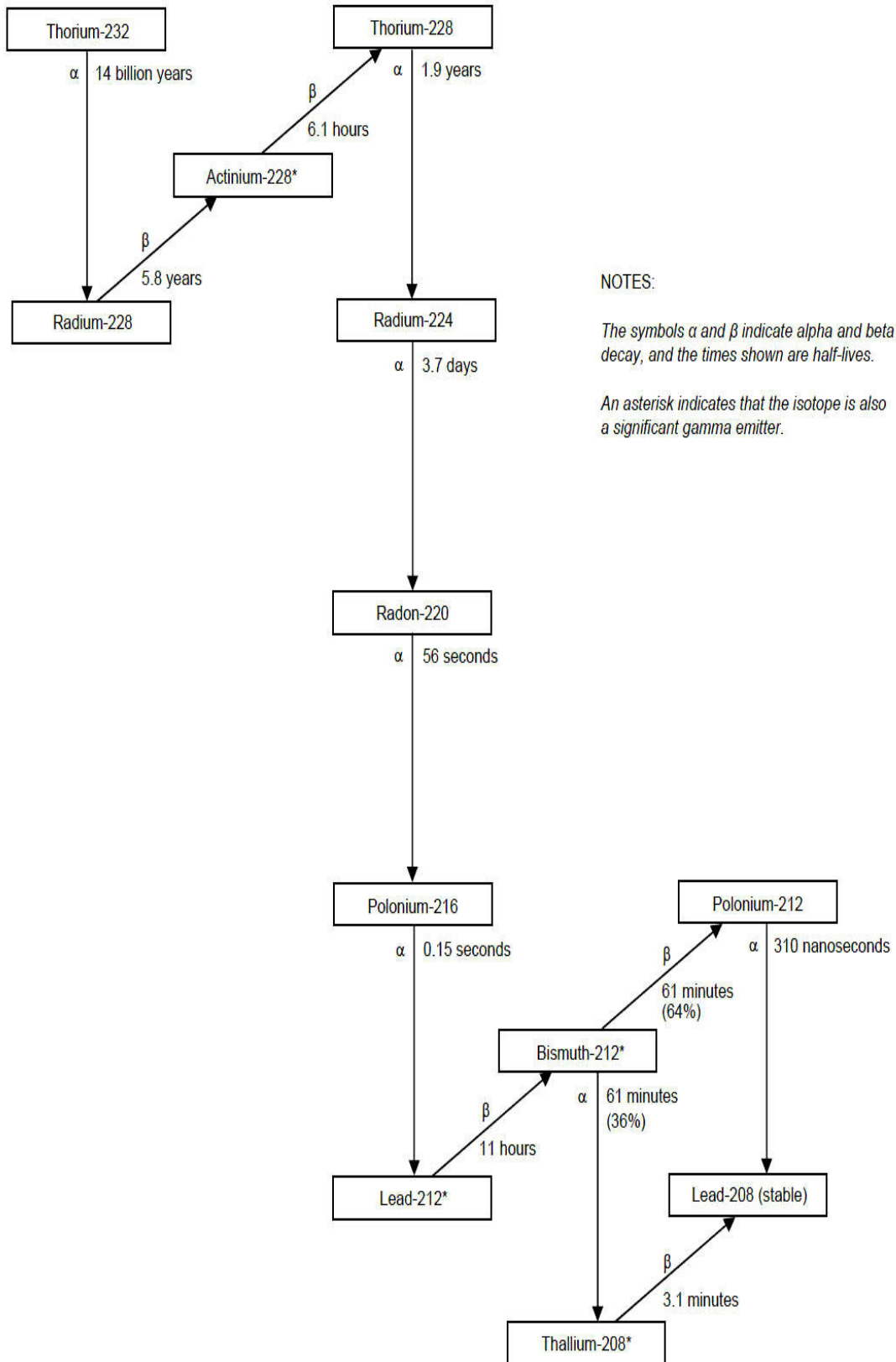


Figure 1.2 Decay diagram of  $^{232}\text{Th}$  series with the half-life of each radionuclide.

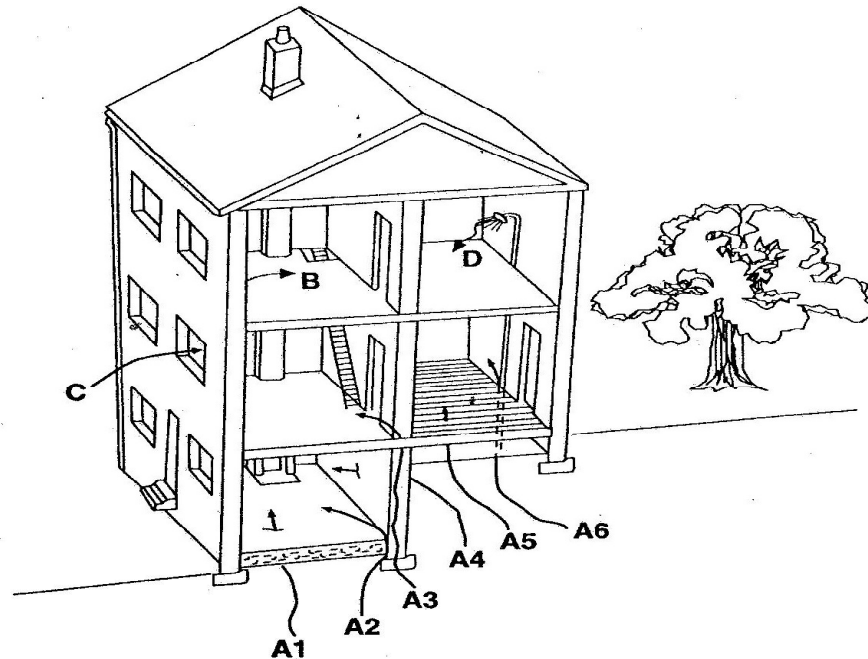
## 1.2 Indoor radon and thoron

The environmental studies of outdoor radon started with the exposures resulting from industrial processes-primarily the mining and milling of uranium which increased the accessibility of radon to the outdoor atmosphere (Gessell *et al.*, 1980). The concentrations of radon were found to be higher in the homes and other buildings in the vicinity of these mining and milling places than average inside homes. These radionuclides have the ability to transport through small spaces between the soils particles called “pores” inside the earth. The transportation of radon from the source to the environment (gas or liquid medium) is accomplished by the process called Emanation. In this process, radon is released into small air or water contained in pores between soil and rock particles which is facilitated by diffusion and convection. And the process of transportation from soil pores to the atmosphere through the surface of the earth is called “exhalation”. When a dwelling is present, they may migrate into this structure and accumulate indoors in sufficient quantities. The concentration of radon in soil is influenced by soil moisture content, barometric pressure variations, temperature and structure of soil. The major source of indoor radon are (1) soil gas emanation from soils and rocks (2) through water and natural gas used which later off-gas into indoor air (3) building materials and (4) directly from the outdoor air through openings like doors, windows, ventilations, etc. Figure 1.3 shows the typical radon sources and entry routes.

The process of exhalation also takes place from a building materials used in constructing dwellings as it is well known that building materials have been extracted from the naturally existing materials found in the earth. Radon and thoron exhaled from the earth’s surface into the free atmosphere is rapidly dispersed and diluted by natural convection and turbulence. When a dwelling is present, the exhaled gases from the soil have a much higher chance to migrate into the indoor as compared to their dispersion process into the atmosphere. Besides, the higher concentration of radon/thoron inside the



dwelling may be due to the contribution of building materials. Ventilation rate – which is air circulation rate of the building with the outside environment, also plays a vital role in the accumulation of indoor radon, thoron and their progeny. Higher the ventilation rate, lower will be the indoor concentration and vice versa.



- A Entry of radon from soil through:**
- A1 - Cracks in solid floors
  - A2 - Construction joints
  - A3 - Cracks and cavities in walls
  - A4 - Cracks in walls below ground level
  - A5 - Gaps in suspended floors
  - A6 - Gaps around service pipes
- B Radon exhalation from building materials**
- C Entry of radon with outdoor air**
- D Radon released from water**

**Figure 1.3** Typical radon sources and entry routes

### 1.3 Radon measurement

Exposure to radon, thoron and their progenies contribute significantly to the radiological dose among the general population. As a result, investigation of radon and thoron concentrations have become more numerous and territorial mapping of radon concentrations have been or are being conducted in many countries, with the aims to establish the average long term radon/thoron exposure. Radon and thoron are found in

measurable amounts in soil, rock, ocean water, ocean sediments and in the atmosphere. As the isotopes of radon produced from uranium and thorium diffuse continuously into the atmosphere from soil, some get trapped in the soil or among rock particles while some atoms may get dissolved in ground water flowing through the area. The rate of escape will depend on the concentration of radon gas, nature of the soil and local geological and meteorological conditions.

Radon, thoron and their progeny concentrations were measured over the past 50 years in many countries, with the improvement of experimental apparatus and technical formulation. With these improvements, the seismicity and tectonic conditions and radon anomalies were also monitored in the Himalayan range since 1980s (Ramachandran *et al.*, 2004). In this observation, the precursory nature of radon anomalies were found to correlate with some of the micro- earthquake recorded. As for the correlation with earthquakes, by continuous monitoring of radon concentration in a specific area, there has been a high deviation on the concentration of radon before or after the earthquake. In 1979, radon anomalies were observed prior to earthquakes in California, Kobe in Japan in 1995, Tangshan in China in 1976, etc (Ramachandran *et al.*, 2004). The Nuclear Engineering Section of the National Technical University of Athens (Petropoulos *et al.*, 2001), has been studying radon exhalation rate from building materials. The radon, thoron and progeny concentrations vary from place to place and also depend on the building material in case of indoor concentration.

In India, radon concentrations were continuously monitored by Guru Nanak Dev University, Amritsar and Palampur Station, Himachal Pradesh. Their data recorded shows 25 anomalies correlated to earthquakes in the region (Virk, 1994). Both Chamobi and Bhuj earthquake that occurred in March 29, 1999 and January 26, 2001 respectively were postdicted by correlation of radon anomalies recorded at Palampur in the soil-gas and ground water (Ramchandran *et al.*, 2004). Studies of radon and thoron levels in Mysore

City have also been done and radon concentrations were found within  $33 \text{ Bq/m}^3$  in more than 50% of the dwellings studied (Chandrashekara and Paramesh, 2008). Nambi *et al.*, (1986) carried out a country wide survey of the external gamma exposures in India and this enabled the generation of Gamma exposure map of India. Meanwhile, Sankaran *et al.*, (1986) also constructed a similar profile for the terrestrial radioactivity. However, measurement of radon/thoron and their progenies is much more complicated due to the short lived daughter products. Attention was given on high background radiation areas and high uranium content in the soil. Subba Ramu *et al.*, (1990) had initiated indoor radon measurement in some dwellings of 15 towns in India which were specially selected on the basis of high uranium content in the soil where high levels of indoor radon were expected. Similarly, Nair *et al.*, (1994) also measured radon concentration in high background areas in Kerala. Meanwhile the study of behaviour of radon and its progenies also was in progress. Radon diffusion in air and solid medium was also studied (Singh *et al.*, 1993). The studies on the equilibrium of thoron and its daughter in monazite areas were undertaken by Pillai *et al.*, (1999). The radon emanation from the building materials in India and the radioactivity studies were also reported (Menon *et al.*, 1987; Shukla *et al.*, 2005; Sahoo *et al.*, 2007).

Measurement of radon and its short lived daughter products are based on the detection of alpha particles associated with their radioactive decay. Several techniques are used to measure the radon/thoron concentration in air. The measurement techniques can be classified as short term and long term or integrated methods. Short term measurement includes the grab sampling techniques in which air sampling is done by sucking the air, radon/thoron are collected on a filter paper and subsequently alpha decay are counted with suitable counter. In long term and integrated method suitable detector are used in which the nuclear track due to alpha decay are recorded and the tracks formed are counted by a counter. Several personnel dosimeters employing tracks detectors have also been

developed. These techniques have been increasingly used for the measurement of radon or thoron in soil gas, uranium exploration, earthquake predictions and geological studies. For the correct choice of the design of a radon and thoron measuring device using track detectors, it is necessary to have information about the response of the detector to radon and its progeny. The mathematical basis for calculation of these dependencies was first developed by Fleischer and Mogro Campero, (1978). Several theoretical papers, based on various calculation techniques to obtain the response of detectors and elements of design, have been reported.

The nuclear track detector technique is one of the most reliable method for the integrated and long-term measurement of indoor radon activity (Ramu *et al.*, 1992). Frank and Benton, (1977) studied the improvement of two-detector devices, where one detector is placed open, and the other is placed inside the chamber closed with an inlet filter. By this method they propose the possibility to determine the equilibrium factor. Twin cup dosimeter was developed, in which membrane is use to filter the inlet of radon chamber. With the improvement of twin cup dosimeter (Eappen 2005), where membrane filter was replaced by a pinhole cap of the radon chamber. In this, one pinhole is used to block the entry of radioactive nuclides other than radon. In 2009, this pinhole cap was again improved by replacing it with 4 holes. The gas measurement is carried out by placing an SSNTD inside a twin-cup dosimeter covered with a filter paper and the system is suspended in the house for sufficiently long periods (about three months). The filters prevent the entry of the progeny nuclides into the dosimeter cup. The gas concentrations present in the cup are related to the tracks formed on the SSNTD placed inside the cup. The specially developed deposition flux integrating passive sensors, named as the direct radon/thoron progeny sensor (DRPS/DTPS) are used for estimating equilibrium equivalent concentrations of radon and thoron. This direct progeny sensor system uses absorber-mounted nuclear track detectors (LR-115) which selectively register the tracks due to alpha

emissions from  $^{212}\text{Po}$  ( $\alpha$  energy 8.78 MeV) and  $^{214}\text{Po}$  ( $\alpha$  energy 7.69MeV) from the deposited atoms of radon and thoron progeny species respectively (Mishra *et al.*, 2008; Mishra *et al.*, 2009; Rohmingliana *et al.*, 2011). Some of the terms that has been connected with measurement of radon and its progenies may be given as:

### 1.3.1 Equilibrium Equivalent Concentration (EEC)

The EEC of a non-equilibrium mixture of short-lived radon (thoron) daughters in air, is that activity concentration of radon (thoron), which would have been in equilibrium with this mixture. If the actual radon concentration is  $C_{Rn}$  and equilibrium factor is  $F$ , then the "Equilibrium Equivalent Concentration" EEC, can be expressed as:

$$EEC = F C_{Rn}$$

where  $EEC$  and  $C_{Rn}$  are expressed in Bq per unit volume.

### 1.3.2 Equilibrium Factor (F)

The Equilibrium Factor (F) is defined as the ratio of the total potential alpha energy for the actual daughter concentrations to the total potential alpha energy of the daughter, which would be in equilibrium with the radon concentration.

Technique for indoor radon measurement developed by Mayya *et al.*, (1998) proved to be very useful in discriminating radon from thoron and again from their progenies. Using this technique, a country-wide radon mapping programme was carried out sponsored by Department of Atomic Energy, India, in which several Universities and Research Institutions participated (Ramachandran *et al.*, 2003). The results obtained from this project show that the radon gas concentrations at different locations vary between 4.6 and 147.3 Bq/m<sup>3</sup> with an overall geometric mean of 23.0 Bq/m<sup>3</sup> (GSD 2.61). Thoron gas concentrations are found to be less than the radon gas concentrations at these locations (3.5 to 42.8 Bq/m<sup>3</sup>) with an overall geometric mean concentration of 12.2 Bq/m<sup>3</sup> (GSD 3.22). The inhalation dose rates due to radon, thoron and their progeny ranged from 0.27 mSv/y at

Kalpakkam to 5.14 mSv/y at Digboi with a geometric mean value of 0.97 mSv/y (GSD 2.49). In general, the indoor thoron and progeny concentrations and corresponding inhalation dose rates are found to be about half of that due to radon and its progeny. Mishra and Mayya, (2008) developed and characterise a new technique for measuring solely the progenies of these gases which are termed as direct progeny sensors (DPS). This technique simplifies the calculation of inhalation dose rates due to radon and thoron in the indoor environment.

It is observed that fewer surveys have been done in the north-eastern part of India, which is expected to have higher concentrations of radon on the basis of its geological and seismic characteristics (Dwivedi and Ghosh, 1991). Measurement of radon, thoron and their progeny concentrations in Mizoram has been done only in 17 dwellings (Ramachandran *et al.*, 2003). Srivastava *et al.*, (1996) had few measurements in the north-eastern part of India in particular locations like Aizawl, Kolasib, Saiha and Khawlian in Mizoram, Shillong in Meghalaya and Silchar in Assam state.

The present study tries to explore the concentration of radon, thoron and their progeny in Mizoram with special reference to Lunglei, Serchhip and Mamit districts which will supplement the mapping of concentration of these gases in Mizoram. According to the 2011 census, Lunglei District is located in the mid-southern part of Mizoram between 23°24'21.96" and 22°29'45.43" N latitudes and 92°20'53.97" and 93°10'01.82" E longitudes having a total population of 154094 with a population density of 34 per km<sup>2</sup>. Serchhip District occupies the central part of Mizoram lying in between 23°35'58.82" and 23°00'20.84" N latitudes and 92°41'06.00" and 92°40'39.63" E longitudes with a total population of 64855 and population density of 46 per sq.km. Mamit District is located in the western part of Mizoram between 23°17' and 24°15' N and 92°17' and 92°40' E having a total population of 85757 with population density of 28 per km<sup>2</sup>. This thesis will reflect the actual abundance of the studied radionuclides in the study area based on the results of

the experimental measurements. In this experimental work, to obtain the time integrated concentration levels of indoor radon and thoron, Solid-state nuclear track detector (SSNTD) based pin-hole dosimeters have been used. To measure the progeny concentration, deposition based Direct Progeny Sensors (DPS) in bare modes have been used. Simultaneous measurement of background gamma radiation level at the spot was done indoor and outdoor at a height of 1 metre from the ground and on the ground level using Survey Meter. The activities of the source radioactive elements viz., uranium and thorium for the considered gases in soil are measured using NaI(Tl) detector in which soil samples are collected and analyzed. This will be used to understand the deposition of the mentioned radioactive elements in Mizoram and can be well correlated with the concentrations of radon and that of thoron in dwellings.

The chapters in the thesis are organized in the following manner:

Chapter 2 will contain the theoretical formulae used in the research work. A complete methodology will also be given in this chapter.

Chapter 3 will present the experimental calibration and determination of operating points of the instruments used which will be followed by the details of results obtained from the experimental determination of indoor radon, thoron and their progenies concentration carried out in the present study. Calculation of equilibrium factors and annual inhalation doses for radon as well as thoron and discussion will also be included.

Chapter 4 will present the experimental measurements of surface radon flux, radioactivity content of collected soil samples and building materials and finally the background gamma radiation measurements. Possible and even critical discussion along with comparison on the results obtained in the present investigation will also be presented.

In chapter 5, we will discuss the conclusion of the whole results and summary of the entire work will be included.

This will be followed by references, appendices, etc.

## Chapter 2

### Theoretical formalism and methodology

Theory and formulae used in the research work and a complete methodology will be discussed in this chapter. It will include the detail description of detectors, instruments and theory of calibration of the instruments used in the present study. A cellulose nitrate film (LR - 115) placed inside a twin cup dosimeter is used as a detector in the present study. The progeny concentrations of radon and thoron are measured using a recently developed Direct Progeny Sensors (DPS). Equilibrium factors and inhalation doses are calculated from the obtained experimental data. Measurement of radon flux is done by a device called RAD7 and NaI (Tl) detector with 1K Multichannel Analyzer (MCA) is used to measure the radioactivity content of soil samples and building materials collected. Classification of measurements is also included in this chapter. The necessary procedures and formulae involved in measuring the concentrations of radon, thoron and their progeny, the radioactivity content of soil samples and building materials along with the calculations of equilibrium factor and inhalation doses are given in this chapter.

#### 2.1 Measurement of radon and thoron concentrations

Instruments, methodology and formulae used for measurement of radon and thoron are given below:

##### 2.1.1 Twin-cup Dosimeter

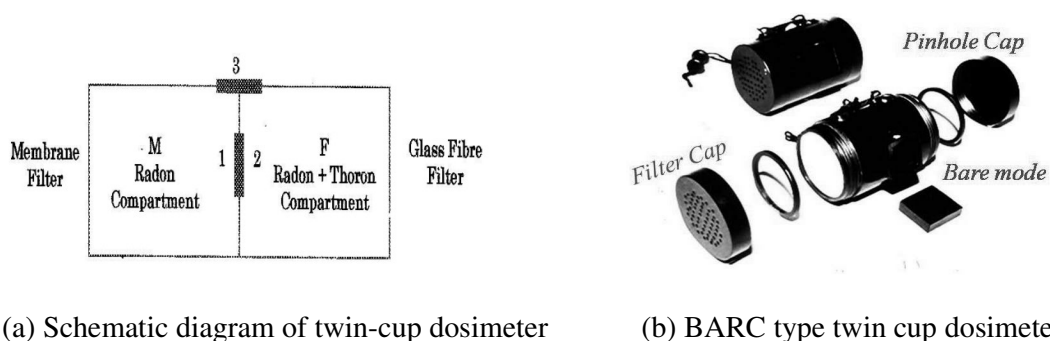
For indoor radon/thoron measurement, Solid State Nuclear Track Detector (SSNTD) based dosimeters developed by BARC (Mayya *et al.*, 1998) have been used. A Cellulose Nitrate films (LR-115 type II) of thickness 12  $\mu\text{m}$ , coloured deep red and coated on a 100  $\mu\text{m}$  thick polyester backing, manufactured by Kodak Pathe are used as detectors.



The chemical composition of LR-115 film is  $C_6H_8O_9N_{12}$  with density varying from 1.3 to 1.6. A 10% (2.5N) solution in distilled water of analytical-grade Sodium hydroxide (NaOH) is the chemical etchant normally used for LR-115. The choice of the detector LR-115 is made in view of the fact that LR-115 detectors do not develop tracks originating from the progeny alphas deposited on them and are unaffected by electrons or by radiations in the electro-magnetic spectrum (such as gamma rays, X-rays, or infra-red radiations, visible light). LR-115 films are suitable for radon in air concentration measurements. They are therefore can be handled without risk where such radiations are present. Nevertheless, care should be taken to avoid any abrasion on the films (Azimi-Garakani *et al.*, 1981).

The detectors are kept inside a twin cup dosimeter, a cylindrical plastic chamber divided into two equal compartments (Nambi *et al.*, 1994). Each chamber has a length of 4.5 cm and radius of 3.1 cm (inner volume of  $135 \text{ cm}^3$ ). The two equal compartments on both sides are filter and pinhole compartments. The filter compartment allows the entry of both radon and thoron gas to pass through inside by covering the cup with a filter paper blocking the entry of the progeny and hence tracks formed on the film in the filter compartment are related to the concentrations of both radon and thoron gases. In the pinhole compartment only radon gas was allowed to enter which has a modification from the earlier twin-cup dosimeter system (Eappen, 2005) by using a cap with a pin hole (0.4 mm diameter and 5 mm thick) in it and diffuses into it from the ambient air through the pinhole. This pin hole is designed in size and thickness of cap so as to block thoron from entry inside by considering the diffusion length and half life of thoron. It allows the build-up of about 90% of the radon gas in the compartment and suppresses thoron gas concentration by more than 99%. One filter paper is used to cover the entry point to block the progenies. There is one small compartment at the external middle attached to it which is usually used for recording the concentration of radon and thoron progenies where the

effects of radon and thoron progenies are difficult to distinguish. With the development of a special device called Direct Progeny Sensor (DPS) recently, the concentrations of progenies are estimated. Therefore, bare mode of this twin cup dosimeter is not used in the present work. The schematic diagram and BARC type of twin cup dosimeter are shown in Figure 2.1 (a) and (b).



(a) Schematic diagram of twin-cup dosimeter

(b) BARC type twin cup dosimeter

**Figure 2.1**

Dosimeters are hanged indoor overhead on the ceiling for a minimum of 90 days. After the exposure period is over, dosimeters are retrieved and replaced with new ones for the next deployment. The exposed films are then etched in an etching bath using 2.5N NaOH solution at 60°C for 90 minutes. Etching of the film helps in obtaining a clear visibility of the tracks produced on the films which is necessary for counting. The tracks recorded in this SSNTD films are then counted using a spark counter, which is an electronic counter operating on high voltage.

### 2.1.2 Standardization of bulk etching rate

Etching of the film is necessary because the tracks produced on the films due to radon, thoron and their progeny are clear for counting only after etching. Etched films are then counted by spark counter. Bulk etching rate is the rate of etching of the film (LR-115) per unit time.

Let  $W$  be the weight of the film in grams,  $A$  be the area in  $\text{cm}^2$  and  $\rho$  be the density in  $\text{gram}/\text{cm}^3$ . Then, the thickness of the film can be calculated by using the equation

$$\text{Thickness} = \frac{W}{A \times \rho} \text{ (cm)} \quad (2.1)$$

If the initial weight be  $w_i$  and final weight be  $w_f$ , then change in weight after etching is given by

$$\Delta W = W_i - W_f \quad (2.2)$$

Bulk Etching Rate ( $V_B$ ) is given by

$$V_B = \frac{\Delta W}{\Delta t \times \rho \times A} \quad (2.3)$$

where  $\Delta t$  is the time of etching in seconds.

By using Eq. 2.3 the bulk etching rate can be easily calculated.

### 2.1.3 Calibration Factor

Calibration factors (CFs) are the quantities, which are used for converting the observed track density rates to the activity concentrations of the species of interest. If  $T$  denotes the track densities observed on a SSNTD due to exposure in a given mode to a concentration  $C$  of given species for a time  $t$ , it is obvious that

$$T = kCt \quad (2.4)$$

where, we define  $k$  as the calibration factor (Eappen and Mayya, 2004).

In the cup mode, only radon or thoron or both enter the cup and the progeny species from the environment will be filtered out. Hence, the total tracks formed on the SSNTD placed inside the cups will be uniquely dependent on the gas concentrations only.

The corresponding calibration factors may be defined as

$$k_{R(P/F)} = \frac{T_{R(P/F)}}{tC_{R(P/F)}} \quad (2.5)$$

$$k_{T(F)} = \frac{T_{T(F)}}{tC_{T(F)}} = \frac{T_{R+T(F)} - T_{R(P)}}{tC_{T(F)}} \quad (2.6)$$

where,  $k_{R(P/F)}$  is the calibration factor of Radon in pinhole cup or filter cup and  $k_{T(F)}$  is the calibration factor of Thoron in the filter cup.  $C_R$  is the gas concentration of Radon in  $\text{Bq/m}^3$

and  $C_T$  is the gas concentration of Thoron in  $\text{Bq/m}^3$ .  $T_{R(P)}$  is the tracks recorded for Radon on the detector in  $\text{tr/cm}^2$  and  $T_{T(F)}$  is the tracks recorded for Thoron on the detector in  $\text{tr/cm}^2$ .  $T_{R+T(F)}$  is the tracks recorded for Radon and Thoron in the filter cup. The subscript  $P$  and  $F$  denote the compartments in the dosimeter.  $P$  represents pinhole compartment and  $F$  represents the filter compartment.

#### 2.1.4 Spark Counter for track counting

Evaluation of etched tracks in solid state nuclear track detectors (SSNTDs) by an optical microscope is a difficult, time-consuming and expensive task. This drawback is clearly found, for example, in absolute fission-rate measurements, where the whole area of the exposed track detector has to be scanned (Azimi- Garakani and Williams, 1977) and/or, in a national large scale survey of radon, when dealing with a number of samples (Azimi- Garakani *et. al.*, 1988). The attempts to automate track counting have led to the use of image analyzer instruments and spark counting systems. The Spark counting technique, which is applicable to plastic detectors, provides a convenient, cheap and fast method for track counting.

The Spark detector consists of two parts viz., the acrylic detector base and the Counter weight. The acrylic detector base has a fixed disc of  $1 \text{ cm}^2$  area (accurate to 3 decimal) and a spring-loaded contact. The positive high voltage is applied to the disc while the other contact is grounded. The entire assembly is made optically plane and polished to a high degree of flatness. The counter weight has a flat circular glass window to press the film during spark counting. When the plastic track detector is chemically etched, the through holes are produced along the tracks. The thin detector (about  $10 - 20 \mu\text{m}$  thick) is placed on top of a thick conductive electrode, commonly made of brass and covered with an aluminized plastic foil namely a very thin layer of aluminium evaporated onto a Mylar backing. The aluminized side of the plastic foil is in contact with the thin detector. When

the high voltage is applied across the capacitor  $C$ , an electrical discharge or spark takes place through a track-hole. The voltage pulse produced across a load resistor,  $R$ , can easily be counted electronically by a counter (Azimi-Garakani *et al.*, 1981). The spark passing through a track hole has enough energy to evaporate the thin layer of aluminium coating (less than  $1\mu\text{m}$  thick) and produces a much larger circular spot in the aluminium electrode. After the short-circuit, the spark is stopped, the capacitor  $C$  is charged again but a second spark cannot occur in the same track hole, because of the evaporation of the aluminium on the electrode. The spark, therefore, jumps randomly from one track hole to another until all track holes are counted. The evaporated spots on the aluminium, which have the diameter of about  $100\mu\text{m}$  are equal to the number of sparks and hence to the number of track holes in the plastic track detector. The aluminium replica can easily be counted by an optical microscope or a microfiche reader. The schematic diagram of a spark counter is given in Figure 2.2.

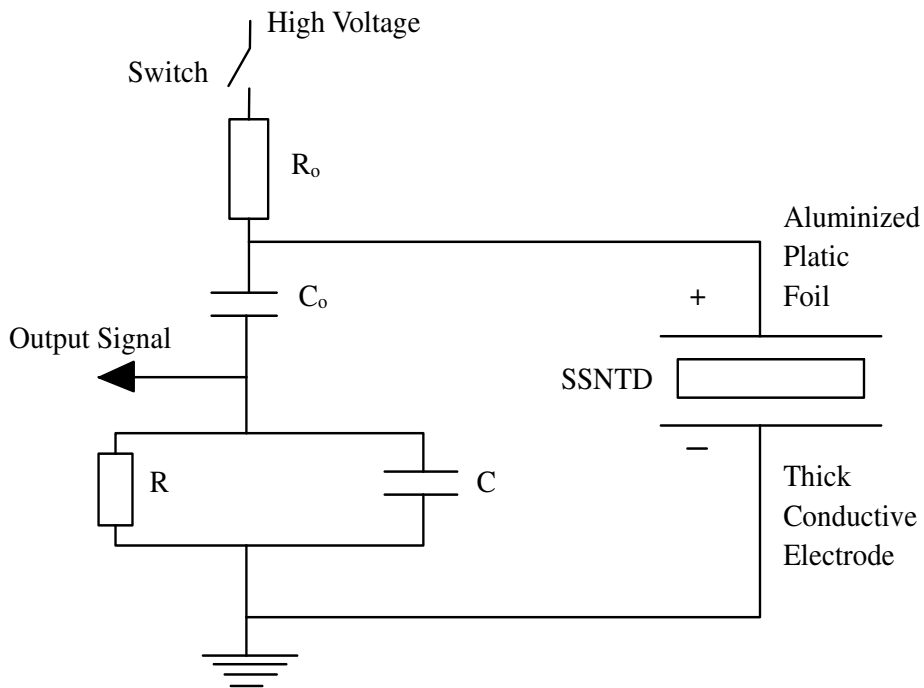


**Figure 2.2** Schematic diagram of a spark counter.

### 2.1.5 Operating Voltage of a Spark Counter

Operating voltage of a Spark counter is that specific voltage by which the counting of tracks should be done. When graph is plot between applied voltages and counts, a plateau region is produced. The plateau curve of a spark counter is similar to that of a Geiger tube, with the optimum operating voltage being at the centre of plateau (Malik and Durrani, 1974). The operating applied voltage for track counting is usually around 400 to 600 V. This plateau region shows that even with a small change in the applied voltage the number of tracks count by the counter remains constant. Hence, with the fluctuation of the applied voltage, the counts will remain the same. It is always necessary to apply a higher voltage to the track detector to punch out those tracks which have not been completely etched through. In practice pre-sparking at 700 to 900 V is carried out before the actual track counting. The graph plotted between applied voltage and the tracks obtained per unit area (counts) is shown in Figure 2.3.

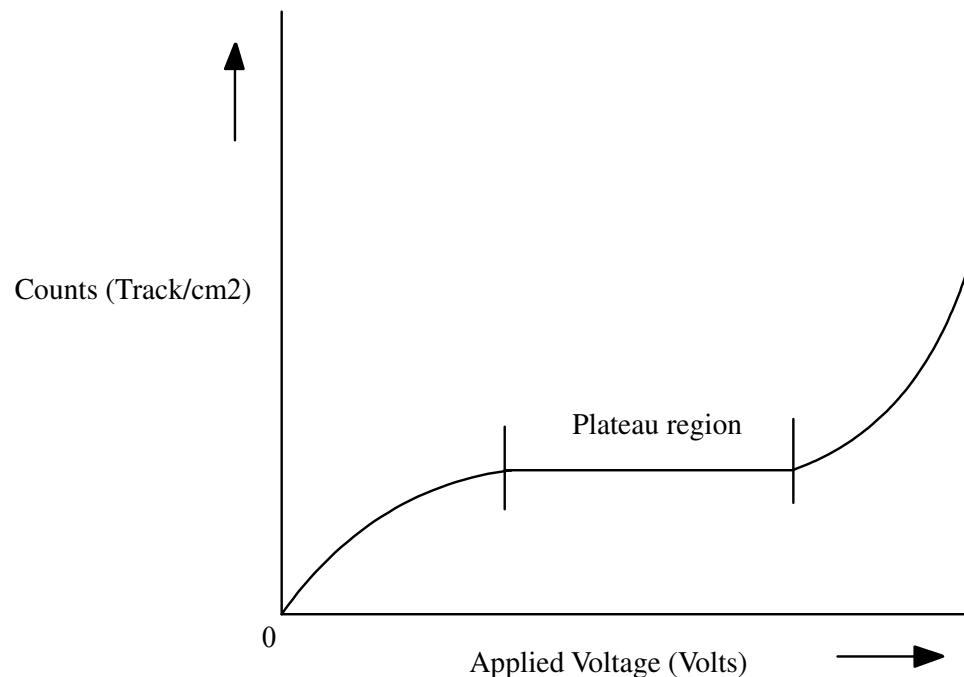


**Figure 2.3** Applied Voltage vrs Count showing the plateau region.

One of the disadvantages of spark counting technique is overlapping track spots. For small track densities, it is not a problem. But, at high track densities (above about 3000 tracks.cm<sup>-2</sup>), the track spots start overlapping since the average diameter of the aluminium spots is about 100 µm. Bhagawat *et al.*, (1976) had observed that mylar thickness as well as capacitance of the spark counter affects the size of the sparking area in the mylar films. Increase in thickness of aluminum decreases the hole size, while increase in capacitance increases the hole size.

### 2.1.6 Formulae used for calculations of concentrations of radon and thoron

The track density obtained from the spark counter is then used to calculate the concentration of that particular gas producing the α-emissions using the following formulae.

Radon concentration from the track density of pinhole compartment of the dosimeter is given as

$$C_R (Bq / m^3) = \frac{T_P}{\text{Calibration factor} \times \text{Exposure period (days)}} \quad (2.7)$$

where  $C_R$  is the radon concentration in  $Bq/m^3$  and  $T_P$  is the track density (Tracks/cm<sup>2</sup>) of films in pin hole compartment.

For calculating thoron concentration from filter compartment, the following formula was used.

$$C_T (Bq / m^3) = \frac{T_F - T_P}{\text{Calibration factor} \times \text{Exposure period (days)}} \quad (2.8)$$

where  $C_T$  is the thoron concentration,  $T_F$  is the track density of films in filter compartment and  $T_P$  is that for pinhole compartment (Mayya *et al.*, 1998). Calibration factor is the

quantity, which is used for converting the observed nuclear track density rates to the activity concentration.

The concentrations obtained using the above formulae are in  $\text{Bq/m}^3$ .

## 2.2 Radon and thoron progeny concentrations

For measurements of radon and thoron progeny concentrations, the methodology and formulae used are given as follows:

### 2.2.1 Equilibrium Equivalent Concentration (EEC)

Equilibrium equivalent concentration (EEC) of a non-equilibrium mixture of short-lived radon (thoron) daughters in air is that activity concentration of radon (thoron), which would have been in equilibrium with this mixture (Ramachandran *et al.*, 2003). The deposition based passive detector system named as DTPS (Direct Thoron Progeny Sensor) and DRPS (Direct Radon Progeny Sensor) in bare modes were used to measure the progenies of radon and thoron (Mishra *et al.* 2009). This system uses absorber-mounted nuclear track detectors (LR-115 type II) which selectively register the tracks due to alpha emissions from  $^{212}\text{Po}$  ( $\alpha$  energy 8.78 MeV) and  $^{214}\text{Po}$  ( $\alpha$  energy 7.69MeV) from the deposited atoms of radon and thoron progeny species, respectively. The diagrammatic view of the detector element is shown in Figure 2.4.

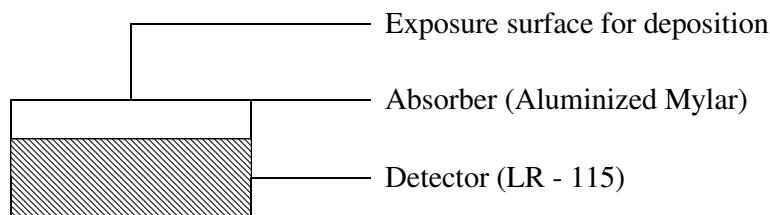


**Figure 2.4** Diagram of the detector element (Direct Progeny Sensor (DPS)).

The track densities registered on the LR-115 detectors after the complete decay of all the deposited atoms were determined using the standard track etching protocols followed by counting with a spark counter. The track density obtained using DTPS can be



used directly in calculating Equilibrium Equivalent Thoron Concentration (EETC). Since this is the highest alpha energy in the natural radioactivity decay series, there will be no interference from other alpha emissions. But, in case of Equilibrium Equivalent Radon Concentration (EERC), since we have a mixed radon and thoron progeny environment,  $\alpha$  energy of  $^{212}\text{Po}$  (thoron progeny) is higher as compared to that of  $^{214}\text{Po}$  (radon progeny). This can have some interference from the alpha particles from  $^{212}\text{Po}$  which needs to be subtracted using the thoron progeny sensor data. So, the track density obtained using DRPS should be used to eliminate the interference on the DRPS by  $^{212}\text{Po}$ . This is done by simple subtraction method. The Equilibrium Equivalent Concentrations of Radon (EERC) (Mishra *et al.*, 2009) and Thoron (EETC) (Mishra *et al.*, 2008) are calculated using the given formulae as follows

$$EERC(\text{Bq} / \text{m}^3) = \frac{T_{DRPS}}{\text{Calibration factor} \times \text{Exposure period (days)}} \quad (2.9)$$

$$EETC(\text{Bq} / \text{m}^3) = \frac{T_{DTPS}}{\text{Calibration factor} \times \text{Exposure period (days)}} \quad (2.10)$$

where  $T_{DRPS}$  and  $T_{DTPS}$  are the track densities obtained by counting tracks in the etched film of DRPS and DTPS respectively.

### 2.2.2 Equilibrium Factor (F) for radon and thoron

The equilibrium factor or the sensitivity factor for the radon ( $F_R$ ) and thoron ( $F_T$ ) are the quantity of ultimate interest in passive dosimetry applications. To convert absolute radon/thoron concentration to Equilibrium Equivalent Radon (EER) and Equilibrium Equivalent Thoron (EET) in an atmosphere, Equilibrium factor for particular area is determined by simultaneous measurement of radon/thoron concentration and radon/thoron daughter concentration (Srivastava, 2008). In the literature on inhalation dosimetry, it is conventional to express  $F_T$  as the track density expected for 1-day exposure to an environment containing  $1 \text{ Bq/m}^3$  of EETC (Mishra *et al.*, 2008; Vanchhawng, 2012).

Likewise,  $F_R$  represents the track density expected for 1-day exposure to an environment containing 1 Bq/m<sup>3</sup> of EERC after subtracting the track density expected from 1 Bq/m<sup>3</sup> of EETC. The equilibrium factor for radon ( $F_R$ ) and thoron ( $F_T$ ) are calculated using the formulae as follows (Mishra *et al.*, 2009)

$$F_R = \frac{EERC (Bq / m^3)}{C_R (Bq / m^3)} \quad (2.11)$$

and

$$F_T = \frac{EETC (Bq / m^3)}{C_T (Bq / m^3)} \quad (2.12)$$

where  $C_R$  and  $C_T$  are the concentrations of radon and thoron calculated using track density from Pin-hole and filter compartments and  $EERC$  and  $EETC$  are the Equilibrium Equivalent Concentration of radon and thoron.

### 2.2.3 Inhalation dose rate (D) of radon and thoron

Inhalation dose can be calculated using the obtained concentrations of the parent nuclei and the progenies. The dosimeters along with the DPS (DTPS and DRPS) were exposed simultaneously in different selected houses for a period of at least 90 days. The track densities registered on the LR-115 detectors after the complete decay of all the deposited atoms were determined using the standard track etching protocols followed by counting with a spark counter. The track densities were converted into radon, thoron and their progeny concentrations using appropriate calibration factors. Several models have been developed to assess the inhalation dose rates to the population due to radon, thoron and their progeny (Subba Ramu, *et al.*, 1988; Jacobi, 1993). Lung dose distribution assessment carried out by different agencies right from 1956 to 2000 given in details in UNSCEAR reports (UNSCEAR, 1993; 2000) shows a large variation in dose conversion factors. The estimated dose conversion factors varied drastically based on the breathing rate as well as the target tissue mass. In the present study, the dose conversion factors reported

by UNSCEAR (2000) have been used to estimate the indoor inhalation dose rates ( $D$ ,  $\mu\text{Sv/h}$ ) due to radon, thoron and their progeny as shown below:

$$D = 10^{-3} [(0.17 + 9 F_R) C_R + (0.11 + 40 F_T) C_T] \quad (2.13)$$

where numerical numbers given in Eq. 2.13 are the dose conversion factors for gas and progeny concentrations (UNSCEAR, 2000).  $F_R$  and  $F_T$  represent the equilibrium factor of radon and thoron progenies respectively.  $C_R$  and  $C_T$  represent the radon and thoron concentration respectively. Table 2.1 demonstrates the inhalation dose estimate from global averaged radon and thoron concentration.

**Table 2.1** Global averaged radon and thoron inhalation dose.

Average concentration levels of radon, thoron and their progeny in air and corresponding annual effective doses*							
Radionuclide	Location	Concentration ( $\text{Bq.m}^{-3}$ )		Effective dose equivalent ( $\text{nSv/Bq.h.m}^{-3}$ )		Annual effective dose ( $\mu\text{Sv}$ )*	
		Gas	EEC <sup>+</sup>	Gas	EEC	Gas	EEC
Radon	Outdoor	10	6	0.17	9	3	95
	Indoor	40	16	0.17	9	48	1009
<b>Total (numerical)</b>							<b>1155</b>
Thoron	Outdoor	10	0.1	0.11	40	2.0	7.0
	Indoor	10	0.3	0.11	40	8.0	84
<b>Total (numerical)</b>							<b>101</b>
<b>Total Annual Effective dose equivalent due to radon and thoron (<math>\mu\text{Sv}</math>)</b>							<b>1256</b>

<sup>+</sup> It is the equilibrium equivalent concentration (EEC) of radon and thoron and calculated multiplying gas concentration with equilibrium factor (F). The equilibrium factor (F) has been taken as 0.6 for outdoor and 0.4 for indoor in the case of radon. In the case of thoron F is taken as 0.01 for outdoor and 0.03 for indoor. \*The annual effective dose is calculated taking occupancy factor of 0.2 for outdoor and 0.8 for indoor (UNSCEAR, 2000).

### 2.3 Radon in Soil (Surface Radon Flux)

The radon exhalation flux at the soil surface depends on the transport properties of the medium and the concentration of its parent nucleus, radium-226 (Richon *et al.*, 2010). The transport of radon can be divided into two stage process. The first stage is emanation from the material and the second is exhalation from the matrix. In emanation process radon is transport from the solid mineral grains to the air-filled pores while in exhalation process it transport from air-filled pores to the atmosphere (Sahoo, 2008). The potential of radon emission over the soil surface is governed by the physical quantity called ‘radon flux’ and is used as a source term for the atmospheric radon dispersion modelling. The rate of radon exhalation is measured by using a recently developed ‘accumulator’ or the inverted cup technique (Mayya, 2004). The measurement of in-situ radon flux can be carried out using a set up consisting of an accumulator in line connected to continuous radon monitor (RAD7). An accumulator (cylindrical metallic shaped cup of diameter 15.5 cm and height 17.5 cm) is placed in an inverted position in the soil area of interest and accumulating the radon gas for a specified period of time. The gas concentration built in the cup is converted into the exhalation rates through appropriate formulae. In this method, flux entering the accumulator gradually reduces from its initial ‘free’ value to a much smaller ‘bound’ value due to a build up of gas concentration inside the cup (Mayya, 2004).

The time variation of the radon concentration inside the accumulator is monitored and related to the flux through growth kinetic equations (Sahoo, 2008).

$$C(t) = \frac{J_s A}{V \lambda_e} (1 - e^{-\lambda_e t}) + C_0 e^{-\lambda_e t} \quad (2.14)$$

where,  $C(t)$  is the Radon concentration in the accumulator at time  $t$  ( $\text{Bq m}^{-3}$ );  $J_s$  is the Radon flux from soil ( $\text{Bq m}^{-2}\text{s}^{-1}$ );  $V$  is the Volume of the accumulator ( $\text{m}^3$ );  $\lambda_e$  is the effective time constant ( $\text{h}^{-1}$ ) of  $^{222}\text{Rn}$  for the given set up and it is the sum of leakage rate, radon decay constant and back diffusion rate;  $A$  is the area of soil surface covered by accumulator ( $\text{m}^2$ ) and  $C_0$ , the radon concentration inside the accumulator at time  $t = 0$ . Radon flux can be

determined by fitting the exponential growth equation given in Eq. 2.14 to the concentration data inside accumulator obtained from the measurement set up. As the exact form of the equation is not available in the standard software for the fitting procedure, hence the available general growth equation is given by

$$Y(x) = Y_o + A_1 e^{-x/t_1} \quad (2.15)$$

where,  $Y_o$ ,  $A_1$  and  $t_1$  are the fitting parameters.

Comparing Eq. 2.14 and Eq. 2.15,

$$Y(x) = C(t), Y_o = \frac{J_s A}{V \lambda_g}, A_1 = \frac{-J_s A}{V \lambda_g} + C_o, x = t \text{ and } t_1 = \frac{1}{\lambda_g}$$

In order to avoid interference of initial radon concentration ( $C_o$ ) present in the accumulator ' $J_s$ ' should be obtained from the fitting parameter ' $Y_o$ ' i.e.

$$J_s = \frac{Y_o V}{t_1 A} = \frac{Y_o}{t_1} H \quad (2.16)$$

where  $Y_o$  and  $A$  are the calculated parameters from the software,  $V$  is the volume of the accumulator and  $A$  is the area covered by the accumulator. Hence  $V/A$  is the height of the accumulator ( $H$ ) (Sahoo, 2008).

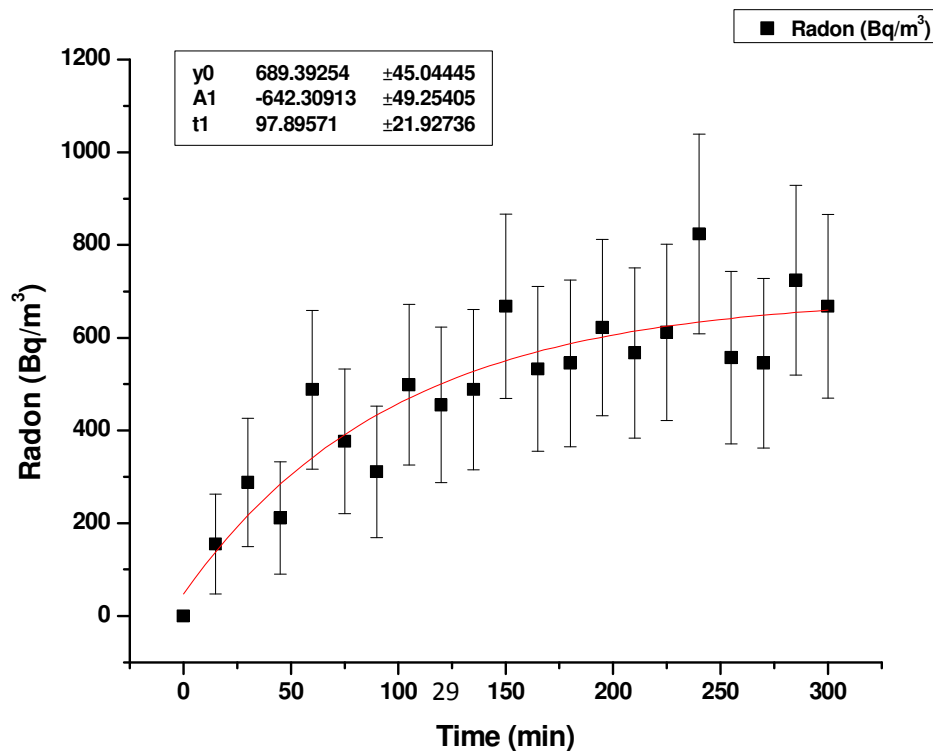


**Figure 2.5** Building up of radon concentrations with time inside the accumulator.

The radon concentration build up in the accumulator is monitored by RAD7 and it is used for fitting exponential growth curve using Origin Pro as shown in Figure 2.5 from which the parameters  $Y_0$ ,  $A_I$  and  $t_I$  are obtained and these values are put in Eq. 2.16 to calculate surface radon flux ( $J_s$ ) in  $\text{mBq/m}^2/\text{s}$ .

### 2.3.1 RAD7

The outdoor radon/thoron concentration was measured with an active device called RAD7. This device is used for short term as well as long term and continuous measurement of radon and thoron concentration from air as well as soil gas. The DURRIDGE RAD7 uses a solid state alpha detector that converts alpha radiation directly to an electrical signal. It has the ability to electronically determine the energy of each alpha particle which makes it possible to tell exactly which isotope (polonium-218, polonium-214, etc.) produced the radiation. The RAD7 is immune to the buildup of lead-210.

The RAD7's internal sample cell is a 0.7 liter hemisphere, coated on the inside with an electrical conductor. A solid-state, Ionimplanted, Planar, Silicon alpha detector is at the center of the hemisphere. The high voltage power circuit charges the inside conductor to a potential of 2000 to 2500 volts, relative to the detector, creating an electric field throughout the volume of the cell. The electric field propels positively charged particles onto the detector.

A radon-222 nucleus that decays within the cell leaves its transformed nucleus, polonium-218, as a positively charged ion. The electric field within the cell drives this

positively charged ion to the detector, to which it sticks. When the short-lived polonium-218 nucleus decays upon the detector's active surface, its alpha particle has a 50% probability of entering the detector and producing an electrical signal proportional in strength to the energy of the alpha particle. Subsequent decays of the same nucleus produce beta particles, which are not detected, or alpha particles of different energy. Different isotopes have different alpha energies, and produce different strength signals in the detector. The RAD7 amplifies, filters, and sorts the signals according to their strength. In Sniff mode, the RAD7 uses only the polonium-218 signal to determine radon concentration, and the polonium-216 signal to determine thoron concentration, ignoring the subsequent and longer-lived radon daughters.

This device produces the radon and/or thoron concentrations along with errors, temperature, relative humidity and time, automatically after each pre-set time intervals through its LCD Display. The readings can also be printed instantly with the infra-red connected printer included along with it.

#### **2.4 Background Gamma Radiation Survey**

The background gamma radiation are measured using a Micro-R survey meter at ground level and 1m height inside and outside the house during deployment and retrieving of the dosimeters (Vanchhawng *et al.*, 2009). This device manufactured by Nucleonix systems is a low level radiation (photon/gamma) measuring device or instrument and automatically displays the background gamma radiation values after each gate time of 8 seconds which is noted suitably as required. The gamma detector probe is a 1" x 1" NaI(Tl) Scintillator optically coupled to a 1" Photo Multiplier Tube (PMT). The variation of background gamma radiation helps in tracing the origin of these radiations viz., whether it is cosmic or terrestrial.

#### **2.5 Radioactivity content in soil and building materials**

The radium content of the soil and building materials is typically given as an activity concentration per unit mass. The most convenient and accurate method largely used for the determination of natural occurring radionuclides is by means of gamma spectrometry on individual samples previously dried, powdered and packed in small plastic containers with a given geometry (Nazaroff *et al.*, 1988a; Ibrahim, 1999; Bojanowski *et al.*, 2001). The amount of  $^{238}\text{U}$  present in the soil and building materials mainly determine the amount of  $^{226}\text{Ra}$  present in it. Since  $^{222}\text{Rn}$  is formed as result of decay of  $^{226}\text{Ra}$ , and hence knowing the amount of  $^{238}\text{U}$  present in the soil and/or building materials, the level of radon concentration can be predicted or assumed. A gamma spectrometry of the  $^{232}\text{Th}$  content considering the peaks of the intermediate gamma emitters,  $^{228}\text{Ra}$  and  $^{228}\text{Ac}$ , is a good indicator of the rate of  $^{220}\text{Rn}$  production within the reference soil or building material because the intermediate radioelements in the  $^{232}\text{Th}$  series to  $^{224}\text{Ra}$  have relatively short half-life in terms of geological time scales and are not altered to any extent by natural physical and/or chemical processes (Vanchhawng, 2012).

Gamma ray spectrometry method was employed to estimate the activity of  $^{226}\text{Ra}$ ,  $^{232}\text{Th}$  and  $^{40}\text{K}$  in the soil and building materials. Soil samples are collected from places near the house where dosimeters are hanged. These samples are then powdered to small particle sizes, weighed packed and sealed in 250 ml leak-proof plastic containers and stored for at least 30 days so as to attain secular equilibrium between radon and thoron with their parent nuclides before counting (Vanchhawng *et al.*, 2011; Shashikumar *et al.*, 2008). After attainment of secular equilibrium, each of the prepared samples measured using a high efficiency NaI (Tl) detector coupled with 1K Multichannel Analyzer (MCA) which is previously calibrated using standard radioactive sources. Each sample was counted for 30,000 seconds since the activity of the samples analysed is found to be low (Shukla *et al.*, 2005). Spectrum obtained in the 1K MCA is used to obtain the net peak area for each



nuclide. From this net peak area, the activity can be calculated using the following formula.

$$\text{Activity} = \frac{\text{Net Peak Area} / \text{Counting Time}}{\eta} \text{ (Bq/g)} \quad (2.17)$$

where  $\eta$  is efficiency obtained using standard source, counting time is in second.

## 2.6 Classification of parameters for measurements

As we know that radon and thoron exhaled from soil and building materials, their concentration varies widely depending on the meteorological and geographical conditions, emanation rate from the building material, pseudo-ventilation rate of the dwellings, etc. The contribution of building materials in large structures may be the dominating source for the indoor radon level. The importance of studies of radon emanation from building materials is given by the fact that this source is more readily controllable than the other radon sources. Radon generated at the level of material grain by alpha decay of radium may enter into the pore space (by recoil or diffusion in the solid phase) and then migrate through these pores to the surrounding air (Cosma *et al.*, 2001). In building materials the dominant radon transport mechanism is diffusion driven by concentration gradients (Stranden, 1988). So the physical parameters used for a quantitative description of radon exhaled from building materials are radium content, emanation fraction, diffusion coefficient or diffusion length and porosity (Cosma *et al.*, 2001). The radiation exposure from building materials creates prolonged exposure situation as individuals spend more than 80% of their time indoors (ICRP, 1999).

Taking into consideration the different factors influencing the concentration of radon, thoron and their progeny, the following selection of monitoring locations are done for the present work.

### 2.6.1 Geographical classification and seasonal variation of concentration of gases

Geographical comparison includes the comparison of results in the three districts viz., Lunglei, Serchhip and Mamit Districts. The pseudo-ventilation rate greatly influenced the indoor radon concentrations. The change in temperature during different seasons results in change in ventilation rate of dwellings. Hence, seasonal variation of indoor radon as well as thoron has been monitored. In this study, complete one year is divided into three seasons viz., rainy season (June - September), winter season (October – January) and summer season (February – May).

### **2.6.2 Geological Conditions**

The geological conditions of the place/area in the selected locations are carefully taken into considerations which are then sub-divided as follows:

#### ***a) Fault Region***

The regions where faults are observed are termed as fault region. These places are located using the available geological mapping of the state. Since the exhalation of radon and thoron are expected to increase in the area where fault is present. Hence, the study of concentration of these gases in these areas will be important.

#### ***b) Unrepresented areas***

These are places where no geological distinctiveness like fault or fossils regions are indicated and they may be treated as having normal soil also referred to as unrepresented area. These areas covered mostly the habitats/dwellings in Mizoram.

### **2.6.3 Selection of Types of Houses**

#### ***(a) Gamma level survey***

The houses in each district were selected on the basis of the spot survey based gamma radiation levels, geological characteristics of the area and the construction types of

the houses. A Micro-R Survey Meter was used for measurement of Gamma Background Radiation level which gives the dose rates in the unit of  $\mu\text{R/h}$ . Measurement of dose rate were done on ground level as well as at 1 m height from the ground both indoor and outdoor in the vicinity of the dwellings selected for deployment of dosimeters. During the retrieval of the dosimeters after about three to four months, survey meter readings of gamma background radiation were recorded again in the same manner.

***(b) Construction type of houses***

As the building material contributes the indoor radon, thoron and their progenies concentration, hence the material used for roof, wall and floor and elevation of the building from the ground are considered for selection of different types of houses. The different types of houses are selected as follows:

***i) Reinforced Cement Concrete (R.C.C.)***

The building material used for this type is reinforced cement concrete using iron rod. The wall is usually made up of bricks plastered with cement, while the roof and floors are all made up of concrete cement. However, the construction of this type of building may not be fully concrete at all. In such cases, the type of material will be indicated clearly whether the roof, wall or floor material is made of different materials.

***ii) Assam Type***

In this type of house, walls are mostly made up of asbestos (tile) while some are wooden and bamboo where in some cases G.I. sheets are also used as walls. The roofs are usually made up of G.I. Sheets and the floors are mostly concrete while some are wooden and some are bare.

## Chapter 3

# Experimental determination of indoor radon, thoron and their progeny concentrations in Lunglei, Serchhip and Mamit Districts

The experimental determination of indoor radon, thoron and their progeny concentrations, equilibrium factor and inhalation dose in Lunglei, Serchhip and Mamit Districts has been presented in this chapter. Instrumental calibrations and the measurement details are also included.

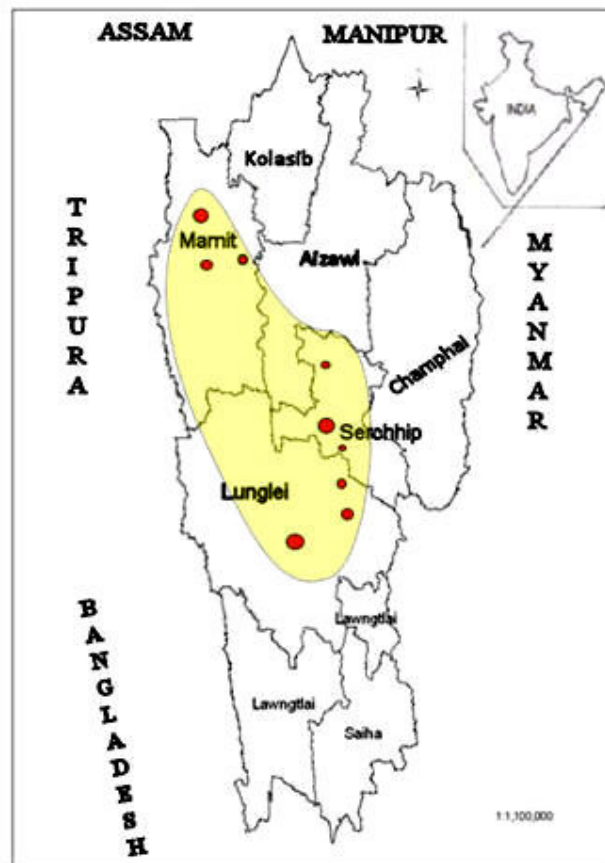


**Figure 3.1:** A map of Mizoram showing the sampling sites covering Lunglei, Serchhip and Mamit Districts.

This will be followed by the details of results obtained from the experiments carried out in the present study and the possible discussion on the results obtained will also be included. The results obtained will also be compared with the global and national average level whenever possible. Figure 3.1 shows the study area for measuring the indoor radon/thoron concentrations in Lunglei, Serchhip and Mamit districts in Mizoram.

### **3.1 Indoor radon and thoron measurements**

For indoor radon/thoron measurement, solid state nuclear track detector (SSNTD) based dosimeters developed by Bhabha Atomic Research Centre (BARC), Mumbai, were used for the survey. The dosimeter system is a cylindrical plastic chamber divided into two equal compartments. Cellulose nitrate film (LR-115, Type II) are used as detectors. The detectors are cut into a smaller pieces ( $3 \times 3 \text{ cm}^2$ ) placed inside the twin cup dosimeters. The dosimeters are hanged over on the ceiling of the selected houses at a height of minimum 1.5 m from floor and at least 10 cm away from any surface for a period of about 90 days. Bedroom ceiling is preferred as this is a room where one has maximum occupancy. After the exposure period is over the detector is retrieved and replaced with new ones for the next deployment. In this study each exposed dosimeters are replaced three times in a year to have seasonal variations in concentrations of these gases particularly during rainy, winter and summer seasons in the study area.

The exposed films are chemically etched using 2.5 N NaOH solution at constant temperature of 60°C for 90 minutes. The etched SSNTD films are then counted by using a spark counter. The track density obtained from the spark counter is then used to calculate the radon and thoron concentration using the formulae given in Eq. 2.7 and Eq. 2.8. The

standard calibration factor for radon in pinhole compartment is  $0.023 \text{ Tr.cm}^{-2}/\text{Bq.d.m}^{-3}$  and for thoron in filter compartment is  $0.016 \text{ Tr.cm}^{-2}/\text{Bq.d.m}^{-3}$ .

### 3.1.1 Calibration of dosimeter

The actual calibration of twin cup dosimeter was also performed at the Environmental Assessment Division (EAD), BARC, Mumbai. The calibration chamber used is a cubical stainless steel chamber having a capacity of  $1\text{m}^3$ . Inside it there are small fan (for achieving spatial uniformity in the concentration of the gases and aerosols dosimeter), mounting bar, inlets, outlets and a tube light. Radon and Thoron source can be kept inside the chamber while their activity concentrations can be measured continuously using RAD7 as shown in Figure 3.2 below. In this experiment, radium is used as radon source and thorium nitrate is used as thoron source.

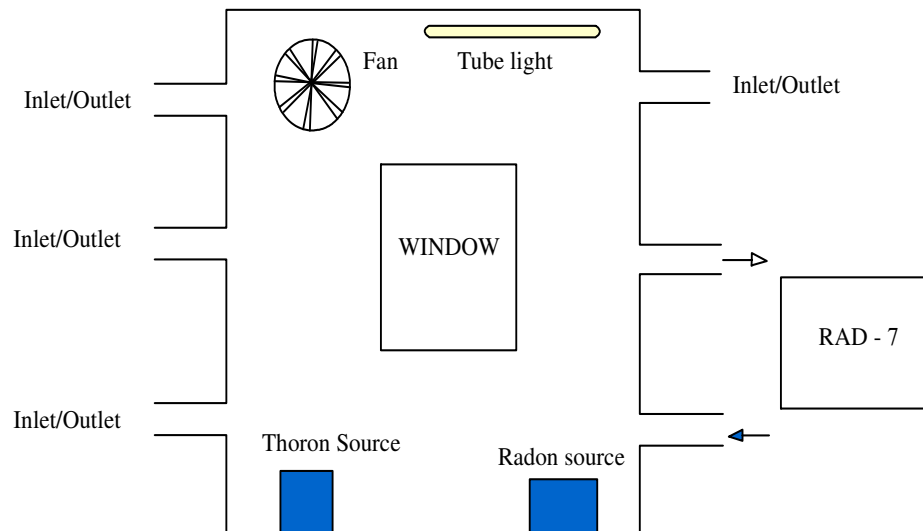


**Figure 3.2** Block diagram of the calibration chamber for calibrating twin cup dosimeter.

Twin cup dosimeters containing SSNTD films were placed on a mounting bar which was fixed inside the calibration chamber. The calibration of twin cup dosimeter using radon source was done for a period of 0.66 days (i.e. 15hrs 45min). After the period

was over, dosimeters are taken out and the films are chemically etched. The tracks formed in the etched films are counted with a spark counter. From the experimentally obtained data, the calibration factor for radon was found to be  $\sim 0.016$  which is near to standard value, 0.023 (Eappen *et al.*, (2004) which is shown in Appendix – I (a). But in case of thoron, the obtained average value of calibration factor using thoron source for a period of 23hrs was unacceptably small (i.e. 0.009) as compared to the standard value, 0.016 (Eappen *et al.*, 2004; Eappen, 2005; Eappen *et al.*, 2008) which is shown in Appendix – I (b). This is because during the experiment, there was a radon source building up inside the calibration chamber after the source has removed and radon gas was also pumped out from the chamber.

For the present study, twin cup dosimeters used for the measurement of radon and thoron concentrations are supplied from BARC, Mumbai which were well pre-calibrated. As per the advice from BARC, the standard calibration factor was used instead of the experimental result obtained which involved some error in the experimental procedure.

### 3.1.2 Experimental Standardization of etching rate

The term etching means the process of removal of a layer of a substance. Etching of the film is necessary because the tracks produced on the films due to radon, thoron and their progeny are visible for counting only after etching. Etched films are then counted by spark counter. Bulk etching rate is the rate of etching of the film (LR-115) per unit time. The standardization of etching rate of the LR-115 film has been performed by the author in BARC, Mumbai. The experimental details are shown in Appendix – II. By using Eq. 2.3, the bulk etching rate is calculated. The average bulk etching rate calculated from the experiments is  $4.122\mu\text{m/h}$  without stirring which is in good agreement with experimentally obtained standard value ( $4\mu\text{m/h}$ ) (Eappen, 2005). The standard parameter set for the above experiment is 90 mins etching at constant  $60^\circ\text{C}$  without magnetic or any other stirring device.

The etched SSNTD films are counted by using a spark counter. The applied voltage to the spark counter determines the electric field between the plates which influence the number of spark counts from the etched film. The operating voltage of a spark counter is firstly determined using the following method:

### 3.1.3 Determination of Operating voltage of a Spark counter

The SSNTD film is pre-sparked using a spark counter at a voltage of 900 V to fully develop the partially etched track holes. After pre-sparking the film, the voltage is set at 100V, the tracks are counted and counting is repeated by increasing the applied voltage. When graph is plot between applied voltages and counts, the corresponding middle voltage of the plateau region is taken as the operating voltage for the spark counter. This plateau region shows that even with a small change in the applied voltage the number of tracks count by the counter remains constant. The detail experimental work for operating voltage of spark counter is shown in Appendix – III.

From the experimental results, the average value for the operating voltage of the spark counter was found to be ~ 450V. The graph plotted between applied voltage and counts is shown in Figure 3.3 below.

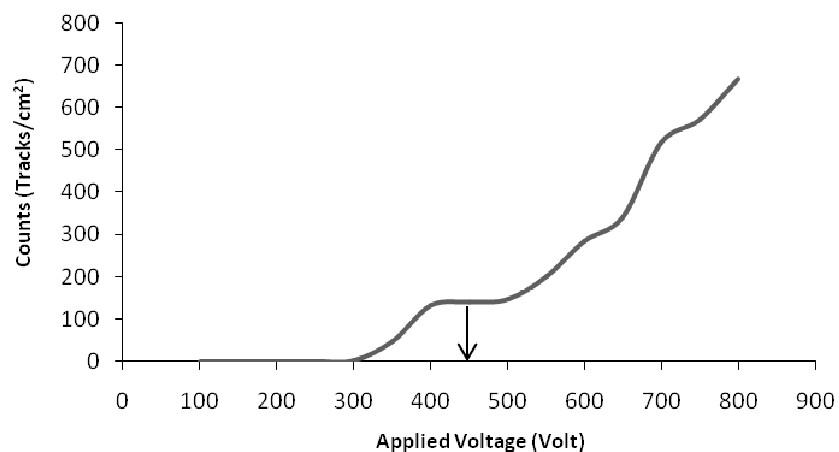


**Figure 3.3** Operating voltage of the spark counter used in the present study.



The same exposed film was sent to BARC, Mumbai for inter-comparison of data using the same type of spark counter. It was found that the operating voltage of spark counter was found to be 500V. Hence, as per the advice from BARC, the operating voltage of spark counter used is 500V.

#### 3.1.4 Results and discussions

The measurements of indoor radon and thoron concentrations were carried out successfully in 111 dwellings of Lunglei, Serchhip and Mamit Districts in Mizoram during the period from June 2009 to May 2010. During this period, three types of seasons were observed, which may be written as rainy season (June-Sept. 2009), winter season (Oct.2009 – Jan.2010) and summer season (Feb. – May.2010).

The experimentally determined value of annual average concentration of radon in the whole study area ranges from 28.053 Bq/m<sup>3</sup> to 88.493 Bq/m<sup>3</sup> with a geometric mean (GM) of 48.287 Bq/m<sup>3</sup> and geo-standard deviation (GSD) of 1.253 and that of thoron ranges from 5.990 Bq/m<sup>3</sup> to 69.304 Bq/m<sup>3</sup> with geometric mean of 19.770 Bq/m<sup>3</sup> and GSD 1.695. The study area has higher average indoor concentrations of radon and thoron as compared to average global level of 40 Bq/m<sup>3</sup> and 10 Bq/m<sup>3</sup> as well as national level of 42 Bq/m<sup>3</sup> and 12.2 Bq/m<sup>3</sup> respectively (Mishra *et al.*, 2009; UNSCEAR, 2000). The concentrations of the gases obtained in this work show no significant radiological risks and lies in the range covered by nationwide survey result (Ramu *et al.*, 1992) as well as the ICRP regulations (ICRP, 1993).

In Lunglei District, Lunglei (District Headquarters), Hnahthial and Thiltlang were selected for deployment of dosimeters and the altitudes of these study area are measured using Geo-Positioning System (GPS) and it shows that the altitude of Lunglei District ranges from 775m to 954m. A total of 44 dosimeters were first deployed, however, at the end of the last season i.e., summer in 2010, only 39 dosimeters could be retrieved and the

average values of the gases could be obtained from these 39 dosimeters. Table 3.1 shows the detail values of concentrations of radon and thoron in Lunglei District.

**Table 3.1** Concentrations of radon and thoron in Lunglei District.

Dwelling Nos.	Rainy		Winter		Summer		Annual Average	
	Radon (Bq/m <sup>3</sup> )	Thoron (Bq/m <sup>3</sup> )	Radon (Bq/m <sup>3</sup> )	Thoron (Bq/m <sup>3</sup> )	Radon (Bq/m <sup>3</sup> )	Thoron (Bq/m <sup>3</sup> )	Radon (Bq/m <sup>3</sup> )	Thoron (Bq/m <sup>3</sup> )
1	39.38	2.72	48.35	9.28	49.90	9.24	45.88	7.08
2	40.01	17.21	133.17	41.01	78.89	6.87	84.03	21.70
3	31.98	30.12	69.37	25.47	58.57	13.10	53.30	22.90
4	58.44	94.20	107.20	27.19	63.65	35.01	76.43	52.14
5	31.35	83.79	102.40	17.27	74.85	9.45	69.53	36.83
6	62.54	29.21	68.61	17.91	62.15	7.95	64.44	18.36
7	44.74	59.10	68.91	6.26	52.59	6.23	55.42	23.86
8	50.96	7.39	55.20	63.26	57.53	30.19	54.56	33.61
9	25.83	12.00	79.27	29.78	59.89	14.03	55.00	18.61
10	33.82	10.30	44.01	14.35	49.54	9.14	42.46	11.26
11	22.84	7.02	79.72	12.95	75.42	6.16	59.33	8.71
12	57.19	14.56	41.74	34.13	35.41	9.66	44.78	19.45
13	16.67	28.90	65.63	27.61	38.40	36.30	40.24	30.93
14	16.05	22.18	37.05	13.91	50.65	14.60	34.58	16.90
15	36.31	56.23	41.29	45.43	27.79	6.23	35.13	35.96
16	32.57	33.15	43.40	17.39	37.20	14.18	37.73	21.57
17	37.71	17.47	34.68	4.53	40.08	12.97	37.49	11.66
18	26.34	26.21	77.32	12.52	46.14	20.62	49.93	19.78
19	31.17	17.25	62.16	6.69	48.06	39.97	47.13	21.30
20	31.48	7.17	74.47	14.46	33.87	14.46	46.60	12.03
21	24.69	72.12	45.94	55.25	56.93	66.58	42.52	64.65
22	40.29	47.62	62.61	10.79	60.66	15.46	54.52	24.62
23	20.07	38.23	64.11	7.99	52.14	18.04	45.44	21.42
24	25.00	79.21	56.75	26.33	93.38	10.09	58.38	38.55
25	25.20	9.06	52.10	14.24	79.64	27.92	52.31	17.07
26	47.06	12.99	47.33	25.87	49.16	42.53	47.85	27.13
27	21.97	26.88	44.61	1.96	57.37	8.59	41.32	12.48
28	19.79	23.30	47.18	13.91	49.45	12.67	38.81	16.63
29	42.85	5.82	53.08	24.13	49.60	15.68	48.51	15.21
30	43.64	9.06	39.79	9.50	86.05	21.48	56.49	13.35
31	43.48	73.14	30.78	7.55	69.75	23.65	48.00	34.78
32	35.60	6.79	27.18	8.20	68.24	6.73	43.67	7.24

<b>33</b>	40.64	15.63	81.38	22.23	60.69	9.55	60.90	15.80
<b>34</b>	20.79	14.49	42.34	12.73	42.57	4.99	35.24	10.74
<b>35</b>	21.90	21.29	51.80	27.63	41.67	27.56	38.45	25.49
<b>36</b>	35.92	24.00	52.10	35.40	50.27	4.99	46.10	21.46
<b>37</b>	34.88	6.18	32.13	11.44	53.44	4.99	40.15	7.54
<b>38</b>	33.92	33.20	48.95	16.40	42.57	27.78	41.81	25.79
<b>39</b>	53.51	20.60	79.87	44.68	34.42	18.45	55.94	27.91

The altitude of the study areas in Serchhip District ranges from 689m to 1032m and the sites for deployment of dosimeters are Serchhip (District Headquarters), Chhingchhip and Keitum. In this district, initially 40 dosimeters were deployed out of which the average annual values of track reading could be counted from 36 dosimeters. Table 3.2 shows the detail values of concentrations of radon and thoron in Serchhip District.

**Table 3.2** Concentrations of radon and thoron in Serchhip District.

Dwelling Nos.	Rainy		Winter		Summer		Annual Average	
	Radon (Bq/m <sup>3</sup> )	Thoron (Bq/m <sup>3</sup> )	Radon (Bq/m <sup>3</sup> )	Thoron (Bq/m <sup>3</sup> )	Radon (Bq/m <sup>3</sup> )	Thoron (Bq/m <sup>3</sup> )	Radon (Bq/m <sup>3</sup> )	Thoron (Bq/m <sup>3</sup> )
<b>1</b>	19.38	78.58	43.86	56.52	38.80	8.90	34.01	48.00
<b>2</b>	34.66	14.49	46.12	13.91	54.95	8.68	45.24	12.36
<b>3</b>	38.75	4.76	49.00	5.65	57.52	32.77	48.42	14.39
<b>4</b>	45.37	3.85	49.15	9.57	27.23	18.73	40.58	10.71
<b>5</b>	29.93	4.30	63.97	10.87	32.94	9.05	42.28	8.07
<b>6</b>	35.76	4.98	51.27	15.00	41.67	4.99	42.90	8.32
<b>7</b>	21.90	3.85	36.29	9.13	25.97	4.99	28.05	5.99
<b>8</b>	18.43	13.36	36.90	17.83	41.52	33.85	32.28	21.68
<b>9</b>	31.82	6.79	56.71	3.70	48.46	37.33	45.66	15.94
<b>10</b>	20.54	12.13	39.64	6.69	25.66	25.61	28.62	14.81
<b>11</b>	46.82	59.98	45.79	29.14	32.00	9.77	41.54	32.96
<b>12</b>	40.29	38.69	104.05	21.15	43.18	6.08	62.51	21.97
<b>13</b>	46.34	27.47	84.38	121.29	49.52	11.28	60.08	53.35
<b>14</b>	73.58	21.29	92.34	42.09	39.55	13.02	68.49	25.47
<b>15</b>	27.71	14.42	71.47	10.14	41.36	14.32	46.85	12.96
<b>16</b>	18.95	17.63	99.84	14.24	38.65	14.54	52.48	15.47
<b>17</b>	24.84	12.59	83.63	17.91	42.27	27.56	50.25	19.36
<b>18</b>	37.27	12.82	27.48	11.44	51.48	30.60	38.74	18.29
<b>19</b>	44.43	90.66	104.50	8.42	68.54	54.04	72.49	51.04
<b>20</b>	16.72	19.69	36.78	8.63	58.88	11.07	37.46	13.13
<b>21</b>	24.69	23.81	27.33	15.76	50.42	13.02	34.14	17.53
<b>22</b>	21.98	5.72	57.35	26.12	37.74	13.02	39.02	14.95
<b>23</b>	15.45	8.24	26.12	9.71	52.84	19.31	31.47	12.42
<b>24</b>	19.91	5.49	58.55	4.32	46.35	9.11	41.60	6.31
<b>25</b>	25.48	27.01	43.84	13.17	26.12	6.08	31.81	15.42
<b>26</b>	54.15	11.45	45.79	7.77	34.42	16.28	44.79	11.83
<b>27</b>	33.76	18.09	55.70	30.86	38.65	6.94	42.70	18.63

28	36.31	49.45	58.55	39.93	47.55	18.66	47.47	36.01
29	41.41	11.22	48.20	14.68	34.57	3.26	41.39	9.72
30	23.89	7.78	37.39	17.48	42.41	38.60	34.56	21.29
31	16.24	10.30	73.72	15.76	41.80	8.55	43.92	11.54
32	24.05	7.10	45.49	80.72	55.99	10.53	41.84	32.78
33	20.70	10.53	97.74	16.19	41.50	21.05	53.31	15.92
34	28.03	11.22	79.42	8.85	37.38	12.28	48.28	10.78
35	39.02	8.47	118.61	71.44	59.19	14.47	72.27	31.46
36	27.23	11.45	103.75	26.98	41.95	15.79	57.64	18.07

In Mamit district, the altitudes of the study area ranges from 808m to 868m and the sites for deployment of dosimeters are Mamit (District Headquarters), Rawpuichhip and Lengpui. In this area, out of 41 dosimeters deployed 36 could be used for taking the average values for radon and thoron. Table 3.3 shows the detail values of concentrations of radon and thoron in Mamit District.

**Table 3.3** Concentrations of radon and thoron in Mamit District.

Dwelling Nos.	Rainy		Winter		Summer		Annual Average	
	Radon (Bq/m <sup>3</sup> )	Thoron (Bq/m <sup>3</sup> )	Radon (Bq/m <sup>3</sup> )	Thoron (Bq/m <sup>3</sup> )	Radon (Bq/m <sup>3</sup> )	Thoron (Bq/m <sup>3</sup> )	Radon (Bq/m <sup>3</sup> )	Thoron (Bq/m <sup>3</sup> )
1	53.03	15.57	44.89	13.17	29.58	24.66	42.50	17.80
2	49.37	27.47	96.39	51.15	36.23	86.73	60.66	55.12
3	43.48	50.14	83.33	49.21	64.48	38.05	63.76	45.80
4	28.19	8.24	82.43	12.09	33.57	14.46	48.06	11.59
5	42.60	38.72	52.40	39.71	30.32	18.92	41.77	32.45
6	40.61	5.49	103.75	14.68	41.11	14.88	61.82	11.68
7	45.71	8.47	96.84	15.76	37.41	32.95	59.99	19.06
8	72.62	27.24	148.64	9.71	44.22	10.20	88.49	15.72
9	63.29	32.87	35.37	27.25	52.20	11.48	50.29	23.87
10	59.74	83.10	73.60	9.62	33.72	6.38	55.69	33.03
11	36.23	37.96	43.81	8.02	38.75	22.11	39.60	22.70
12	40.26	8.10	70.57	10.76	57.53	11.90	56.12	10.26
13	60.39	20.14	65.16	9.39	33.72	25.51	53.09	18.35
14	77.62	125.23	39.35	64.35	47.91	4.46	54.96	64.68
15	84.54	131.48	51.14	46.03	30.76	30.40	55.48	69.30
16	35.91	50.46	55.44	13.05	34.01	49.11	41.79	37.54
17	32.37	17.36	81.25	34.58	55.01	18.28	56.21	23.41
18	30.92	9.03	57.19	24.05	51.91	32.53	46.67	21.87
19	42.35	32.18	77.58	31.37	45.10	8.93	55.01	24.16
20	88.08	22.45	60.06	22.67	48.36	23.38	65.50	22.84
21	68.76	135.42	41.26	16.72	33.72	9.14	47.91	53.76
22	44.61	17.59	37.28	9.85	55.01	45.92	45.63	24.45
23	65.86	32.87	46.52	11.22	32.98	10.20	48.45	18.10
24	62.00	77.55	35.37	46.49	34.31	17.64	43.89	47.23
25	100.00	47.22	47.63	17.18	42.59	7.65	63.41	24.02
26	56.68	58.33	73.76	5.04	49.84	11.48	60.09	24.95
27	60.87	8.10	86.51	8.93	36.53	21.05	61.30	12.69
28	102.58	8.56	55.92	21.30	53.53	8.29	70.68	12.72

<b>29</b>	64.41	13.43	69.78	20.84	33.13	15.52	55.77	16.59
<b>30</b>	100.97	9.72	47.95	29.54	36.82	11.05	61.91	16.77
<b>31</b>	82.77	29.63	53.37	15.34	50.43	9.57	62.19	18.18
<b>32</b>	47.50	20.60	51.78	17.63	42.59	18.49	47.29	18.91
<b>33</b>	50.72	51.16	51.30	10.31	53.53	12.33	51.85	24.60
<b>34</b>	56.84	27.55	65.48	24.96	32.24	9.14	51.52	20.55
<b>35</b>	25.44	17.59	61.33	8.70	24.99	15.09	37.26	13.80
<b>36</b>	38.16	34.03	42.69	16.95	30.32	16.37	37.06	22.45

### Geographical (District-wise) comparison

Table 3.4 and Table 3.5 shows the annual average concentrations of radon and thoron in Lunglei, Serchhip and Mamit Districts. Minimum value (Min), maximum value (Max) and geometric mean (GM) are shown along with geometric standard deviation (GSD).

**Table 3.4** Annual average concentration of radon in Lunglei, Serchhip and Mamit Districts.

<b>Radon (Bq/m<sup>3</sup>)</b>			
	<b>Lunglei District</b>	<b>Serchhip District</b>	<b>Mamit District</b>
<b>Min</b>	34.584	28.053	37.059
<b>Max</b>	84.025	72.490	88.493
<b>GM</b>	<b>48.389</b>	<b>43.840</b>	<b>53.065</b>
<b>GSD</b>	1.264	1.271	1.204

**Table 3.5** Annual average concentration of thoron in Lunglei, Serchhip and Mamit Districts.

<b>Thoron (Bq/m<sup>3</sup>)</b>			
	<b>Lunglei District</b>	<b>Serchhip District</b>	<b>Mamit District</b>
<b>Min</b>	7.078	5.990	10.257
<b>Max</b>	64.649	53.351	69.304
<b>GM</b>	<b>19.648</b>	<b>16.927</b>	<b>23.245</b>
<b>GSD</b>	1.659	1.710	1.625

Mamit district has the highest average concentration of radon and thoron while Serchhip district has the lowest concentration of radon and thoron. Mamit district is located in the mid-western part of Mizoram. Geologically, the soil especially inside Mamit town is not steady. During the month of August in 2010 there was a huge landslide in Mamit town

and several houses were destroyed and evacuated. As a result of this landslide, cracks were formed on the floors and walls of the dwellings near the landslide area. The radon concentration was also measured after the landslide took place but did not show much variation before the landslide took place. However, the annual average radon or thoron concentration is still much below the WHO (2009) or ICRP (1993) action limit. The average annual concentration in other districts also showed that they are within the acceptable limit.

### **Seasonal variation**

In Lunglei District, the concentrations of radon vary from 16.051 Bq/m<sup>3</sup> to 62.539 Bq/m<sup>3</sup> with a geometric mean of 32.884 Bq/m<sup>3</sup> (GSD 1.41) during rainy season. During winter season, it ranges from 27.175 Bq/m<sup>3</sup> to 133.175 Bq/m<sup>3</sup> with a geometric mean of 55.262 Bq/m<sup>3</sup> (GSD 1.42). Likewise, during summer season, the radon concentration varies from 27.790 Bq/m<sup>3</sup> to 93.381 Bq/m<sup>3</sup> with a geometric mean of 52.861 Bq/m<sup>3</sup> (GSD 1.31). Comparing the geometric mean concentrations of each season, radon level is highest in winter season and minimum in rainy season. The annual average concentration of radon in Lunglei District ranges from 34.584 Bq/m<sup>3</sup> to 84.025 Bq/m<sup>3</sup> with a geometric mean (GM) of 48.389 Bq/m<sup>3</sup> and geo-standard deviation (GSD) of 1.232.

In case of thoron, the concentration varied from 2.717 Bq/m<sup>3</sup> to 94.203 Bq/m<sup>3</sup> with a geometric mean of 20.401 Bq/m<sup>3</sup> (GSD 2.33) in rainy season and the level ranges from 1.957 Bq/m<sup>3</sup> to 63.261 Bq/m<sup>3</sup> with a geometric mean of 16.639 Bq/m<sup>3</sup> (GSD 2.05) during winter. In summer season, the concentration varies from 4.991 Bq/m<sup>3</sup> to 66.581 Bq/m<sup>3</sup> with a geometric mean of 13.996 Bq/m<sup>3</sup> (GSD 1.935). Comparing the geometric mean concentrations of each season, thoron level is highest in rainy season and minimum in summer season. The annual average concentration of thoron ranges from 7.078 Bq/m<sup>3</sup> to 64.649 Bq/m<sup>3</sup> with geometric mean of 19.648 Bq/m<sup>3</sup> and GSD 1.671.

In Serchhip District, during rainy season, radon concentrations vary from 15.448 Bq/m<sup>3</sup> to 73.579 Bq/m<sup>3</sup> with geometric mean of 29.131 Bq/m<sup>3</sup> (GSD 1.45) whereas in winter season, it was found to be varying from 26.124 Bq/m<sup>3</sup> to 118.61 Bq/m<sup>3</sup> with geometric mean of 56.265 Bq/m<sup>3</sup> (GSD 1.50). It ranges from 25.664 Bq/m<sup>3</sup> to 68.539 Bq/m<sup>3</sup> with geometric mean of 41.836 Bq/m<sup>3</sup> (GSD 1.27) in summer. Comparing the geometric mean concentrations, radon level is maximum in winter and minimum in rainy season. The annual average concentration of radon in Serchhip District ranges from 28.053 Bq/m<sup>3</sup> to 72.490 Bq/m<sup>3</sup> with a geometric mean (GM) of 43.840 Bq/m<sup>3</sup> and geo-standard deviation (GSD) of 1.271

The concentration of thoron in Serchhip district vary from 3.850 Bq/m<sup>3</sup> to 90.659 Bq/m<sup>3</sup> with geometric mean of 13.226 Bq/m<sup>3</sup> (GSD 2.25) during rainy season whereas in winter season, it ranges from 3.696 Bq/m<sup>3</sup> to 121.295 Bq/m<sup>3</sup> with geometric mean of 16.226 Bq/m<sup>3</sup> (GSD 2.20). In summer season, thoron level is ranging from 3.255 Bq/m<sup>3</sup> to 54.036 Bq/m<sup>3</sup> with geometric mean of 13.688 Bq/m<sup>3</sup> (GSD 1.897). Comparing the geometric mean concentrations, thoron level is maximum in winter and minimum in rainy season. The annual average concentration of thoron ranges from 5.990 Bq/m<sup>3</sup> to 53.351 Bq/m<sup>3</sup> with geometric mean of 16.927 Bq/m<sup>3</sup> and GSD 1.710

In Mamit District, during rainy season, radon concentrations vary from 25.443 Bq/m<sup>3</sup> to 102.576 Bq/m<sup>3</sup> with geometric mean of 53.545 Bq/m<sup>3</sup> (GSD 1.433) whereas in winter season, the level was found to be varying from 35.367 Bq/m<sup>3</sup> to 148.639 Bq/m<sup>3</sup> with geometric mean of 59.998 Bq/m<sup>3</sup> (GSD 1.391). In summer, it ranges from 24.993 Bq/m<sup>3</sup> to 64.478 Bq/m<sup>3</sup> with geometric mean of 40.248 Bq/m<sup>3</sup> (GSD 1.260). Comparing the geometric mean concentrations, radon level is maximum in winter and minimum in summer season. The annual average concentration of radon in Mamit District ranges from 37.059 Bq/m<sup>3</sup> to 88.493 Bq/m<sup>3</sup> with a geometric mean (GM) of 53.065 Bq/m<sup>3</sup> and geo-standard deviation (GSD) of 1.204.

The concentrations of thoron in Mamit district vary from 5.495 Bq/m<sup>3</sup> to 135.417 Bq/m<sup>3</sup> with geometric mean of 26.156 Bq/m<sup>3</sup> (GSD 2.324). Whereas in winter season, the level of thoron is from 5.038 Bq/m<sup>3</sup> to 64.351 Bq/m<sup>3</sup> with geometric mean of 18.000 Bq/m<sup>3</sup> (GSD 1.853) and it ranges from 4.464 Bq/m<sup>3</sup> to 86.735 Bq/m<sup>3</sup> with geometric mean of 16.309 Bq/m<sup>3</sup> (GSD 1.858) in summer. Comparing the geometric mean concentrations, thoron level is maximum in rainy and minimum in summer season. The annual average concentration of thoron ranges from 10.257 Bq/m<sup>3</sup> to 69.304 Bq/m<sup>3</sup> with geometric mean of 23.245 Bq/m<sup>3</sup> and GSD 1.625.

The seasonal variations of indoor radon and thoron concentration which is obtained by combining all the three districts for a complete one year are obtained. During rainy season, radon concentrations vary from 15.448 Bq/m<sup>3</sup> to 102.576 Bq/m<sup>3</sup> with geometric mean of 37.033 Bq/m<sup>3</sup> (GSD 1.557). Whereas in winter season, radon level was found to be varying from 26.124 Bq/m<sup>3</sup> to 148.639 Bq/m<sup>3</sup> with geometric mean of 57.087 Bq/m<sup>3</sup> (GSD 1.440) and in summer season, the radon level is ranging from 24.993 Bq/m<sup>3</sup> to 93.381 Bq/m<sup>3</sup> with geometric mean of 44.853 Bq/m<sup>3</sup> (GSD 1.320). With the comparison of the geometric mean, radon concentration is maximum in winter and minimum in rainy season.

In case of thoron, during rainy season, it vary from 2.717 Bq/m<sup>3</sup> to 135.417 Bq/m<sup>3</sup> with geometric mean of 19.214 Bq/m<sup>3</sup> (GSD 2.407) and that it ranges from 1.957 Bq/m<sup>3</sup> to 121.295 Bq/m<sup>3</sup> with geometric mean of 16.930 Bq/m<sup>3</sup> (GSD 2.04) in winter. In summer, thoron level is ranging from 3.255 Bq/m<sup>3</sup> to 86.735 Bq/m<sup>3</sup> with geometric mean of 14.602 Bq/m<sup>3</sup> (GSD 1.906). With the comparison of the geometric mean, thoron concentration is maximum in rainy and minimum in summer.

The annual average value of radon gases combined for the three districts ranges from 28.05 Bq/m<sup>3</sup> to 88.49 Bq/m<sup>3</sup> with a geometric mean of 48.29 Bq/m<sup>3</sup> (GSD 1.25) and



the annual average value of thoron gases varies from 5.99 Bq/m<sup>3</sup> to 69.30 Bq/m<sup>3</sup> with a geometric mean of 19.77 Bq/m<sup>3</sup> (GSD 1.7).

Figure 3.4 shows the variation of indoor radon levels during rainy season, winter season and summer season along with annual average in Lunglei, Serchhip and Mamit districts as well as the combined study areas. In the entire three districts, indoor radon level is highest during winter and lowest during rainy season except in Mamit district where the indoor radon level is lowest in summer season. This is due to the fact that during winter, temperature in the study area becomes minimum among the three seasons, which results in less ventilation rate (Vaupotic *et al.*, 1999) and air exchange rate of indoor with the outdoor environment was low as windows and doors were closed for more duration. It becomes easy for radon to accumulate that results in high concentration of the gas in indoor. Consequently, overall concentrations of radon reach its maximum in winter as compared to other seasons (Vanchhawng *et al.*, 2011).

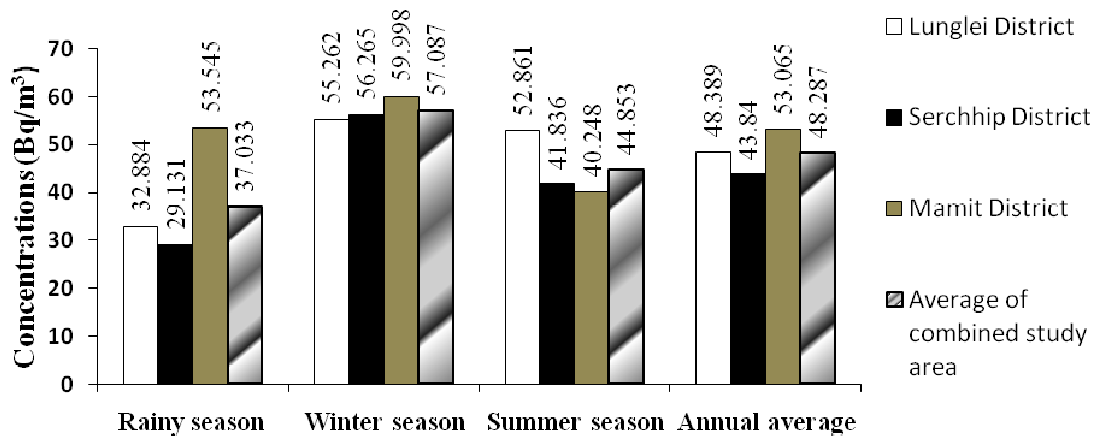


**Figure 3.4** Indoor radon concentrations in each district along with the combined study area for different seasons including the annual average value.

In summer, because of high temperature, ventilation rate was high as doors and windows were opened regularly and also ceiling fan, table fan, etc. were used as comfort for the occupant. As a result, the concentrations of the gas were found to be low during this particular season (Wilkening, 1986). The decrease of the concentrations of radon in rainy

season is due to the fact that the soil is saturated with water and the rain washout during this period.

Figure 3.5 shows the variation of indoor thoron levels during rainy season, winter season and summer season along with annual average in Lunglei, Serchhip and Mamit districts as well as the combined study areas. The seasonal variation is different as compared to that of indoor radon levels. This is due to the fact that ventilation rate does not affect indoor thoron levels because of its short diffusion length and to its short half life.

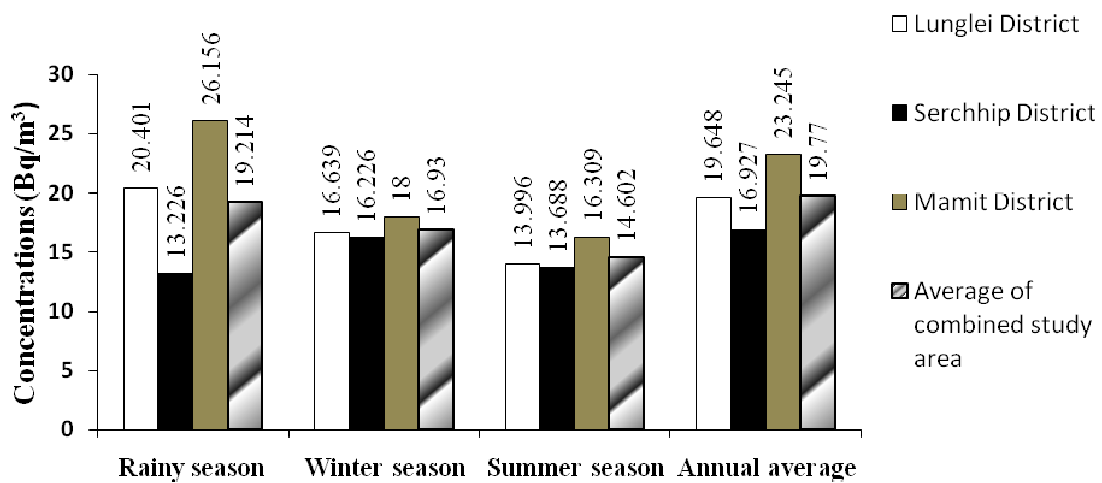


**Figure 3.5** Indoor thoron concentrations in each district along with the combined study area for different seasons including the annual average value.

The indoor thoron level is highest in rainy season in Lunglei and Mamit districts while in Serchhip district, the highest thoron level is found in winter season. The lowest indoor thoron level is found in summer season in Lunglei and Mamit districts as well as in the whole study area while in Serchhip district, the lowest thoron level is found in rainy season. Due to higher concentration observed during rainy season in Lunglei District, the overall concentrations become highest during rainy season even though maximum concentration is expected during winter. The climate of the State of Mizoram is moderate throughout the year. The temperature varies between 20°C – 30°C during summer and 11°C – 21°C during winter. It is also difficult to draw a clear cut division of a complete one year

into different seasons. This explains why thoron reaches its maximum during rainy season (Vanchhawng *et al.*, 2011). Though it is maximum in rainy season, the concentration of thoron is low. This behavior may be due to the low emanation rate of  $^{220}\text{Rn}$  during the rainy season. It cannot escape easily from the soil capillaries that are mostly occupied by water during the rainy season (Sathish *et al.*, 2001).

It is clear from the results that the concentrations of radon and thoron in this study area are low. This is due to overall low concentration of radon and thoron in the environment (David *et al.*, 2008; Khan *et al.*, 1993; Kumar *et al.*, 1994; Gupta *et al.*, 2012; Ramu *et al.*, 1992; EPA, 1993). Since the radon level in the environment is low, the rate of indoor accumulation is low even in winter season. We have found that radon has higher concentrations as compared to thoron. There have been many factors affecting radon, thoron and their progeny concentrations in the environment. The ventilation rate and air exchange rate in dwellings plays a vital role in indoor radon and thoron concentrations. The study area has higher average indoor concentrations of radon and thoron as compared to average global level of  $40 \text{ Bq/m}^3$  and  $10 \text{ Bq/m}^3$  as well as national level of  $42 \text{ Bq/m}^3$  and  $12.2 \text{ Bq/m}^3$  respectively (Mishra *et al.*, 2009; UNSCEAR, 2000). However, the observed values of radon and thoron are well below the action level as prescribed by ICRP 65 (1993) which is  $200 \text{ Bq/m}^3 - 600 \text{ Bq/m}^3$  and WHO which is  $200 \text{ Bq/m}^3 - 300 \text{ Bq/m}^3$ .

### **House type comparison**

The comparison of indoor radon as well as thoron concentrations has been done with different types of dwellings depending on the materials used for construction of buildings. As already mentioned in section 2.6.3, the selected houses are classified into two main groups, viz., Reinforced Cement Concrete (R.C.C) and Assam type houses. They are then sub-divided into five types depending on the building materials, namely, full R.C.C., R.C.C. with GI sheet roof, Assam type with wooden/bamboo walls, Assam type with asbestos walls and Assam type with GI sheet walls.

The detail experimental observations of measured indoor radon and thoron concentrations in different house types in Lunglei, Serchhip and Mamit Districts along with the whole study area are shown in Table 3.6. It is clear from the table that RCC type of buildings has the maximum indoor radon and thoron concentrations in each district as well as in the combined study areas.

**Table 3.6** Annual average indoor radon and thoron concentrations for different house types in the three districts along with the combined study area.

Type of Houses		Lunglei District		Serchhip District		Mamit District		whole study area	
		Radon (Bq/m <sup>3</sup> )	Thoron (Bq/m <sup>3</sup> )	Radon (Bq/m <sup>3</sup> )	Thoron (Bq/m <sup>3</sup> )	Radon (Bq/m <sup>3</sup> )	Thoron (Bq/m <sup>3</sup> )	Radon (Bq/m <sup>3</sup> )	Thoron (Bq/m <sup>3</sup> )
Full RCC	Min	35.235	10.739	42.90	8.32	43.89	10.26	35.24	8.32
	Max	76.431	52.135	62.51	53.35	65.50	64.68	76.43	64.68
	GM	50.71	23.12	51.28	19.31	54.71	24.28	52.39	22.29
	GSD	1.27	1.56	1.14	1.74	1.13	1.83	1.19	1.73
RCC with GI sheet roof	Min	40.235	12.028	72.49	51.04	41.79	18.18	40.24	12.03
	Max	46.605	30.935	72.49	51.04	62.19	53.76	72.49	53.76
	GM	42.63	16.68	72.49	51.04	50.71	28.74	49.89	25.86
	GSD	1.07	1.55	1.00	1.00	1.14	1.47	1.20	1.66
Assam Type with Wooden/Bamboo Walls	Min	37.725	15.801	28.05	5.99	37.26	11.68	28.05	5.99
	Max	84.025	27.909	53.31	17.53	70.68	45.80	84.03	45.80
	GM	50.20	21.18	38.91	12.65	54.59	17.80	46.82	16.75
	GSD	1.30	1.24	1.25	1.37	1.26	1.58	1.32	1.49
Assam Type with Asbestos Walls	Min	34.584	7.241	31.47	9.72	37.06	12.69	31.47	7.24
	Max	58.379	64.649	72.27	48.00	88.49	69.30	88.49	69.30
	GM	45.83	17.94	41.48	18.08	52.46	23.01	46.40	19.63
	GSD	1.18	1.89	1.25	1.59	1.25	1.48	1.26	1.67
Assam Type with G.I.Walls	Min	35.128	7.078	34.56	6.31	50.29	23.87	34.56	6.31
	Max	64.436	35.964	68.49	32.78	50.29	23.87	68.49	35.96
	GM	50.08	18.78	43.23	15.11	50.29	23.87	47.40	17.57
	GSD	1.19	1.75	1.24	1.82	1.00	1.00	1.22	1.78

A chart plotted using the geometric mean of indoor radon and thoron concentrations with the construction type of buildings in Lunglei District is shown in Fig.

3.6. From the graph, in Lunglei District, the full RCC type of building has the highest average concentrations of indoor radon and thoron.

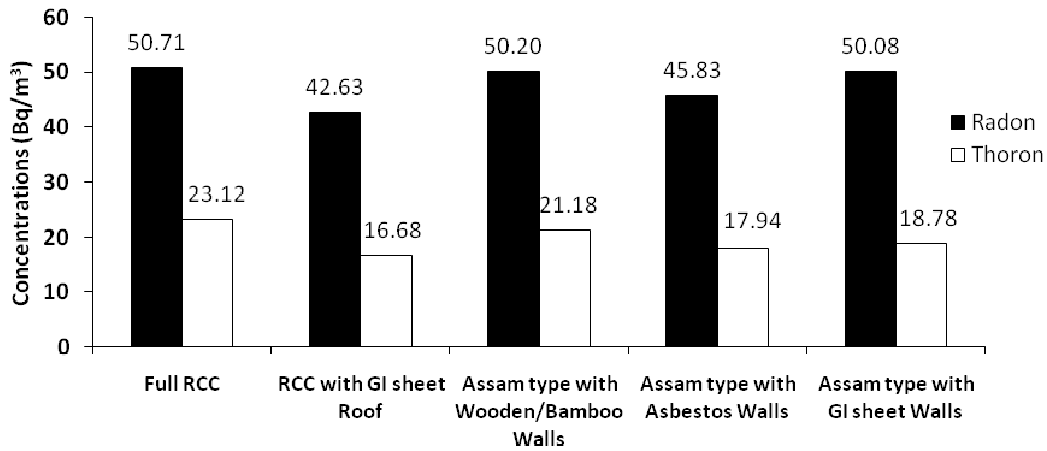


**Figure 3.6** Indoor radon and thoron concentrations of different types of buildings in Lunglei District.

Fig. 3.7 shows a chart plotted using the geometric mean of indoor radon and thoron concentrations with the construction type of building in Serchhip District.

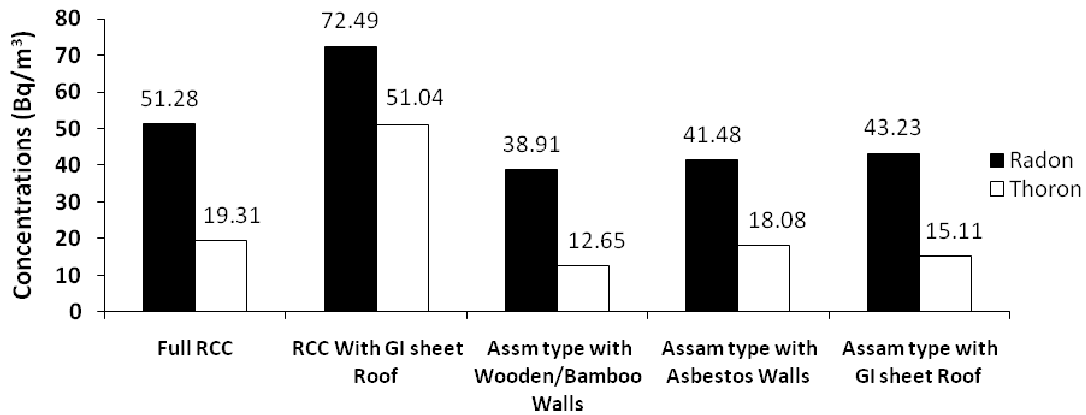


**Figure 3.7** Indoor radon and thoron concentrations of different types of buildings in Serchhip District.

Hence, it is clearly seen from the figure that in Serchhip District, the RCC with G.I. Sheet roof type of building has the maximum indoor concentrations as well as thoron concentrations.

Fig. 3.8 display a chart plotted using the geometric mean of indoor radon level as well as thoron level with the construction type of buildings in Mamit District. It is clearly seen from the figure that the indoor radon level is highest in full RCC type of buildings and the thoron level is highest in RCC with GI Sheet roof type of buildings.

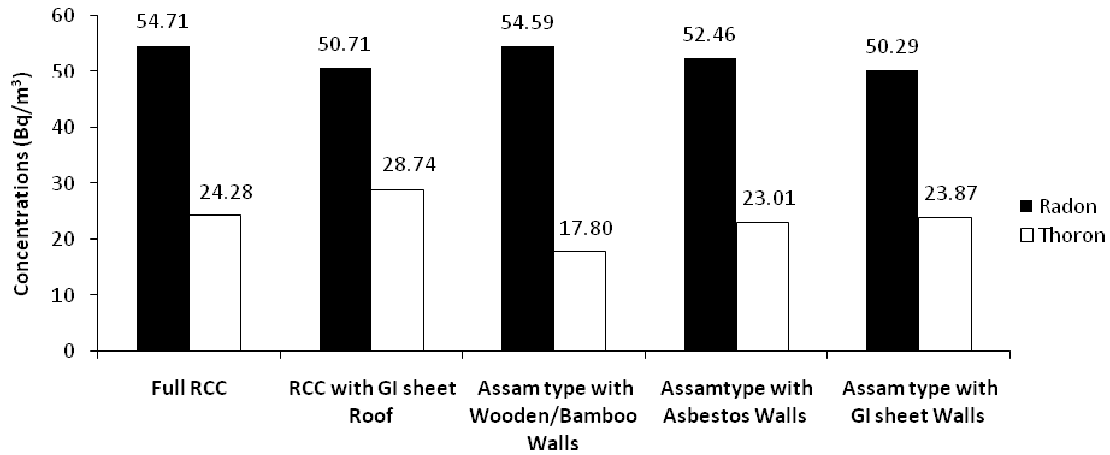


**Figure 3.8** Indoor radon and thoron concentrations of different types of buildings in Mamit District.

A chart plotted between the geometric mean of indoor radon and thoron concentrations and the construction type of buildings in the combined area of study is shown in Fig. 3.9. It is clear that the full RCC type of buildings has the maximum indoor radon concentrations and the RCC with G.I. Sheet roof type of buildings has the next highest radon concentrations. The RCC with G.I. Sheet roof type of buildings has the maximum thoron concentrations and the full RCC type of buildings has the next highest thoron concentrations. Hence RCC type of buildings has higher values of indoor radon as well as thoron levels as compared to other type of buildings in the whole study areas.

From the result, the RCC type of construction having materials of higher natural radioactivity content (Menon *et al.*, 1987) has higher radon/thoron concentrations as expected compared to Assam type buildings. In Assam type buildings with asbestos walls have high radon/thoron level which could be attributed due to the higher natural activity content of asbestos material (Porstendorfer, 1994). Also, we found that those with G.I.

sheet as walls have high radon/thoron level which can be due to lesser ventilation rate and its ability to block radon from escaping outside. It is also found that the ground floor of some houses is directly constructed on top of soil with a coating of mud. The ground floor allows more radon to diffuse inside the houses because of the higher porosity of materials used (Ramola *et al*, 1998).

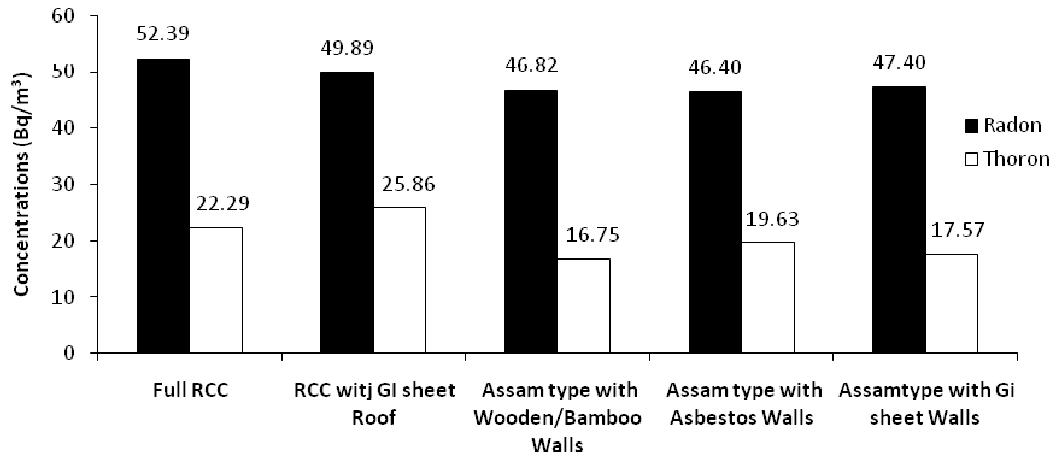


**Figure 3.9** Indoor radon and thoron concentrations of different types of buildings in the combined study area.

Uses of improper mixture of materials for construction of the houses led to several cracks in the foundations, walls, and basic slabs through which radon could easily enter the rooms (Vaupotic *et al.*, 1999). In general, radon and thoron concentration was found higher in cemented houses than in Assam type houses. This is due to the higher natural radioactivity content of materials used, exhalation of radon and thoron from the walls, floors, ceilings and cracks from the cement houses.

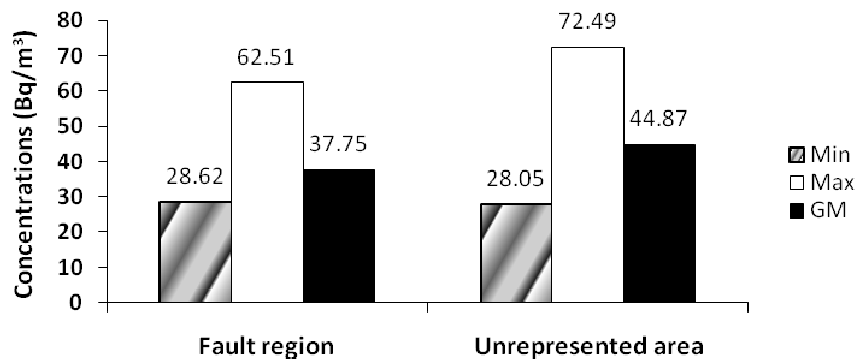
### Geological comparision

The measurement of indoor radon and thoron concentrations depending on the geological conditions has been done in Serchhip District only due to the limited availability of the geologically known regions in the study area. Thus, the study area is divided into Fault region and Unrepresented area. Fault region covers Ramthlun Veng, Hmar Veng and

Zion Veng localities in Serchhip town. These places are located using the available geological mapping done by the department of Geology and Mining, Govt. of Mizoram. Unrepresented area includes where no information of geological distinctiveness like fault or fossils regions are indicated and they may be treated as geologically unknown areas.

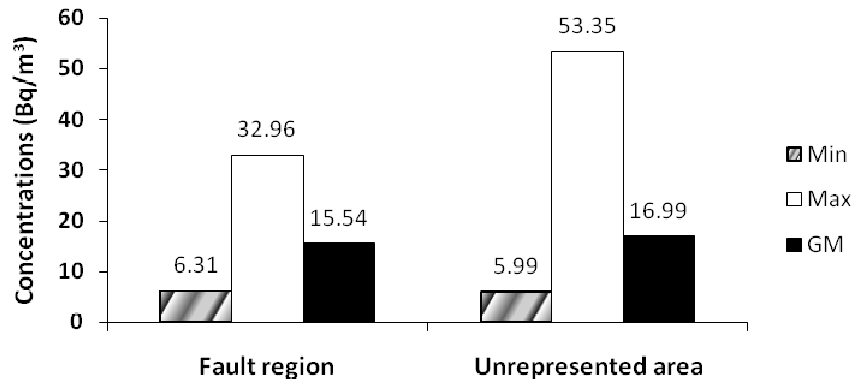
The annual average concentration of indoor radon ranges from 28.62 Bq/m<sup>3</sup> to 62.51 Bq/m<sup>3</sup> with GM 37.75 Bq/m<sup>3</sup> and 1.26 GSD in fault region while in dwelling (unrepresented) area it ranges from 28.05 Bq/m<sup>3</sup> to 72.49 Bq/m<sup>3</sup> with GM 44.87 Bq/m<sup>3</sup> and 1.28 GSD. In case of thoron, the annual average concentrations vary from 6.31 Bq/m<sup>3</sup> to 32.96 Bq/m<sup>3</sup> with GM 15.54 Bq/m<sup>3</sup> and 1.56 GSD in fault region while in dwelling (unrepresented) area, the annual average thoron concentrations vary from 5.99 Bq/m<sup>3</sup> to 53.35 Bq/m<sup>3</sup> with GM 16.99 Bq/m<sup>3</sup> and 1.85 GSD.

Fig. 3.10 and Fig. 3.11 show the comparison of the annual average of indoor radon and thoron levels among each of the selected geological areas.



**Figure 3.10** Annual average concentration of indoor radon in geological areas.





**Figure 3.11** Annual average concentration of indoor thoron in geological areas.

The movement of soil due to earthquake or landslide is supposed to enhance radon exhalation from the soil to surrounding atmosphere by providing more gaps for exhalation to surrounding atmosphere. From the two figures, it is clear that the annual average indoor radon and thoron levels in dwelling (unrepresented) area is higher than in fault region which is in contradictory to the expected one. This may be the influence of the material used for the construction of buildings and the ventilation rate. The geologically unknown regions could also contain rich radon and thoron sources which is not pre-determined.

### 3.2 Progeny concentrations measurement

The progenies of radon and thoron were measured by Equilibrium Equivalent Radon Concentrations and Equilibrium Equivalent Thoron Concentrations (EERC & EETC) using deposition based Direct Progeny Sensors (DPS) in bare modes (Mishra *et al.*, 2009). Since the system is intended for use in the deposition mode, it is necessary to avoid uncontrolled static charges from affecting the deposition rates and hence aluminized side of the mylar is chosen to act as the deposition surface (Mishra, 2008). The DRPS and DTPS are pasted separately on a separate piece of cardboard with cellotape. The dosimeters along with the DRPS and DTPS were exposed in different houses of Lunglei, Serchhip and Mamit districts for a period of 3 months each during rainy season, winter and summer season. After the exposure period is over, the detectors were retrieved and chemically

etched. The tracks were counted using spark counter and the track densities were converted into radon, thoron and their progeny concentrations using Eq. 2.7, Eq. 2.8, Eq. 2.9 and Eq. 2.10 and appropriate calibration factors. The calibration factor used for the progeny concentration of radon is 0.09 and that of thoron is 0.94 (Mishra *et al.*, 2008).

The progeny concentrations are given in terms of equilibrium equivalent concentration (EEC). EEC of a non-equilibrium mixture of short lived radon/thoron daughters in air is that activity concentration of radon/thoron, which would have been in equilibrium with this mixture. This value is essential in estimating the equilibrium factor for each of these gases respectively.

### 3.2.1 Results and discussions

A total of 60 DPS were exposed, 20 each in the three districts. From the total of 60 DPS exposed, 15 DPS (5 DPS each from each districts) were sent to Bhabha Atomic Research Centre (BARC) for inter-comparison. The exposure period starts from April 2009 and ends at April 2010. The experimentally determined value of EERC varies from a minimum of  $1.93\text{Bq/m}^3$  to a maximum of  $67.59\text{Bq/m}^3$  with a geometric mean of  $9.46\text{Bq/m}^3$  and 2.72 GSD during rainy season. It ranges from  $1.96\text{Bq/m}^3$  to  $173.91\text{Bq/m}^3$  with GM  $22.51\text{Bq/m}^3$  and 2.55 GSD during winter season. In summer, it ranges from  $0.36\text{Bq/m}^3$  to  $23.10\text{Bq/m}^3$  with GM of  $6.89\text{Bq/m}^3$  and 2.31 GSD. The annual average value of EERC ranges from a minimum of  $4.21\text{Bq/m}^3$  to a maximum of  $71.87\text{Bq/m}^3$  with a geometric mean of  $15.26\text{Bq/m}^3$  and GSD 1.94.

The EETC value varies from a minimum of  $0.61\text{Bq/m}^3$  to a maximum of  $3.37\text{Bq/m}^3$  with a geometric mean of  $1.22\text{Bq/m}^3$  and 1.64 GSD during rainy season. It ranges from  $0.59\text{Bq/m}^3$  to  $4.73\text{Bq/m}^3$  with GM  $1.56\text{Bq/m}^3$  and 1.7 GSD during winter season. In summer, it ranges from  $0.46\text{Bq/m}^3$  to  $2.08\text{Bq/m}^3$  with GM of  $0.92\text{Bq/m}^3$  and 1.44 GSD. The annual average value of EETC ranges from a minimum of  $0.63\text{Bq/m}^3$  to a maximum of  $3.40\text{Bq/m}^3$  with a geometric mean of  $1.26\text{Bq/m}^3$  and GSD 1.53.

The obtained value of EERC and EECT becomes highest in winter and lowest in summer season as expected. The high value may be due to the poor ventilation rate and low air exchange rate as doors and windows are closed more duration in winter. In summer, the air exchange rate of indoor with outdoor environment becomes higher, resulting in lower EERC and EECT values. The obtained value of EERC ( $15.26\text{Bq/m}^3$ ) is comparable and in good agreement with the global value which is  $16\text{Bq/m}^3$ . In case of EETC, the obtained value ( $1.26\text{Bq/m}^3$ ) is higher than the global value which is  $0.3\text{Bq/m}^3$  (UNSCEAR, 2000). The detail data obtained for EERC and EECT in the study areas are shown in Table 3.7.

**Table 3.7** Detail values of EERC and EETC in the study area.

Dwelling Nos.	Rainy		Winter		Summer		Annual Average	
	EERC ( $\text{Bq/m}^3$ )	EETC ( $\text{Bq/m}^3$ )	EERC ( $\text{Bq/m}^3$ )	EETC ( $\text{Bq/m}^3$ )	EERC ( $\text{Bq/m}^3$ )	EETC ( $\text{Bq/m}^3$ )	EERC ( $\text{Bq/m}^3$ )	EETC ( $\text{Bq/m}^3$ )
1	1.93	1.66	49.81	2.49	23.10	0.80	24.95	1.65
2	7.54	3.22	36.40	3.38	5.92	1.45	16.62	2.68
3	16.30	0.61	26.18	2.21	16.46	0.76	19.65	1.20
4	15.22	0.78	19.10	2.59	10.00	1.29	14.77	1.56
5	15.02	1.00	17.64	1.48	4.58	0.97	12.41	1.15
6	7.20	0.74	46.51	1.24	13.49	0.65	22.40	0.88
7	25.91	1.78	173.91	1.79	15.81	1.20	71.87	1.59
8	3.00	0.93	13.87	0.86	9.35	0.65	8.74	0.81
9	5.94	0.98	2.65	1.40	4.04	0.73	4.21	1.03
10	6.31	0.80	15.92	1.52	4.91	0.52	9.04	0.95
11	38.95	3.37	26.41	4.73	9.81	2.08	25.05	3.40
12	6.63	1.11	9.87	0.95	2.75	0.83	6.42	0.96
13	6.67	1.06	28.11	1.63	6.30	1.12	13.69	1.27
14	3.58	0.67	25.20	0.75	4.65	0.46	11.14	0.63
15	2.69	1.04	29.64	0.78	7.07	0.85	13.13	0.89
16	17.47	2.05	17.91	2.72	11.07	1.02	15.48	1.93
17	8.90	0.86	36.07	0.87	0.36	0.62	15.11	0.78
18	2.07	1.30	1.96	2.07	10.02	1.03	4.68	1.47
19	61.68	2.20	32.85	1.91	9.86	1.22	34.80	1.78
20	67.59	2.27	38.61	1.59	5.10	1.50	37.10	1.78
21	12.44	0.90	37.51	0.59	8.94	0.86	19.63	0.78

In Lunglei District, a total of only 8 DPS could be used for seasonal comparison of the readings out of 20 DPS deployed. Table 3.8 shows the equilibrium equivalent concentration of radon and thoron for different seasons in Lunglei District. It is clear from the table that both the EECR values and the EECT values are highest in winter.

**Table 3.8** The EEC values of radon and thoron in Lunglei District.

	Rainy		Winter		Summer		Annual Average	
	EECR (Bq/m <sup>3</sup> )	EECT (Bq/m <sup>3</sup> )	EECR (Bq/m <sup>3</sup> )	EECT (Bq/m <sup>3</sup> )	EECR (Bq/m <sup>3</sup> )	EECT (Bq/m <sup>3</sup> )	EECR (Bq/m <sup>3</sup> )	EECT (Bq/m <sup>3</sup> )
<b>Min</b>	1.93	0.61	13.87	0.86	4.58	0.65	8.74	0.81
<b>Max</b>	25.91	3.22	173.91	3.38	23.10	1.45	71.87	2.68
<b>GM</b>	8.61	1.15	34.02	1.85	10.94	0.93	19.51	1.34
<b>GSD</b>	2.32	1.69	2.13	1.52	1.66	1.34	1.79	1.44

A total of only 9 DPS could be used for seasonal comparison of the readings out of 20 DPS deployed in Serchhip District. The equilibrium equivalent concentration of radon and thoron for different seasons in Serchhip District is shown in Table 3.9. It is clear from the table that both the EECR values and the EECT values are highest in winter.

**Table 3.9** The EEC values of radon and thoron in Serchhip District.

	Rainy		Winter		Summer		Annual Average	
	EECR (Bq/m <sup>3</sup> )	EECT (Bq/m <sup>3</sup> )	EECR (Bq/m <sup>3</sup> )	EECT (Bq/m <sup>3</sup> )	EECR (Bq/m <sup>3</sup> )	EECT (Bq/m <sup>3</sup> )	EECR (Bq/m <sup>3</sup> )	EECT (Bq/m <sup>3</sup> )
<b>Min</b>	2.69	0.67	2.65	0.75	0.36	0.46	4.21	0.63
<b>Max</b>	38.95	3.37	36.07	4.73	11.07	2.08	25.05	3.40
<b>GM</b>	7.71	1.16	17.44	1.40	4.23	0.83	11.24	1.15
<b>GSD</b>	2.13	1.61	2.14	1.79	2.63	1.53	1.64	1.62

In Mamit District, a total of only 4 DPS could be used for inter-seasonal comparison out of 20 DPS deployed. Table 3.10 shows the equilibrium equivalent concentration of radon and thoron for different seasons in Mamit District. It is clear from the table that both the EECR values and the EECT values are highest in rainy season.

**Table 3.10** The EEC values of radon and thoron in Mamit District.

	Rainy		Winter		Summer		Annual Average	
	EECR (Bq/m <sup>3</sup> )	EECT (Bq/m <sup>3</sup> )	EECR (Bq/m <sup>3</sup> )	EECT (Bq/m <sup>3</sup> )	EECR (Bq/m <sup>3</sup> )	EECT (Bq/m <sup>3</sup> )	EECR (Bq/m <sup>3</sup> )	EECT (Bq/m <sup>3</sup> )
<b>Min</b>	2.07	0.90	1.96	0.59	5.10	0.86	4.68	0.78
<b>Max</b>	67.59	2.27	38.61	2.07	10.02	1.50	37.10	1.78
<b>GM</b>	18.11	1.55	17.48	1.39	8.19	1.13	18.56	1.38
<b>GSD</b>	4.14	1.47	3.54	1.65	1.32	1.23	2.30	1.40

Fig. 3.12 and Fig. 3.13 show the annual average value of EECR and EECT in the study area respectively. The variation of EECR with EECT values are not the same for each dwellings.

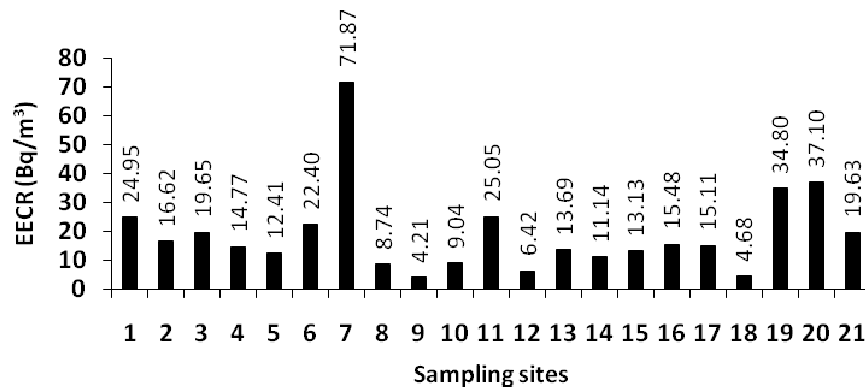


**Figure 3.12** Annual average value of Equilibrium Equivalent Concentration of Radon.

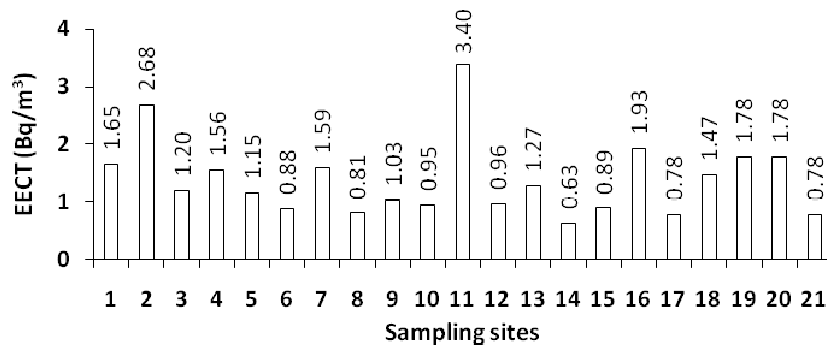


**Figure 3.13** Annual average value of Equilibrium Equivalent Concentration of Thoron.

The results of inter-comparison from Environmental Assessment Division (EAD), BARC, Mumbai, for the value of EECR and EECT are in good agreement with the result obtained as shown above.

### 3.3 Determination of Equilibrium factors for Radon ( $F_R$ ) and Thoron ( $F_T$ )

The equilibrium factors are also referred to as *F-factor* and were globally assumed values in the past years and even the calculation of radon/thoron progenies were inferred using this value (UNSCEAR, 2000). These are understood as representative mean values in

a global sense and might vary across countries and geographical locations, house to house as well as from time to time in a given house. With the advent of passive detection techniques using solid state nuclear track detectors (SSNTDs), direct progeny sensor (DPS) has been developed. The value of equilibrium factor in the indoor air depends mainly on the pseudo-ventilation rates, which is the sum of the air exchange rate and the wall removal rate in the dwelling. In the present work, using the experimental determined values of the progeny concentrations of radon and thoron along with the indoor radon, thoron concentrations the values of equilibrium factor is calculated from the relations given in Eq. 2.11 and Eq. 2.12.

### **3.3.1 Results and discussions**

The calculated value of equilibrium factor for radon ranges from a minimum of 0.04 to a maximum of 1.19 with geometric mean of 0.27 and GSD 2.56 during rainy season. It varies from 0.04 to 1.31 with GM 0.44 and 2.31 GSD during winter season. In summer, it ranges from 0.01 to 0.68 with GM of 0.16 and 2.20 GSD. The annual average value of equilibrium factor of radon ranges from a minimum of 0.09 to a maximum of 0.72 with a geometric mean of 0.35 and GSD 1.69. The obtained value of radon equilibrium factor becomes highest in winter season and lowest in summer season. This variation is in good correlation with the variation of measured EERC as well as indoor radon concentrations.

The value of equilibrium factor for thoron ranges from a minimum of 0.02 to a maximum of 0.27 with geometric mean of 0.06 and GSD 2.17 during rainy season. It varies from 0.02 to 0.58 with GM 0.12 and 2.43 GSD during winter season. In summer, it ranges from 0.02 to 0.18 with GM of 0.06 and 1.79 GSD. The annual average value of equilibrium factor of thoron ranges from a minimum of 0.04 to a maximum of 0.23 with a geometric mean of 0.09 and GSD 1.69. The obtained value of thoron equilibrium factor becomes highest in winter season and lowest in summer season. This variation is in good correlation

with the variation of measured EETC. Table 3.11 shows the detail values of equilibrium factors in the study areas.

**Table 3.11** Detail values of Equilibrium factors in the study area.

Dwelling Nos.	Rainy		Winter		Summer		Annual Average	
	Radon	Thoron	Radon	Thoron	Radon	Thoron	Radon	Thoron
1	0.06	0.23	0.67	0.17	0.68	0.06	0.47	0.15
2	0.09	0.07	0.64	0.58	0.27	0.03	0.33	0.23
3	0.43	0.04	0.75	0.49	0.41	0.06	0.53	0.19
4	0.91	0.03	0.29	0.09	0.26	0.04	0.49	0.05
5	0.26	0.07	0.42	0.04	0.13	0.10	0.27	0.07
6	0.23	0.02	0.67	0.05	0.23	0.05	0.38	0.04
7	0.65	0.10	1.31	0.04	0.20	0.17	0.72	0.11
8	0.15	0.04	0.29	0.06	0.19	0.05	0.21	0.05
9	0.13	0.02	0.06	0.05	0.13	0.07	0.10	0.05
10	0.38	0.04	0.43	0.18	0.08	0.05	0.30	0.09
11	0.88	0.04	0.25	0.56	0.14	0.04	0.42	0.21
12	0.18	0.09	0.36	0.08	0.05	0.03	0.20	0.07
13	0.26	0.04	0.64	0.12	0.24	0.18	0.38	0.12
14	0.23	0.08	0.96	0.08	0.09	0.02	0.43	0.06
15	0.11	0.04	1.08	0.05	0.14	0.07	0.44	0.05
16	0.95	0.15	0.49	0.15	0.27	0.03	0.57	0.11
17	0.20	0.22	0.73	0.09	0.01	0.03	0.31	0.12
18	0.04	0.03	0.04	0.20	0.19	0.08	0.09	0.10
19	1.01	0.27	0.38	0.21	0.27	0.06	0.55	0.18
20	1.19	0.04	0.52	0.32	0.10	0.13	0.61	0.16
21	0.24	0.08	0.66	0.02	0.20	0.10	0.37	0.07

In Lunglei District, the calculated value of equilibrium factor of radon ranges from 0.06 to 0.91 with GM of 0.26 and 2.4 GSD while thoron values vary from 0.02 to 0.23 with GM of 0.06 and 2.04 GSD during rainy season. In winter, radon equilibrium factor vary from 0.29 to 1.31 with GM of 0.56 and 1.61 GSD while thoron equilibrium factor ranges from 0.04 to 0.58 with GM of 0.11 and 2.7 GSD. During summer season, radon equilibrium factor ranges from 0.13 to 0.68 with GM of 0.26 and 1.61 GSD while thoron values vary from 0.03 to 0.17 with GM of 0.06 and 1.73 GSD. The annual average value of

equilibrium factor of radon ranges from 0.21 to 0.72 with GM of 0.4 and 1.44 GSD and the values of thoron vary from 0.04 to 0.23 with GM of 0.09 and 1.85 GSD.

In Serchhip District, the calculated value of equilibrium factor of radon ranges from 0.11 to 0.95 with GM of 0.28 and 2.07 GSD while thoron values vary from 0.02 to 0.22 with GM of 0.06 and 2.14 GSD during rainy season. In winter, radon equilibrium factor vary from 0.06 to 1.08 with GM of 0.43 and 2.31 GSD while thoron equilibrium factor ranges from 0.05 to 0.56 with GM of 0.11 and 2.04 GSD. During summer season, radon equilibrium factor ranges from 0.01 to 0.27 with GM of 0.10 and 2.35 GSD while thoron values vary from 0.02 to 0.18 with GM of 0.05 and 1.83 GSD. The annual average value of equilibrium factor of radon ranges from 0.1 to 0.57 with GM of 0.32 and 1.63 GSD and the values of thoron vary from 0.05 to 0.21 with GM of 0.09 and 1.58 GSD.

In Mamit District, the calculated value of equilibrium factor of radon ranges from 0.04 to 1.19 with GM of 0.33 and 3.89 GSD while thoron values vary from 0.03 to 0.27 with GM of 0.07 and 2.46 GSD during rainy season. In winter, radon equilibrium factor vary from 0.04 to 0.66 with GM of 0.28 and 3.11 GSD while thoron equilibrium factor ranges from 0.02 to 0.32 with GM of 0.14 and 2.72 GSD. During summer season, radon equilibrium factor ranges from 0.1 to 0.27 with GM of 0.18 and 1.42 GSD while thoron values vary from 0.06 to 0.13 with GM of 0.09 and 1.34 GSD. The annual average value of equilibrium factor of radon ranges from 0.09 to 0.61 with GM of 0.32 and 2.16 GSD and the values of thoron vary from 0.07 to 0.18 with GM of 0.12 and 1.47 GSD.

The annual average value of equilibrium factors of radon and thoron in the study area are shown in Fig. 3.14 and Fig. 3.15 respectively. The observed annual average value of equilibrium factor for radon is 0.35 and that for thoron is 0.09 which is slightly lower values for radon and slightly higher for thoron in comparison to global level of 0.4 and 0.03 respectively (UNSCEAR, 2000).



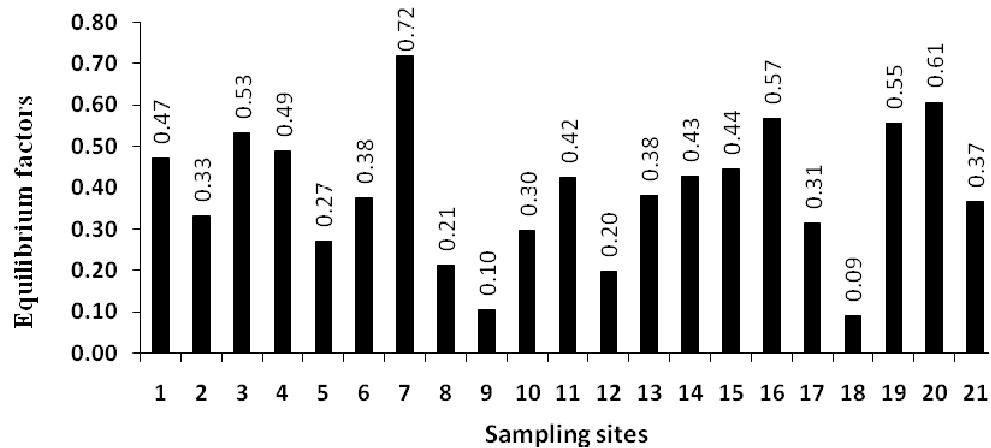


**Figure 3.14** Annual average value of equilibrium factor of radon.

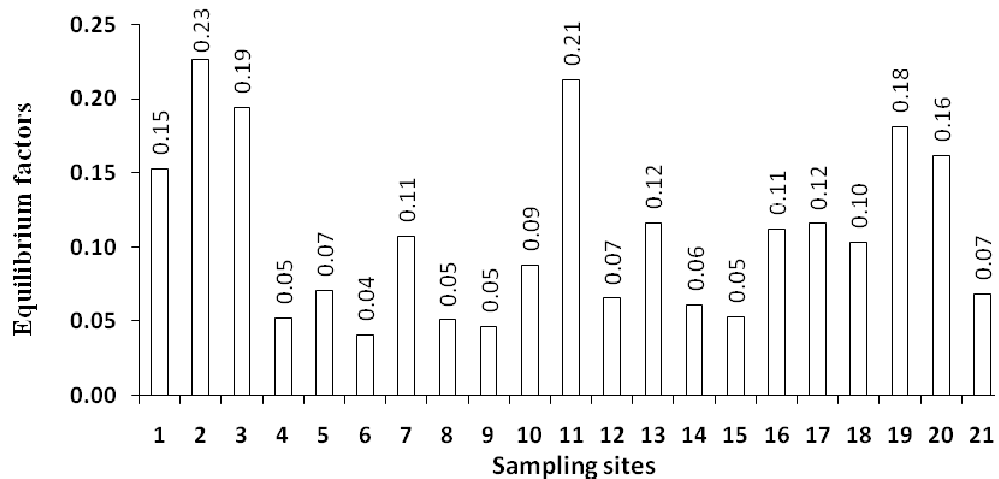


**Figure 3.15** Annual average value of equilibrium factor of thoron.

### 3.4 Estimation of annual inhalation dose for radon and thoron

In the present study, inhalation doses are calculated from the dose conversion factors reported by UNSCEAR, (2000). With the development of DPS system, progeny concentrations of radon and thoron can be obtained directly. Putting the experimentally obtained indoor concentrations of radon and thoron and the calculated values of equilibrium factors of radon and thoron progenies in Eq. 2.13, the annual inhalation dose rate is estimated. The annual inhalation dose rate of indoor radon and thoron in Lunglei, Serchhip and Mamit Districts are given in table 3.12, table 3.13 and table 3.14.

**Table 3.12** Annual inhalation dose rate of radon and thoron in Lunglei District.

	Rainy		Winter		Summer		Annual Average	
	Radon	Thoron	Radon	Thoron	Radon	Thoron	Radon	Thoron
	$\mu\text{Sv/y}$	$\mu\text{Sv/y}$	$\mu\text{Sv/y}$	$\mu\text{Sv/y}$	$\mu\text{Sv/y}$	$\mu\text{Sv/y}$	$\mu\text{Sv/y}$	$\mu\text{Sv/y}$
<b>Min</b>	159.18	185.34	931.31	250.99	330.74	191.03	597.61	240.22
<b>Max</b>	1681.60	935.84	11127.40	951.43	1497.01	450.20	4633.36	779.16
<b>GM</b>	601.53	342.18	2225.94	536.39	744.78	274.22	1292.50	393.27
<b>GSD</b>	2.17	1.65	2.10	1.50	1.63	1.36	1.77	1.42

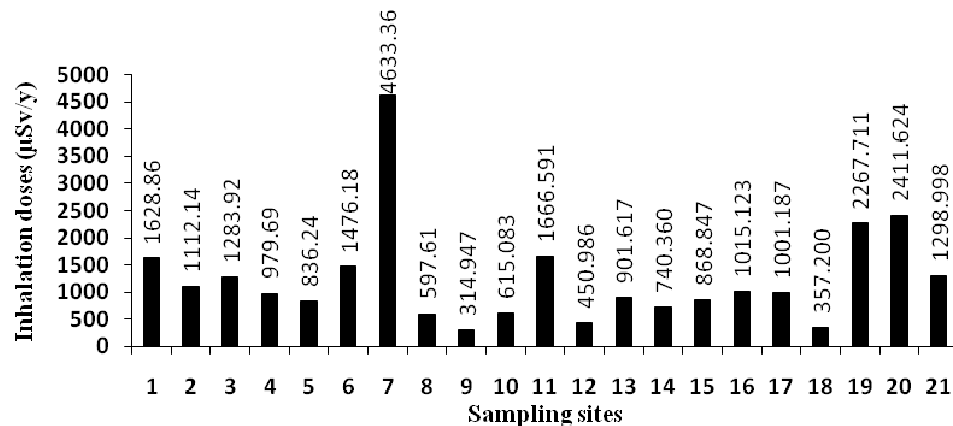
**Table 3.13** Annual inhalation dose rate of radon and thoron in Serchhip District.

	Rainy		Winter		Summer		Annual Average	
	Radon	Thoron	Radon	Thoron	Radon	Thoron	Radon	Thoron
	$\mu\text{Sv/y}$	$\mu\text{Sv/y}$	$\mu\text{Sv/y}$	$\mu\text{Sv/y}$	$\mu\text{Sv/y}$	$\mu\text{Sv/y}$	$\mu\text{Sv/y}$	$\mu\text{Sv/y}$
<b>Min</b>	198.83	194.24	221.64	217.09	54.95	143.93	314.95	185.09
<b>Max</b>	2509.59	1015.87	2333.41	1333.34	747.63	624.41	1666.59	991.21
<b>GM</b>	527.60	345.12	1172.80	405.68	338.20	247.55	761.22	336.80
<b>GSD</b>	2.06	1.61	2.00	1.77	2.08	1.52	1.59	1.62

**Table 3.14** Annual inhalation dose rate of radon and thoron in Mamit District.

	Rainy		Winter		Summer		Annual Average	
	Radon	Thoron	Radon	Thoron	Radon	Thoron	Radon	Thoron
	$\mu\text{Sv/y}$	$\mu\text{Sv/y}$	$\mu\text{Sv/y}$	$\mu\text{Sv/y}$	$\mu\text{Sv/y}$	$\mu\text{Sv/y}$	$\mu\text{Sv/y}$	$\mu\text{Sv/y}$
<b>Min</b>	191.14	259.81	184.96	184.28	381.27	248.82	357.20	230.97
<b>Max</b>	4330.57	679.90	2523.03	588.96	695.50	428.84	2411.62	519.23
<b>GM</b>	1290.64	459.13	1253.64	403.35	574.47	326.72	1262.13	402.41
<b>GSD</b>	3.60	1.47	3.02	1.59	1.27	1.23	2.15	1.39

Fig. 3.16 and Fig. 3.17 show the annual average of the inhalation doses of radon and thoron at each sampling sites respectively.

**Figure 3.16** Annual average of inhalation dose for Radon.

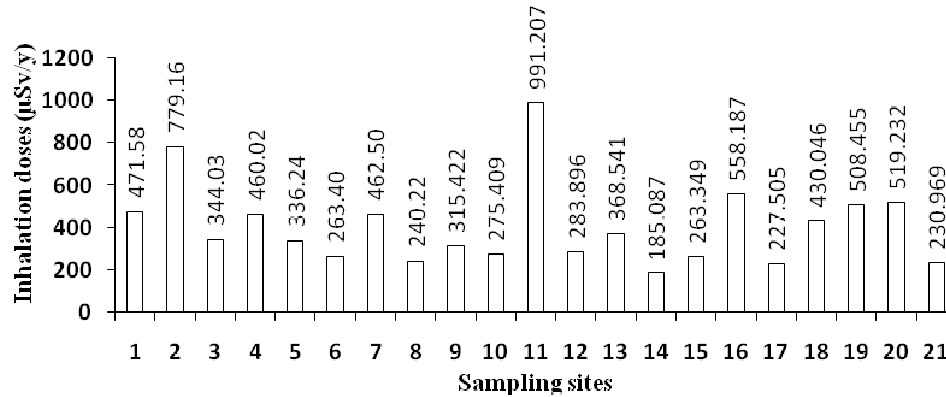


**Figure 3.17** Annual average of inhalation dose for Thoron.

The experimentally determined value of radon inhalation dose rate varies from a minimum of  $159.18\mu\text{Sv/y}$  to a maximum of  $4330.57\mu\text{Sv/y}$  with GM of  $657.66\mu\text{Sv/y}$  (2.55 GSD) in rainy season. It ranges from  $184.96\mu\text{Sv/y}$  to  $11127.4\mu\text{Sv/y}$  with GM of  $1516.19\mu\text{Sv/y}$  (2.36 GSD) during winter whereas it ranges from  $54.95\mu\text{Sv/y}$  to  $1497.01\mu\text{Sv/y}$  with GM of  $505.37\mu\text{Sv/y}$  (1.97 GSD) during summer season. From the result, it is clear that the inhalation dose rate of radon is highest in winter and lowest in summer season.

In case of thoron, the determined value of inhalation dose rate varies from a minimum of  $185.34\mu\text{Sv/y}$  to a maximum of  $1015.87\mu\text{Sv/y}$  with GM of  $363.22\mu\text{Sv/y}$  (1.62 GSD) in rainy season. It ranges from  $184.28\mu\text{Sv/y}$  to  $1333.34\mu\text{Sv/y}$  with GM of  $450.73\mu\text{Sv/y}$  (1.67 GSD) during winter whereas it ranges from  $143.93\mu\text{Sv/y}$  to  $624.41\mu\text{Sv/y}$  with GM of  $271.36\mu\text{Sv/y}$  (1.43 GSD) during summer season. From the result, it is clear that the inhalation dose rate of thoron is highest in winter and lowest in summer season.

The annual average radon inhalation doses vary from  $314.95\mu\text{Sv/y}$  to  $4633.36\mu\text{Sv/y}$  with GM of  $1025.48\mu\text{Sv/y}$  and 1.87 GSD which is slightly higher than the global average value of  $1009\mu\text{Sv/y}$ . In the case of thoron, it varies from  $185.09\mu\text{Sv/y}$  to  $991.21\mu\text{Sv/y}$  with GM of  $369.61\mu\text{Sv/y}$  and 1.52 GSD which is higher than the global

average of 84 $\mu$ Sv/y (UNSCEAR, 2000). The detail values of inhalation dose rate in the study areas are shown in Table 3.15.

**Table 3.15** Detail values of inhalation dose rate in the study areas.

Dwelling Nos.	Rainy		Winter		Summer		Annual Average	
	Radon $\mu$ Sv/y	Thoron $\mu$ Sv/y	Radon $\mu$ Sv/y	Thoron $\mu$ Sv/y	Radon $\mu$ Sv/y	Thoron $\mu$ Sv/y	Radon $\mu$ Sv/y	Thoron $\mu$ Sv/y
1	159.18	469.58	3230.41	709.74	1497.01	235.41	1628.86	471.58
2	573.02	935.84	2363.85	951.43	399.53	450.20	1112.14	779.16
3	1072.77	185.34	1692.86	623.34	1086.12	223.39	1283.92	344.03
4	979.58	241.42	1283.16	748.14	676.32	390.51	979.69	460.02
5	1015.35	290.52	1162.63	440.22	330.74	277.97	836.24	336.24
6	492.30	230.26	3015.84	368.56	920.42	191.36	1476.18	263.40
7	1681.60	512.77	11127.40	534.36	1091.10	340.36	4633.36	462.50
8	212.77	278.63	931.31	250.99	648.75	191.03	597.61	240.22
9	430.57	321.51	221.64	413.99	292.63	210.76	314.947	315.422
10	417.81	240.20	1047.77	431.80	379.66	154.22	615.083	275.409
11	2509.59	1015.87	1789.98	1333.34	700.21	624.41	1666.591	991.207
12	462.82	321.20	655.36	273.79	234.78	256.69	450.986	283.896
13	451.35	319.04	1825.22	466.93	428.28	319.65	901.617	368.541
14	244.30	194.24	1620.66	217.09	356.12	143.93	740.360	185.087
15	198.83	311.11	1901.95	231.64	505.76	247.30	868.847	263.349
16	1123.94	586.20	1173.80	775.05	747.63	313.31	1015.123	558.187
17	615.20	243.91	2333.41	250.60	54.95	188.00	1001.187	227.505
18	191.14	403.52	184.96	588.96	695.50	297.66	357.200	430.046
19	3963.05	623.41	2174.86	543.21	665.23	358.74	2267.711	508.455
20	4330.57	679.90	2523.03	448.96	381.27	428.84	2411.624	519.232
21	845.84	259.81	2433.73	184.28	617.43	248.82	1298.998	230.969

## Chapter 4

### Experimental determination of surface flux, radioactivity content and radon content in soil gas

In this chapter, we present the experimental measurements of surface flux, radioactivity content measurement of soil sample as well as building materials and radon content in soil gas measurement. The details of results obtained will also be compared with the available previous findings in other areas, global and national average level whenever possible. The details of results obtained from the experiments carried out in the present study including the possible discussion will follow.

#### 4.1 Measurement of Surface radon flux

The rate of radon exhalation is measured by using a recently developed accumulator technique. The cylindrical metallic accumulator having 15.5 cm diameter and 17.5 cm height is connected in line to continuous radon monitor (RAD7). The RAD7 is set up in *Sniff mode*, 15 mins cycle, 20 recycle and the Pump is *ON* and Thoron is in *OFF*. The accumulator is placed on the surface of the soil area of interest in an inverted position and the radon concentration is allowed to build up inside the accumulator for a specified period of time (Zoliana *et al.*, 2011) and is monitored by RAD7. Now, the device can take the reading of radon build up inside the accumulator for each 15 minutes and stored in its inbuilt memory. After 20 recycles have been completed, the stored data are printed out using the Infra-red connected printer device.

Time variation of the radon concentration inside the accumulator monitored using RAD7 is related to the flux through growth kinetic equations (Eq. 2.14). By fitting this exponential growth equation to the concentration data inside accumulator obtained from the measurement set up radon flux can be determined. Due to limitation of

availability in the standard software (Origin pro) for the fitting procedure, fitting with the exact form of the equation is not possible, hence, carefully slight calibration have been made for fitting purpose with the available general growth equation (Eq. 2.16). Surface radon flux is obtained from the fitting parameter  $Y_0$  in order to avoid interference of initial radon concentration present in the accumulator (Sahoo, 2008). The accumulator technique takes care of two dimensional non-steady motion of both lateral and vertical diffusion of the trace gas emission into a chamber deployed at the surface of the soil matrix. This type of measurement provides an accurate method for interpreting the concentration data derived from surface deployed chambers without having to worry about insertion depth or deployment duration (Sahoo *et al.*, 2010).

#### 4.1.1 Results and discussions

A total of 15 locations have been selected in the study area depending on the soil conditions of the area. The gamma levels at ground and at 1m height are taken on the selected area and the soil conditions are also noted down. Each flux values are correlated with the indoor radon concentrations measured using dosimeters in dwellings at the vicinity of the surface flux measurements. The measured value of surface radon flux obtained in the study areas is shown in Table 4.1.

**Table 4.1** Measured values of surface radon flux in the study areas.

Sampling sites	Soil Condition	Radon Flux (mBq/m <sup>2</sup> /s)	Sampling sites	Soil Condition	Radon Flux (mBq/m <sup>2</sup> /s)
1	Little moisture soft soil	8.35	9	Dry and soft rocky soil	42.33
2	Little moisture soft soil	5.89	10	Little moisture soft soil	11.35
3	Dry and soft rocky soil	69.62	11	Little moisture soft soil	11.81
4	Moisture and soft rocky soil	32.19	12	Dry and soft rocky soil	64.35
5	Moisture and soft rocky soil	82.23	13	Dry and soft sandy soil	37.14
6	Dry and soft rocky soil	98.05	14	Dry and soft sandy red soil	21.84
7	Dry and soft rocky soil	19.95	15	Dry and soft rocky soil	13.62
8	Dry and soft rocky soil	25.22			

The study area in Lunglei district covers  $022^{\circ}53.175' N$  to  $022^{\circ}53.710' N$  latitude and  $092^{\circ}44.668' E$  to  $092^{\circ}44.860' E$  longitude at a height of 3317 – 3421 ft from sea level. Flux measurement was taken in 2 sampling sites and the soil condition in these areas are soft soil and little moisture and the gamma level is  $15\mu R/h$  –  $16\mu R/h$  at ground and  $16\mu R/h$  –  $17\mu R/h$  at 1m height. Figure 4.1 show the variation of radon flux in Lunglei district and was found in the range of  $5.89\text{mBq/m}^2/\text{s}$  to  $8.35\text{mBq/m}^2/\text{s}$  with geometric mean of (GM) of  $7.01\text{mBq/m}^2/\text{s}$  (GSD 1.19).

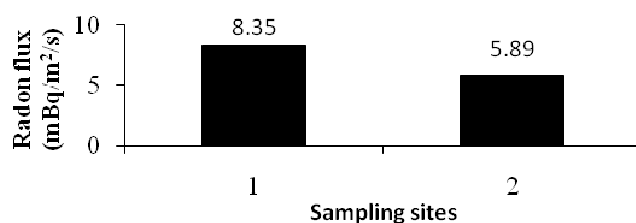


**Figure 4.1** Radon flux at each sampling sites in Lunglei District.

In Serchhip district, 7 sampling sites were selected covering  $023^{\circ}18.505' N$  to  $023^{\circ}28.455' N$  latitude and  $092^{\circ}51.221' E$  to  $092^{\circ}51.662' E$  longitude at a height of 3194 – 3433 ft from sea level. Most of the soils in these areas are soft rocky and dry soil and a little moisture soil is selected in two places. The gamma level is  $14\mu R/h$  –  $17\mu R/h$  at ground and  $13\mu R/h$  –  $16\mu R/h$  at 1m height. The radon flux values lied between  $19.95\text{mBq/m}^2/\text{s}$  and  $98.05\text{mBq/m}^2/\text{s}$  with GM of  $45.19\text{mBq/m}^2/\text{s}$  (GSD 1.77) as shown in Figure 4.2.

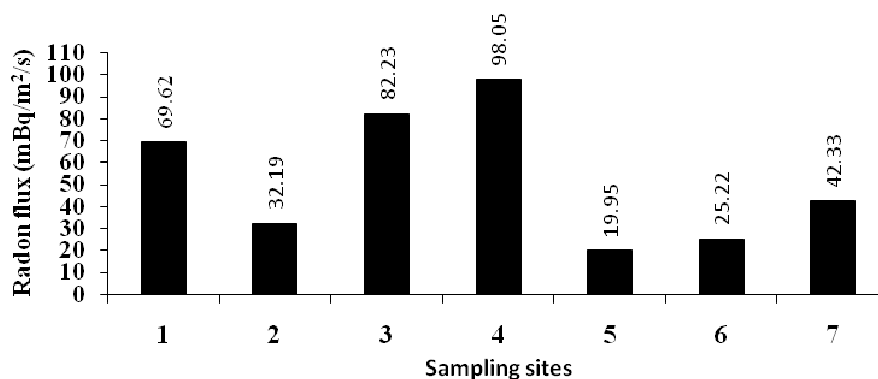


**Figure 4.2** Radon flux at each sampling sites in Serchhip District.

In Mamit district, 6 sampling sites were selected covering  $023^{\circ}55.016' N$  to  $023^{\circ}55.412' N$  latitude and  $092^{\circ}29.492' E$  to  $092^{\circ}29.563' E$  longitude at a height of 2652 – 2848 ft from sea level. The gamma level in these study areas are  $13\mu R/h$  –  $17\mu R/h$  at ground and  $12\mu R/h$  –  $16\mu R/h$  at 1m height. In two sampling sites the soil is dry and soft sandy while in the other two sampling sites it is dry and soft rocky. Soft sandy and little moisture soil is also found in two sampling sites. Figure 4.3 show the variation of radon flux in Mamit district, it varied from  $11.35\text{mBq/m}^2/\text{s}$  to  $64.35\text{mBq/m}^2/\text{s}$  with GM of  $21.37\text{mBq/m}^2/\text{s}$  (GSD 1.90).

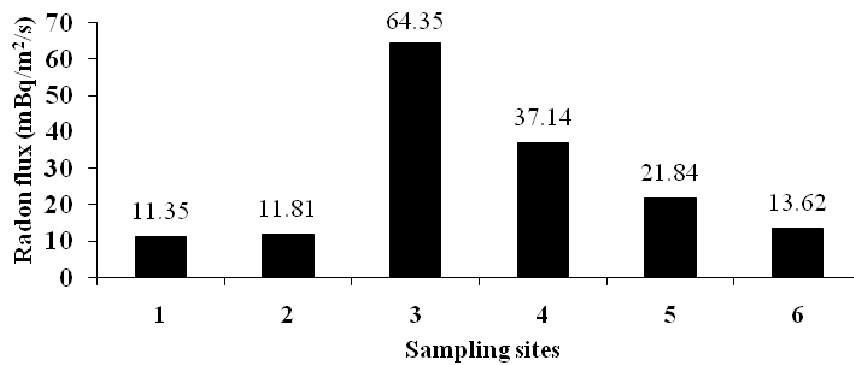


**Figure 4.3** Radon flux at each sampling sites in Mamit District.

Figure 4.4 shows the minimum and maximum values of radon flux in different geographical location with their geometric mean and the overall values. The overall values lied in the range of  $5.89\text{mBq/m}^2/\text{s}$  and  $98.05\text{mBq/m}^2/\text{s}$  with geometric mean of  $26.13\text{mBq/m}^2/\text{s}$  (GSD 2.1). The radon flux obtained in this work is close to the world average of  $22\text{mBq/m}^2/\text{s}$  (Nazaroff, 1992).



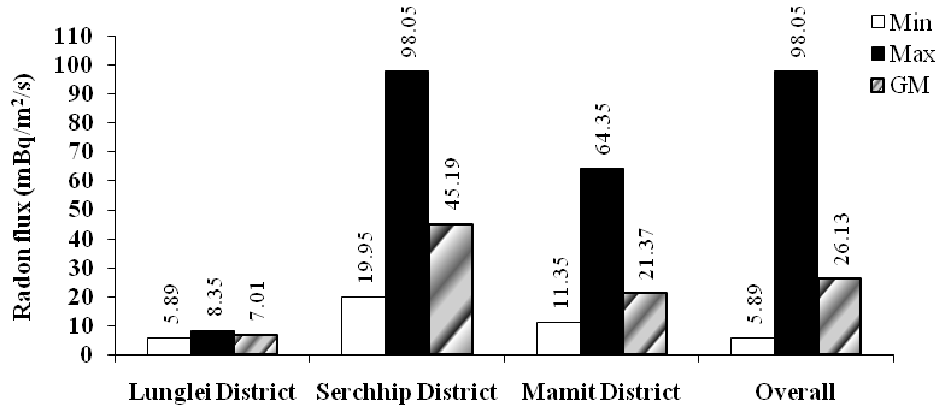


**Figure 4.4** Radon flux at different geographical locations.

The correlation of flux and indoor radon levels at the sampling sites with the help of Excel software is shown in Figure 4.5. From the graph plotted, we see that the gradient of the line is low with correlation coefficient ( $R^2$ ) = 0.253. This may be attributed due to the fact that the method of indoor radon concentration measurement is a time integrated type which took at least 120 days while radon flux measurement is an active method for a duration of about an hour having a cycle of 15 minutes. Owing to the different method of measurements, radon flux and indoor radon concentration, in this case may not be well related.

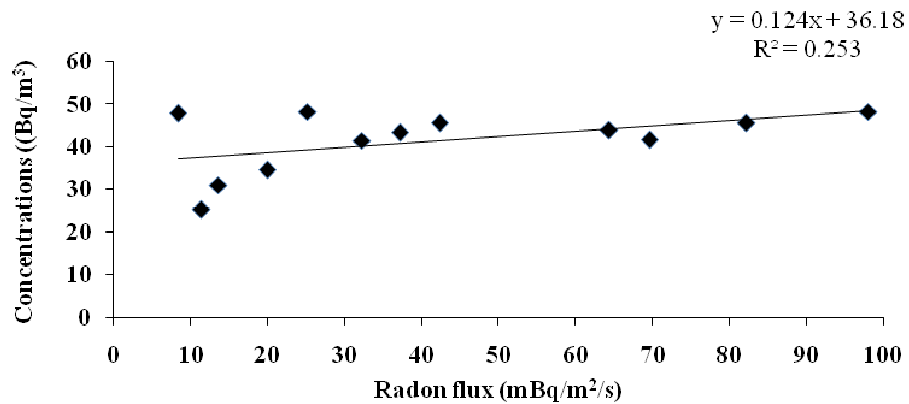


**Figure 4.5** Correlation of radon flux obtained and indoor radon concentration.

## 4.2 Radioactivity content in soil samples and building materials

As soil is the basic ingredient used in construction materials in India, estimation of the radiation risk to the population may also be computed from the activities of the radio-nuclides present in the sample extracted from soils.

Gamma ray spectrometry using NaI(Tl) scintillation detector method was employed to estimate the radioactivity content of  $^{226}\text{Ra}$ ,  $^{232}\text{Th}$  and  $^{40}\text{K}$  from the collected soil samples and samples of building materials. The NaI(Tl) Scintillation Detector was coupled with 1K Multichannel Analyzer (MCA) and had been manually calibrated for each measurement using known activity of standard sources ( $\text{Cs}^{137}$  and  $\text{Co}^{60}$ ). The efficiency measurements were carried out using standard sources whose activities were already determined beforehand at BARC. The calibration of the instrument using the standard sources and the calculation of activity content of soil sample has been performed by the author in Bhabha Atomic Research Centre (BARC), Mumbai. The experimental details are shown in Appendix – IV (a), Appendix – IV (b) and Appendix – IV (c).

Soil samples are collected at several locations near the houses where dosimeters are hanged in different parts of the study area and were grinded into a powder size, weighed and sealed inside a container (250 ml) for a minimum of 30 days in order to reach equilibrium between  $^{238}\text{U}$ ,  $^{232}\text{Th}$  and their respective progenies. After 30 days the samples were placed inside the detector and analyzed for a duration of 30000 secs since the activity of the samples analysed is found to be low.

The activity concentration of  $^{40}\text{K}$  was measured directly by its own gamma ray of energy 1460 keV. As  $^{238}\text{U}$  and  $^{232}\text{Th}$  are not directly gamma emitters, their activity concentrations were measured through gamma rays of their decay products. Decay products taken for  $^{238}\text{U}$  is  $^{214}\text{Bi}$  having energy of 1764 keV whereas for  $^{232}\text{Th}$  is  $^{208}\text{Tl}$

having energy of 2614 keV gamma ray by assuming the decay series to be in equilibrium (Firestone *et al.*, 1998). The spectra were analyzed using the software NETSWIN. Respective count rates after subtracting the background counts of the spectrum obtained for the same counting time were used to calculate the net count rate under the most prominent photo peaks of radium and thorium daughters. Then, the activity of radionuclide was calculated using Eq. 2.17 after subtracting the background area of prominent gamma ray energies. The radioactivity content was obtained in Bq/kg for each sample.

#### 4.2.1 Results and discussions

A total of 14 soil samples have been collected from different area of interest within the study area. From the obtained result, the activity for  $^{40}\text{K}$  ranges within 12.82 Bq/kg and 856.42 Bq/kg with geometric mean (GM) of 171.83 Bq/kg and GSD 2.80. The experimentally obtained activity of  $^{238}\text{U}$  varies from 35.21 Bq/kg to 335.32 Bq/kg with geometric mean of 128.48 Bq/kg and 2.57 GSD. For  $^{232}\text{Th}$ , activity ranges from 42.18 Bq/kg to 456.39 Bq/kg with GM of 150.63 Bq/kg and GSD 2.31. Table 4.2 and Figure 4.6 shows the radioactivity content of soil samples collected from the study areas.

**Table 4.2** Radioactivity content of soil sample (in Bq/kg) collected from the study areas.

Sample No.	$\text{K}^{40}$	$\text{U}^{238}$	$\text{Th}^{232}$	Sample No.	$\text{K}^{40}$	$\text{U}^{238}$	$\text{Th}^{232}$
1	255.40	268.48	456.39	8	57.10	49.01	57.86
2	316.88	335.32	331.89	9	144.87	47.93	42.18
3	331.73	319.30	331.24	10	137.52	292.50	293.56
4	320.08	318.17	328.27	11	108.48	278.82	255.18
5	187.30	35.21	74.71	12	94.26	254.41	239.51
6	762.65	49.72	74.43	13	124.81	255.63	244.82
7	856.42	46.73	70.99	14	12.82	35.85	44.40

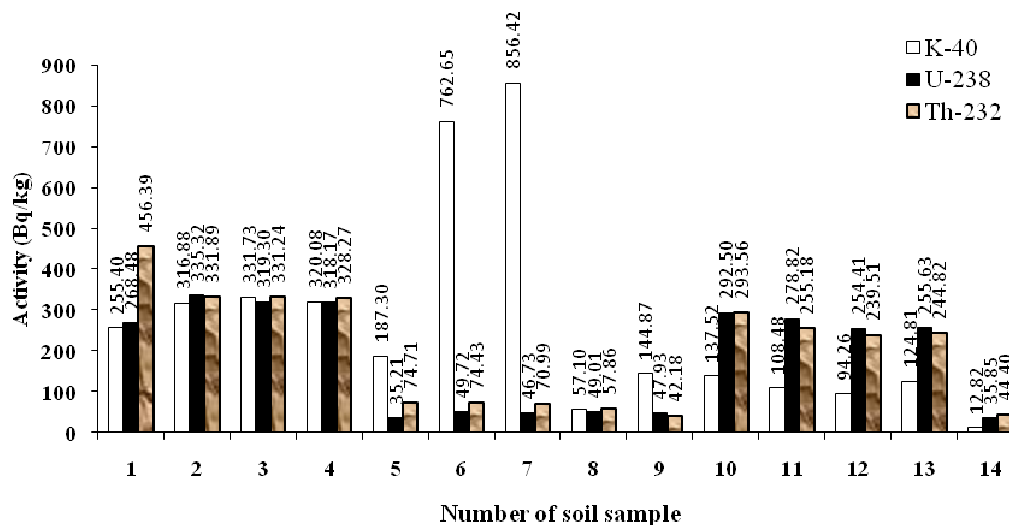


**Figure 4.6** Radioactivity content of soil sample collected from the study areas.

In this study,  $^{238}\text{U}$  and  $^{232}\text{Th}$  are the main concern since these two radionuclides are the parent nuclei of radon and thoron respectively. Hence,  $^{40}\text{K}$  activity can be neglected for the time being. The results obtained in this measurement is slightly higher which may be due to lower obtained efficiency of the particular instruments, experimentally determined using standard source provided from BARC, Mumbai.

The radioactivity content of collected building materials in the study area viz., brick, asbestos, glazed tiles and wood were also analyzed. Table 4.3 and Figure 4.7 shows the radioactivity content in different types of building materials viz., brick, asbestos, glazed tiles and wood in Bq/kg.

**Table 4.3** Activity content in Building materials (in Bq/kg).

Activity of Building materials (in Bq/kg)				
	Brick	Asbestos	Glazed Tiles	Wood
$\text{K}^{40}$	123.12	165.84	154.48	560.22
$\text{U}^{238}$	258.59	311.87	316.62	732.07
$\text{Th}^{232}$	257.29	330.12	252.62	908.48

From the result obtained, it is clear that highest content of potassium has been observed in wood samples while lowest content has been observed in brick samples.

Uranium content is found highest in wood sample; while lowest activity content has been observed in brick. Wood sample has the maximum content of thorium whereas glazed tiles sample has the minimum content. The natural radioactivity content obtained from the collected samples of building materials lies in normal range as compared to other data (Arman, 2007).

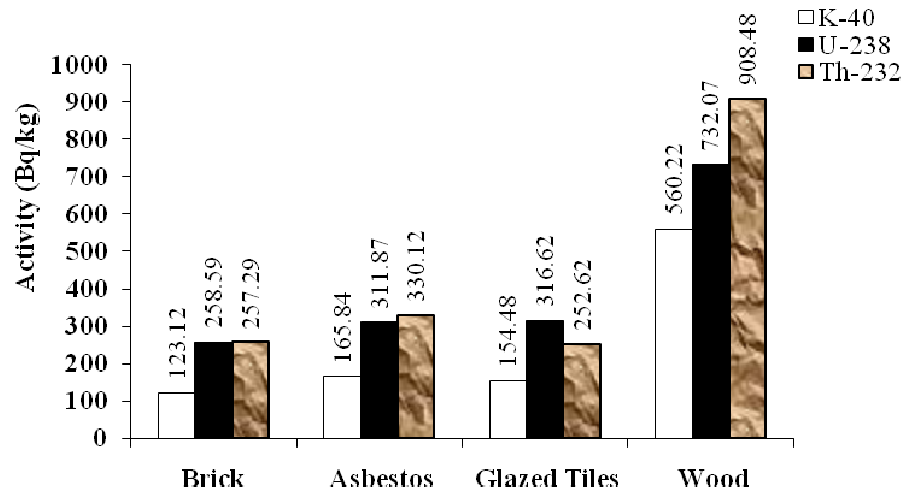


**Figure 4.7** Radioactivity content in Building materials

As shown in Fig. 3.9 of section 3.1.4, the indoor concentrations of radon and thoron in concrete building has the maximum annual average of indoor radon as well as thoron concentrations, while Assam type building with wooden/bamboo and asbestos walls has the lowest indoor radon and Assam type building with wooden/bamboo walls has the lowest indoor thoron concentrations. Even though the maximum contribution was found in case of wooden for its radioactivity content ( $^{238}\text{U}$ ), indoor radon concentration in concrete buildings constructed using bricks and rocks were found to be highest. This is due to the fact that buildings having wooden/bamboo walls have higher average ventilation rate as compared to concrete buildings. There are many spaces between the walls and the roofs in buildings having wooden/bamboo walls. The fact supporting higher indoor concentrations of radon in concrete buildings as compared to

other buildings is that this type of buildings have lower pseudo-ventilation rate where there were no openings between the walls and the roof as well as on the floor.

Fig. 4.8 shows the relation of radon along with the radioactivity content of collected building materials. In order to have a comparable co-relation, obtained indoor radon levels were multiplied by a factor of 5. In buildings with wooden/bamboo walls, the measured indoor radon concentration does not become higher as expected from the radioactivity content. This is due to higher ventilation rate of this type of buildings.

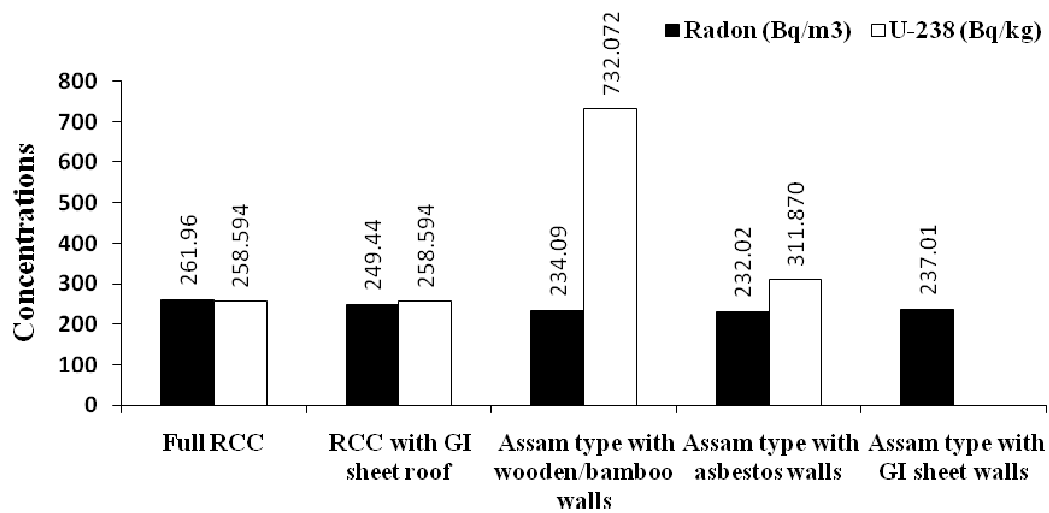


**Figure 4.8** Relation of  $^{238}\text{U}$  content of the building materials with indoor radon concentrations.

Most of the study area has a hilly terrain landscape, buildings are constructed on a steep slope. RCC buildings are constructed in such a way that not only the basement is in contact with the soil, but also the third or even fourth floor may have a wall adjacent to the soil in its sides which may increase radon/thoron emanation from walls in addition to the contribution from the materials of the building. Consequently, in this study, indoor radon/thoron concentrations obtained are higher in RCC buildings as compared to Assam type buildings. Due to limited sources and equipments, in this study we could not measure the radioactivity content from GI sheet.

The higher radioactivity content was found in wooden/bamboo samples in case of  $^{232}\text{Th}$ . Maximum indoor thoron concentration were found in concrete buildings constructed using bricks and rocks. Fig. 4.9 shows the relation of thoron along with the radioactivity content of collected building materials. In order to have a comparable correlation, indoor thoron levels were multiplied by a factor of 15.

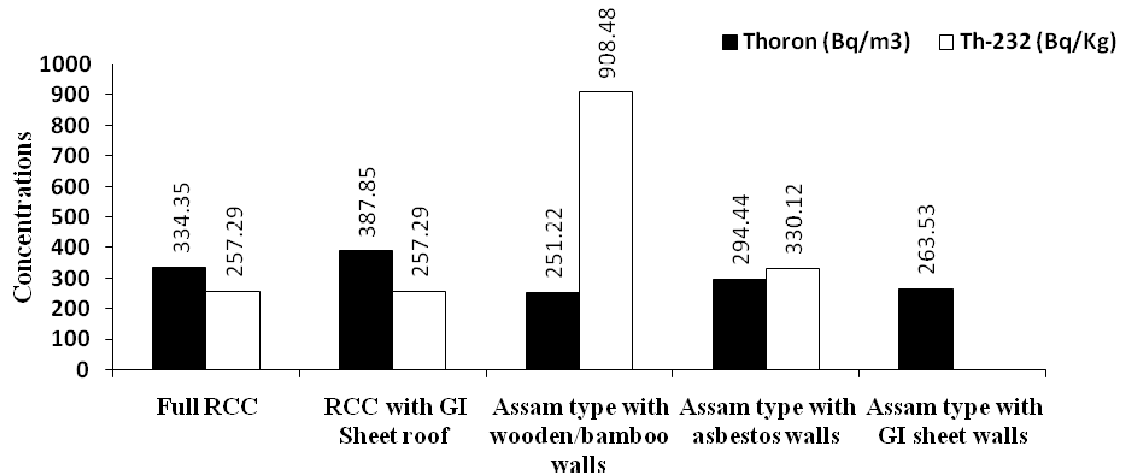


**Figure 4.9** Relation of  $^{232}\text{Th}$  content of the building materials with indoor radon concentrations.

Concrete buildings constructed using bricks and cement has high indoor thoron levels as well as the thorium content. This can be explained similarly as in the case of radon. The RCC building construction type is such a way that due to steep slope of the terrain, even higher walls are still in contact with the soil which does not occur in assam type buildings. Hence, this may increase emanation of thoron from the walls apart from contribution of the building materials in RCC buildings and may increase indoor thoron levels. Since, ventilation rate does not affect indoor thoron concentrations due to its short half life; the main reason affecting indoor thoron concentrations in dwellings seems to be the emanation rate from the soil into the buildings.

The radioactivity content of soil samples collected from the cave called “Chawngchilhi puk” also have been monitored and the activity of  $^{40}\text{K}$  is 304.978Bq/kg

and for  $^{238}\text{U}$ , its activity is 289.777Bq/kg, while the activity of  $^{232}\text{Th}$  is 510.588Bq/kg. In this cave the outside and inside gamma levels were measured using micro-R survey meter. At the outside cave the gamma level reaches 22 $\mu\text{R/h}$  at ground level and 20 $\mu\text{R/h}$  at 1m high. The inside gamma level is slightly higher than the outside gamma level and it reaches 27 $\mu\text{R/h}$  at ground level and 26 $\mu\text{R/h}$  at 1m high.

### 4.3 Radon content in soil gas

A 1.5 m length soil gas probe which is connected to RAD7 is inserted in the selected soil upto 1.2 m depth within the study area. The RAD7 is set up in *Sniff mode*, 5 mins cycle, 4 recycle and the Pump is in *Grab mode*. When the measurement is started, the soil gas is pumped by RAD7 into the detector chamber and the radon concentration is automatically measured.

#### 4.3.1 Results and discussions

Radon content in soil gas was measured in 30 locations in the study areas. The detail measured values are given in Table 4.4.

**Table 4.4** Measured values of radon content in soil gas from the study areas.

Location	Radon Bq/m <sup>3</sup>	Radon Error	Location	Radon Bq/m <sup>3</sup>	Radon Error
1	3600	763.25	16	25400	1965
2	5950	763.25	17	5030	891
3	29900	2110	18	14700	1482.5
4	22000	1822.5	19	11900	1335
5	47300	2675	20	9820	1220
6	30200	2115	21	9740	1217.5
7	24800	1930	22	8300	1132.5
8	9410	1212.5	23	7670	1092.5
9	27700	2045	24	20200	1740
10	3980	817.25	25	8570	1147.5
11	14300	1462.5	26	6290	999
12	15500	1537.5	27	8690	1160
13	12300	1372.5	28	9360	1195
14	24100	1902.5	29	9230	1185
15	18500	1677.5	30	12400	1370



In Lunglei district, radon content in soil gas was measured in five locations and the average value ranging from  $3600\text{Bq/m}^3$  to  $47300\text{Bq/m}^3$  with a geometric mean (GM) of  $14613.52\text{Bq/m}^3$  and GSD 2.40. Figure 4.10 shows the variation of radon in soil gas in Lunglei district.

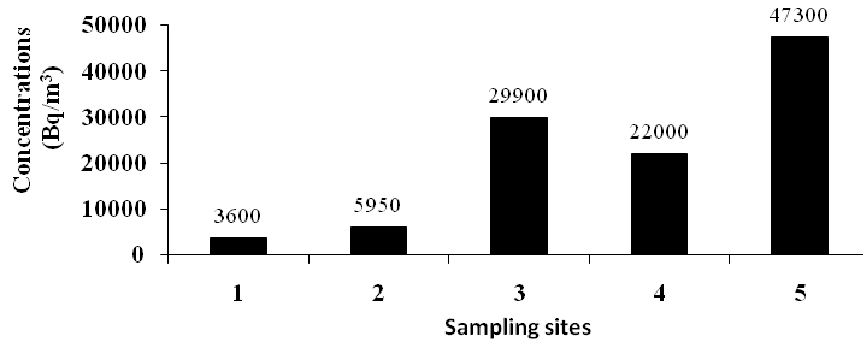


**Figure 4.10** Radon content in soil gas in Lunglei District.

In Serchhip district, radon content in soil gas was measured in 14 locations. The minimum value is  $3980\text{Bq/m}^3$  and the maximum value is  $30200\text{Bq/m}^3$ . The geometric mean is  $14656.54\text{Bq/m}^3$  with GSD 1.81. Figure 4.11 shows the variation of radon in soil gas in Serchhip district.

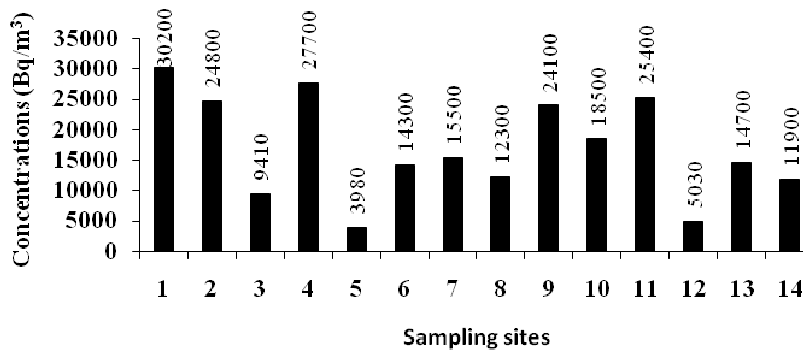


**Figure 4.11** Radon content in soil gas in Serchhip District.

Radon content in soil gas was measured in Mamit district in 11 locations. The highest value is  $20200\text{Bq/m}^3$  and the lowest value is  $6290\text{Bq/m}^3$ . The geometric mean is  $9570.83\text{Bq/m}^3$  with GSD 1.33. Figure 4.12 shows the variation of radon in soil gas in Mamit district.

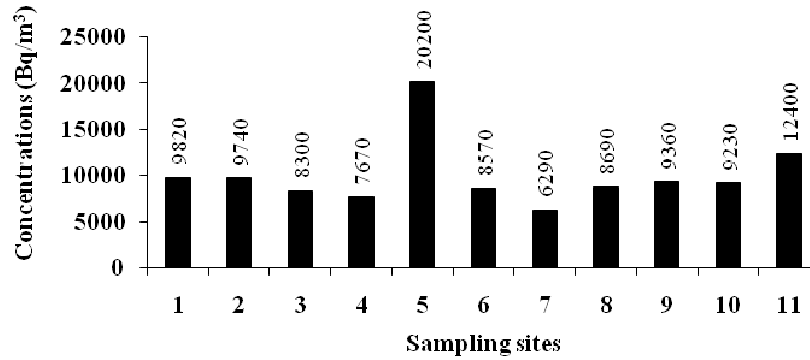


**Figure 4.12** Radon content in soil gas in Mamit District.

Comparing the radon content in soil gas from the three districts, we found that the highest and lowest value are found in Lunglei district ( $47300\text{Bq/m}^3$  and  $3600\text{Bq/m}^3$ ) with a geometric mean (GM) of  $14613.52\text{Bq/m}^3$ . Figure 4.13 shows the comparison of radon in soil gas in the three districts.

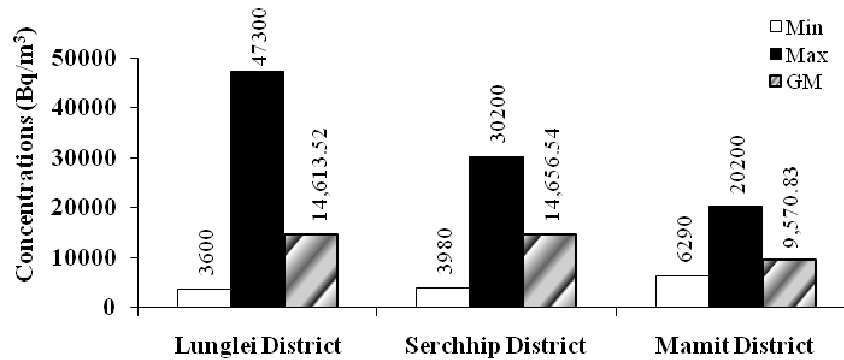


**Figure 4.13** Comparison of radon content in soil gas.

#### 4.4 Background gamma radiation

Gamma background radiation has a terrestrial source as well as cosmic source. The measured levels of background gamma level may also help us in predicting the content of source radioactive elements of radon as well as thoron in the vicinity of the study area. Simultaneous measurement of background gamma radiation level was done on ground level as well as at 1m height from the ground, both indoor and outdoor of the selected dwellings where dosimeters were deployed. The instrument used for this

measurement is a portable device called Micro-R Survey Meter which automatically detects and measures the background gamma radiation for every 8 seconds (gate time).

#### 4.4.1 Results and discussions

Spot measurement of background gamma radiation level ranges from  $10\mu\text{R/h}$  –  $22\mu\text{R/h}$  in indoor and from  $11\mu\text{R/h}$  –  $23\mu\text{R/h}$  in outdoor at ground whereas it ranges from  $9\mu\text{R/h}$  –  $22\mu\text{R/h}$  in indoor and from  $10\mu\text{R/h}$  –  $21\mu\text{R/h}$  in outdoor at 1m height from the ground. The values are slightly higher at ground as compared to 1m height. Obtained background gamma level using Micro-R Survey meter in this study seems to be little higher. This is due to small sample size of the survey meter, which is collected only within 8 sec. IERMON was installed recently in Aizawl City which has larger sample size (5 min analysis). From this instrument, obtained background gamma level was found to be lower, which ranges from  $8.05\mu\text{R/h}$  –  $11.5\mu\text{R/h}$ . The measured background gamma radiation level is comparable with the nationwide survey result which is  $10.05\mu\text{R/h}$  (Nambi *et al.*, 1986).

The background gamma radiation levels do not provide us good and clear cut assumption or prediction for the levels of indoor radon as well as thoron. However, it is clear that terrestrial source is dominant as compared to cosmic source but only with slightly higher value.

## Chapter 5

### Conclusion

Human beings are exposed to ionizing radiations of natural origin, namely terrestrial and extra-terrestrial radiation. Radiation of extra-terrestrial origin is from high energy cosmic ray particles while that of terrestrial origin is due to the presence of naturally occurring radio-nuclides; mainly potassium and the radio-nuclides in the decay chains of uranium and thorium and the internal exposure from radioactive elements through food, water and air. Therefore, estimation of this component is an important task. This calls for time integrated measurements of radon, thoron and progeny concentrations covering diurnal and seasonal variations. With the progress of studies and development of instruments, measurement of these radionuclides has covered some of the states in India (Sadasivan *et al.*, 2003). In some part of India, apart from being determined, continuous monitoring is also in progress. In the north-eastern part of India, very little studies have only been done covering small part of the whole area (Srivastava *et al.*, 1996). In Mizoram, even though some previous studies had been done including only 17 houses, this is far less than the required data to show the exact status of the state (Ramachandran *et al.*, 2003).

From the literature surveyed as discussed in Chapter 1, considerable work on the topic of measurements of radon and thoron exist. However, measurement of population dosimetry particularly in the study area is the novel aspect dealt in the present work. The work regarding measurement of the concentration of these gases in the state of Mizoram is still in the initial stage and very few data are available. But this data is not enough for the study of inhalation doses of these gases contained in the inhaled air in the dwellings as well

as for the study of deposition of radioactive sources in the soil. Keeping this objective in mind, measurement details of indoor radon, thoron and their progeny concentrations and status of the exhalation of these gases from soil in the north-eastern part of India, covering three districts, viz., Lunglei, Serchhip and Mamit Districts in the state of Mizoram, which covers the middle and north-western part of the State is presented in this thesis. It also includes the study of the contribution of the building materials used for dwellings to the radon, thoron and their progeny concentrations besides the atmospheric air and also the determination of the activity content of radioactive elements in and around the dwellings. These constitute the bulk of the studies carried out in the thesis.

Before the actual work had been done, training for acquaintance of the instruments, experimental determination of calibration of instruments etc. was performed using the facilities at Bhabha Atomic Research Center (BARC), Mumbai, some of the results obtained are outlined in Chapter 3 and Chapter 4. Regarding some instruments like Spark counter and NaI (Tl) detector, obtaining the operating voltage and calibration of NaI (Tl) detector has to be done for each specific device. Hence, the operating voltage of the particular Spark counter used in this study has been determined experimentally at the laboratory in Aizawl, but, with the detection of slight change in the track densities, the required final calibration has been done with the scientists from BARC, Mumbai. Calibration of NaI (Tl) detector has also been done experimentally at the laboratory in Aizawl.

We have found that the results obtained in measuring indoor radon and thoron concentrations in this study area are low, which lies in the range covered by nationwide survey result (Ramu *et al*, 1992) as well as the ICRP regulations (ICRP, 1993). The investigation shows no significant radiological risks for the inhabitants and is well within the limits prescribed by UNSCEAR (2006). We have found that radon has higher

concentrations as compared to thoron. Among the three districts, Mamit District has the maximum annual average indoor concentrations of radon as well as thoron, but is minimum in Serchhip District for radon and thoron. There have been many factors affecting radon, thoron and their progeny concentrations in the environment. From the present study, the pseudo-ventilation rate and air exchange rate as well as entry rate from the soil in to the dwellings plays a vital role in indoor radon concentrations while the emanation rate and entry rate from the soil into buildings are the main factors affecting indoor thoron concentrations in the study area.

Monitoring of seasonal variation of these gases as shown in chapter 3, section 3.1.4 shows that indoor radon concentrations was found to be highest in winter season and lowest in rainy season whereas indoor thoron concentration was found to be highest in rainy season and lowest in summer season. In winter, the temperature was lowest among the three seasons and hence ventilation rate was also lowest. Whereas in summer, because of high temperature which results in higher ventilation rate of the dwellings, low concentration of indoor radon as well as thoron were observed during this season. The climate of the State of Mizoram is moderate throughout the year. The State of Mizoram has a pleasant climate. It is generally cool in summer and not very cold in winter. During winter, the temperature varies from 11°C to 21°C and in the summer it varies from 20°C to 30°C. The entire area is under the direct influence of the monsoon. It rains heavily from May to September and the average rainfall is 250 cm (Tiwari, 2006). Hence, rainy season is long in the state and it is also difficult to draw a clear cut differentiation of different seasons within a year. However, the temperature difference is not much in different seasons as the temperature is mild throughout the year. Hence, during rainy season also we have the highest thoron concentration. The ventilation rate is always high during rainy and summer season and does not vary much during these seasons. But, it is still obvious that the air

exchange rate due to ventilation plays the most important role in seasonal variation of radon levels in the state. This is due to the fact that the most contributor of radon gas is the rate of exhalation from soil and building materials, and the removal depends strongly on ventilation rate. Hence high ventilation rate will surely lowers the level and vice versa.

Due to overall low concentration of radon in the environment, the rate of accumulation of radon in indoors air during winter season is not so high even with low ventilation rate or air exchange rate. As a result, with highest radon level observed during winter, this low rate of accumulation may results in low radon level comparing with the other seasons. It can also be concluded that the rate of exhalation of radon from soil and building materials may also be low in the measured areas.

From the results obtained regarding types of materials used in construction of building as discussed in chapter 3, section 3.1.4, we can conclude that indoor radon levels as well as thoron levels are higher in concrete buildings as expected compared to Assam type buildings. This is due to the lower air exchange rate or pseudo-ventilation rate where there exist no openings between the walls and roofs or floors. More openings between the walls and roofs as well as floors of assam type buildings results in more escape rate for radon and thoron and hence results in low indoor radon/thoron levels. Besides this, it was observed that some RCC buildings are constructed on a steep slope in such a way that even the fifth floor have a wall adjacent to the soil on its sides and hence radon/thoron emanation through these walls is supposed to enhance concentration of the gases in addition to the contribution due to building materials. This kind of construction of building is not observed in other types (Assam type) of buildings. This condition supports the observation of higher indoor accumulation of radon/thoron gases in RCC buildings.

A well geological mapping has not been found in the study area and is difficult to locate the exact geological condition. However, in Mamit district, local fault was found

below the hill where Mamit town was located. In Serchhip town area, a small fault region had been identified. In Lunglei district, the identification of fault in the dwelling areas is not clear. Comparing the radon concentration in the available geological conditions and places where it was not identified, the radon/thoron concentration was higher in unrepresented areas than in fault region which is in contradictory to the expected one. This may be the influencing of the material used for the construction of buildings and the ventilation rate or the unidentified region may also contain those areas rich in radon and thoron sources. Hence, this can be the reason for this contradictory result even though it is difficult to have a clear cut conclusion for the time being. It may be mentioned again that due to limited availability of recorded geological conditions to refer to in the study area, measurements of radon and thoron concentration based on geological conditions could not be performed satisfactorily.

The results obtained in the study areas show that the radon gas concentrations are found to be higher than the thoron concentrations in all the parameters considering whether it a geographical, geological or house type distributions. The radon and thoron concentrations obtained in this work lies in the range covered by nationwide survey result (Ramu *et al.*, (1992) as well as the ICRP regulations (ICRP (1993).

Measurement of progeny concentrations of radon and thoron as well as calculations of equilibrium factors and inhalation dose rate have been done only in limited houses from the study area due to limited DPS. The calculated annual average value of equilibrium factor for radon ( $F_R$ ), 0.35 is slightly lower in comparison to average global level, 0.4. Whereas, the calculated annual average value of equilibrium factor for thoron ( $F_T$ ), 0.09 is slightly higher with respect to average global level, 0.03 (UNSCEAR, 2000). This may be due to high indoor concentrations of radon as well as thoron and high EETC values in comparison to average global level. Regarding annual effective doses, the



obtained value for the total annual effective dose rate due to radon as well as thoron are higher than global average value. It has been found that the maximum inhalation dose rate for radon as well as thoron is obtained during winter season, while minimum value is obtained during summer season. Since obtained equilibrium factor for radon is lower and that for thoron is higher hence the inhalation dose value obtained using this factor along with the indoor concentrations gives us lower value for radon but higher value for thoron in comparison to global average value.

The concentration of indoor radon levels in the study area is also depends on the rate of exhalation of radon in the vicinity of the dwellings. As discussed in Chapter 4, section 4.1.1, the correlation of radon flux and indoor radon concentration are not well related which may be due to the different method of measurements, in which radon flux measurement is an active method for a duration of about an hour having a cycle of 15 minutes while indoor radon concentration measurement is a passive time integrated type which took at least 120 days. The results show that radon flux obtained was slightly higher but close to the world average ( $22\text{mBq/m}^2/\text{s}$ ).

It is interesting to note that, in some sampling sites the massive landslides took place and cracks are also observed in the floors and walls of the houses which can cause large damage to the buildings. So, the occupants need to leave their houses due to this massive landslide and cracks. The exhalation of radon gases should be high as compared to unaffected area. But, due to the low concentration of radon in the environment, the exhalation of radon gases in these areas are still not very high as compared to unaffected area.

Natural radioactivity is wide spread in the earth's environment and it exists in soils, rocks, water and sand etc. (Mahur *et al.*, 2010). Distribution of naturally occurring radio-nuclides mainly  $^{238}\text{U}$ ,  $^{232}\text{Th}$  and  $^{40}\text{K}$  and other radioactive elements depends on the

distribution of rocks from which they originate and on the processes through which they are concentrated. The measurement of activities of naturally occurring radio-nuclides is important for the estimation of radiation risk. From the result obtained, the radioactivity content of  $^{40}\text{K}$  is highest (GM 171.83 Bq/kg) and the radioactivity content of  $^{238}\text{U}$  is lowest (GM 128.48 Bq/kg) in the study area. Due to this lower radioactivity content of  $^{238}\text{U}$  and  $^{232}\text{Th}$ , the exhalation of radon and thoron from the soil is less which affects less concentration of indoor radon and thoron. From the analysis of building materials, wood has the highest radioactivity content of  $^{40}\text{K}$ ,  $^{238}\text{U}$  and  $^{232}\text{Th}$ . The soil radioactivity measurement will help in understanding the type and available radioactive series present in the soil of the area of measurement.

The measurement of radon content in soil gas as discussed in Chapter 4, section 4.3.1 shows that the average value of measured radon content in soil gas is lower as compared to previous research findings in other areas (Singh *et al.*, 2010). This also helps in explaining the overall slightly lower determined radon levels in the whole study area as compared to previous findings in other areas.

It is observed that the inner surfaces of the cave is made up of rocks, the background gamma radiation level inside the cave is slightly high as compared to gamma radiation level at outside the cave as well as inside the dwellings.

It is hoped that the studies and observations discussed here will be of considerable help in generating large scale dosimetric data on the inhalation doses to the populations and contributes the status of Mizoram as well as north-eastern India in the mapping of radon and thoron in India.

Inspite of the best efforts being put into this research, there are still some inadequacy to be found somewhere. 'To err is human' as the saying goes, there are still some errors here and there. Some errors are committed without any knowledge and in some

case there are no other alternative available. Here are some of the errors which has been observed:

### *1. Calibration factor of Pin-hole cup for thoron discrimination*

For indoor radon/thoron measurement, Solid State Nuclear Track Detector (SSNTD) based dosimeters developed by BARC have been used. Cellulose Nitrate films (LR-115 type II) are used as detectors. The dosimeter system is a cylindrical plastic chamber divided into two equal compartments. The two equal compartments on both sides are filter and pinhole compartments. The filter compartment allows the entry of both radon and thoron gas to pass through inside by covering the cup with a filter paper blocking the entry of the progeny and hence tracks formed on the film in the filter compartment are related to the concentrations of both radon and thoron gases. In the pinhole compartment only radon gas was allowed to enter which has a modification from the earlier twin-cup dosimeter system (Eappen, 2005) by using a cap with a pin hole in it. This pin hole is designed in size and thickness of cap so as to block thoron from entry inside by considering the diffusion length and half life of thoron. Initially, this pinhole cap was provided with only one pin-hole with a calibration factor of 0.023. Later, it was found that the shape and size of this pin-hole was not appropriate and the cup was provided with four holes in it. However, the calibration factor for these four pin-holes cup was not clearly stated and the old single pin-hole cup calibration factor was used for all calculations.

### *2. RAD7 for radon concentration, flux and soil gas measurement*

The presence of high quantity moisture causing error in using RAD7 is also a big issue in this study. Mizoram receives good amount of rainfall from monsoon starting as early as March to October in a year. Hence, dry season is less and the accuracy of the readings during these wet seasons pose some questions. For accurate readings the humidity readings in RAD7 instrument is suppose to fall below 10 in the LCD screen which is quite

difficult to achieve during monsoon months. Soil gas measurements had also been taken from several locations in the study areas in Mizoram. However, the data seems to fluctuate on a wide range and hence found to be not fitting for reproduction.

### *3. Gamma radiation measurement*

The instrument used for measuring gamma level is Nucleonix made Micro-R Survey meter (GM based) for spontaneous measurement, which gives the dose rate in the unit of  $\mu\text{R/h}$ . Obtained background gamma level in this study seems to be a little higher. This is due to the small sample size of survey meter, which is collected only within 8 seconds. IERMON was installed recently In Aizawl which has larger sample size (5 min analysis). From this instrument, obtained background gamma level was found to be lower as compared to that obtained in the same area using Micro-R Survey meter which ranges from  $8.05\mu\text{R/h} - 1.5\mu\text{R/h}$ . Hence, calibration between these two instruments needs to be maintained.

## References

- Amgarou, K., Font, Ll., Domingo, C., Fernández, F., Baixeras, C. (2001). Simultaneous measurements of radon, radon progeny and thoron concentrations using Makrofol-DE detectors. *Rad. Meas.*, **34 (1-6)**, 139 – 144.
- Arman Erkan. (2007). An Investigation on the Natural Radioactivity of Building Materials, Raw Materials and Interior Coatings in Central Turkey. *Turk. J. Med. Sci.*, **37**, 199 – 203.
- Azimi-Garakani, D., Shahbazi, M., and Latifi, G., (1981). A New Automatic Spark Counting System. *Nucl. Tracks*, **4**, 141 – 148.
- Bhagwat, A. M., Soman, S. D., (1976). Spark counting technique for the automatic counting of alpha particle tracks in thin films of cellulose nitrate (CN). *IARP 5/27*.
- Bhagwat, A. M., Hari Singh., Soman, S. D., (1976). Correlation for the observed track-hole densities in the spark counting of fission tracks. *Nucl. Instr. And Methods*, **138**, 173 – 177.
- Bojanowski, R., Radescki, Z., Campbell, M. J., Burns, K. I. and Trinkl, A. (2001). Report on the intercomparison run for the determination of radionuclides in soils IAEA-326 and IAEA-327. IAEA/AL./100 Report. Vienna, Austria.
- Chandrashekara, M. S., and Paramesh, L. (2008). Studies of Radon/Thoron levels in Mysore City, India. *Proc. of DAE – BRNS Theme Meeting, Radon – 2008*, 87 – 90, Dated March 11 – 13, 2008.
- Cosma, C., Dancea, F., Jurcut, T., Ristoiu, D., (2001). Deyermination of <sup>222</sup>Rn emanation fraction and diffusion coefficient in concrete using accumulation chambers and the

- influence of humidity and radium distribution. *Applied Radiat. And Isotopes*, **54**, 467 – 473.
- David, J. N. and John, D. H. (2008). Seasonal radon variations in Utah testing results: Short term test results within 10% of the EPA threshold (4.0 pCi/L) should be repeated in a different season. Proceedings of the American Association of Radon Scientists and Technologists 2008 International Symposium Las Vegas NV, September 14 – 17, 2008.
- Durrani S. A. and Bull R. K. (1987). Solid State Nuclear Track Detection. Pergamon Press, Oxford, First Edition, 169 – 173.
- Dwivedi, K. K., and Ghosh, S., (1991). Prospects and Potentials of Radon Monitoring in North-Eastern India. *Proc. of Second Workshop on Radon Monitoring in Radioprotection Environmental Radioactivity and Earth Sciences*, ICTP, Trieste, Italy, 25 November – 6 December.
- Eappen, K. P., Mayya, Y. S. (2004). Calibration factors for LR-115 (type-II) based radon thoron discriminating dosimeter. *Rad. Meas.*, **38**, 5 – 17.
- Eappen, K. P., (2005). Development of a passive dosimeter for the estimation of inhalation dose due to radon and thoron. A Thesis submitted to University of Mumbai for the Degree of Doctor of Philosophy (Physics).
- Eappen, K. P., Sahoo, B. K., Ramachandran, T. V., Mayya, Y. S. (2008). Calibration factors for thoron estimation in cup dosimeter. *Rad. Meas.*, **33**, S418 – S421.
- Elster, J. and Geitel, H. (1901). Uber eine fernere Analogie in dem elektrischen Verhalten der atirlichen und der durch Becquerelstrahlen abnorm leitend gemachten Luft [On a further similarity in electrical content between natural air and that made abnormally conductive by Becquerel rays]. *Physik Z.*, **2**, 590 – 593.

- Final Report to ONGC, (2008). Environmental Impact Assessment For Exploratory Drilling at Hortoki Village, Kolasib, Mizoram, SENES Consultant India, Kolkata. February.
- Firestone, R. B., Shirely, V. S., (1998). Table of Isotopes, eight edn. (John Wiley, New York).
- Fleischer, R. L., Mogro-Campero, A. (1978). Mapping of integrated radon emanation for detection of long-distance migration of gases within the earth: Techniques and principles. *J. Geophys. Res.*, **83**, 3539 – 3549.
- Frank, A. L. & Benton, E. V., (1977). Radon Dosimetry using Plastic Nuclear Track Detectors. *Nucl. Track Det.*, **1**, 149 – 179.
- Gessell, T. & Lowder, W. M., (1980). Natural Radiation Environment III, *Proc. of Symposium*, Houston, Texas. Springfield, Virginia.
- Guo Q., Shimot M., Ucebet Y., Minatof S. (1992). The study of thoron and radon concentrations in dwellings in progeny Japan. *Radiat. Prot. Dosim.* **45**, 357 – 359.
- Gupta, M., Mahur, A. K. and Verma, K. D. (2012). Indoor radon levels in some dwellings surrounding the National Thermal Power Corporations (NTPCs), India. *Adv. Appl. Sci. Res.*, **3(3)**, 1262 – 1265.
- Ibrahim, N. (1999). Natural activities of  $^{238}\text{U}$ ,  $^{232}\text{Th}$  and  $^{40}\text{K}$  in building materials. *J. Environ. Radioactivity*, **43**, 255 – 258.
- ICRP, (1984). International Commission for Radiological Protection Publication No. 39, Principles of Limiting Exposure of the Public to Natural Sources of Radiation, Pergamon Press, Oxford.
- ICRP (1993). Protection against  $^{222}\text{Rn}$  at Home and at Work. ICRP Publication 65, *Annals of ICRP* 23.
- ICRP (1999). Protection of the Public in Situations of Prolonged Radiation Exposure, Publication 82, Elsevier Science B.V.

- Jacobi, W., (1993). The History of the Radon Problems in Mines and Homes, *Ann. ICRP*, **23**, 39 – 45.
- Khan, H. A. and Haseebulah (1993). Indoor radioactive pollution due to radon and its daughters. *Journal of Islamic Academy of Sciences*, **5:4**, 249 – 255.
- Kumar, S., Gopalani, D. and Jodha, A. S. (1994). Indoor radon levels in India. *Bull. Radiat. Prot.* **17(3&4)**, 41– 45.
- Lubin, J. H., (1994). Lung Cancer and Exposure to Residential Radon, *Am. J. Epidemio.*, **140**, 323 – 332.
- Mahur, A. K., Kumar, Rajesh., Mishra, M., Ali, S. A., Sonkawade, R. G., Singh, B. P., Bhardwaj, V. N., and Prasad, Rajendra., (2010). Study of radon exhalation rate and natural radioactivity in soil samples collected from East Singhbhum Shear Zone in Jaduguda U-Mines Area, Jharkhand, India and its radiological implications. *Ind. J. Pure & Applied Physics*, **48**, 486 – 492.
- Malik S. R., Durrani S. A. (1974). Spatial distribution of uranium in meteorites, tektites, and other geological materials by spark counter. *Int. J. Applied Radiation and Isotopes*, **25** (1), 1 – 8.
- Mayya, Y. S., (2004). Theory of radon exhalation into accumulators placed at the soil – atmosphere interface. *Radiat. Prot. Dosim.* **3 (3)**, 305 – 318.
- Mayya, Y. S., Eappen, K. P., and Nambi, K. S. V., (1998). Methodology for Mixed Field Inhalation Dosimetry in Monazite areas using a Twin Cup Dosimeter with Three Track Detectors. *Radiat. Prot. Dosim.* **77**, 177 – 184.
- Majumdar D., (2000). Radon in the Environment and Associated Health Problems, *Resonance* July, 44 – 55.
- Menon, M. R., Lalith, B. Y., and Shukla, V. K., (1987). Natural radioactivity in building materials in India. *Bull. Radiat. Prot.*, **14**, 45 – 48.



- Mishra, R., and Mayya, Y. S., (2008). Study of a Deposition-based Direct Thoron Progeny Sensor (DTPS) Technique for Estimating Equilibrium Equivalent Thoron Concentration (EETC) in Indoor Environment. *Radiat. Meas.*, **43**, 1408 – 1416.
- Mishra Rosaline, Mayya Y.S., Kushwaha H.S., (2009). Measurement of  $^{220}\text{Rn}/^{222}\text{Rn}$  progeny deposition velocities on surfaces and their comparison with theoretical models. *Aerosol Science* **40**, 1 – 15.
- Nagaratnam, A., (1994). Radon : A Historical Overview, *Bull. of. Rad. Prot.*, **17**, 1 – 10.
- Nair, N. B., Eapen, C. D., Eappen, K. P., Boban, T. G., Ramachandran, T. V., Ramu Subba, M. C., and Nambi, K. S. V., (1994). Indoor radon-thoron inhalation doses in the HBRA, Chavara, Kerala, Proc. 3<sup>rd</sup> National Symposium on Environment, Thiruvananthapuram, 3<sup>rd</sup> – 5<sup>th</sup> March.
- Nambi, K. S. V., Bapat, V. N., David, N., Sundaram, V. K., Sunta, C. M., Soman, S. D., (1986). Natural background radiation and population dose distribution in India. Internal Report, Health Physics Division, BARC.
- Nambi, K. S. V., Subba Ramu, M. C., Eappen, K. P., Ramachandran, T. V., Muraleesharan, T. S. and Shaikh, A. N. (1994). A new SSNTD method of combined measurement of radon and thoron working levels in atmosphere. *Bull. of Radiat. Prot.*, **17**, 34 – 35.
- Nazaroff, W.W. (1988a). Soil as a Source of Indoor Radon: Generation, Migration and Entry, in Nazaroff, W.W. and Nero, A. V., eds., Radon and its Decay Products in Indoor Air. New York, Wiley, 57 – 112.
- Nazarof, W. W., and Nero, A. V., (1988). Radon and its Decay Products in Indoor Air. Wiley, New York.
- Nazaroff, W. W., (1992). Radon transport from soil to air. *Rev. Geophys.* **30 (2)**, 137 – 160.

- Petropoulos, N. P., Anagnostakis, M. J., Simopoulos, S. E. (2001). Building materials radon exhalation rate: ERRICCA intercomparison exercise results. *The Sc. of the Tot. Environ.*, **272**, 109 – 118.
- Pillai, P. M. B., and Paul, A. C., (1999). Studies on the equilibrium of thoron and its daughters in the atmosphere of a monazite plant and its environs. *Radiat. Prot. Dosim.*, **82**, 229 – 232.
- Porstendorfer, J., (1994). Properties and behaviour of radon and thoron and their decay products in air. *J. Aerosol Sci.*, **25**, 219 – 263.
- RAD7 manual extracted from [www.durridge.com/products\\_rad7.shtml](http://www.durridge.com/products_rad7.shtml)
- Ramachandran, T. V., Mayya, Y. S., Sadashivan, S., Nair, R. N., and Eappen, K. P., (2003). Radon-Thoron Levels and Inhalation Dose Distribution Patterns in Indian Dwellings, *BARC Report.*, BARC/2003/E/026. Bhabha Atomic Research Center, Mumbai, Government of India, 1– 43.
- Ramachandran, T. V., Mayya, Y. S., Shaikh, A. N., Khan, A. H., Puranik, V. D., and Raj, Venkat, V., (2004). Radon Monitoring and its Application for Earthquake Prediction, *BARC Report.*, BARC/2004/E/035. Bhabha Atomic Research Center, Mumbai, Government of India, 1– 43.
- Ramola, R. C., Kandari, M. S., Rawat, R. B. S., Ramachandran, T. V. and Choubey, V. M., (1998). A Study of Variations of Radon Levels in Different Types of Houses. *J. Environ. Radioactivity* **39**, 1 – 7.
- Ramu, S., M. C., Shaikh, A. N., Muraleedharan, T. S., and Ramachandran, T. V. (1992). Measurements of Indoor Radon Levels in India using Solid-State Nuclear Track Detectors: Need for Standardisation. *Def. Sc. J.*, **42**, 219 – 225.
- Richon, Patrick., Klinger, Yann., Tapponnier, Paul., Li, Chen-Xia., Van Der Woerd, Jerome., Frederic Perrier., (2010). Measuring radon flux across active faults:

- Relevance of excavating and possibility of satellite discharges. *Rad. Meas.*, **45**, 211 – 218.
- Rohmingliana, P. C., Vanchhawng, Lalmuanpuia, Thapa, R. K., Sahoo, B. K., Singh, O. P., Zoliana, B., Mayya, Y. S., (2009). Measurement of Indoor Radon and Thoron Concentrations in Correlation to Geographical Location and Construction types of Buildings in Mizoram.(with special reference to Aizawl, Champhai and Kolasib districts). *Proc. VI<sup>th</sup> Conference of Physics Academy of North East*, Tripura University, April 3 – 4.
- Rohmingliana, P.C., Vanchhawng, Lalmuanpuia., Thapa, R.K., Sahoo, B.K., Mishra, R., Mayya, Y.S. and Zoliana, B. (2011). Seasonal Variations of Radon/Thoron and Their Progeny Concentrations in Saiha District, Mizoram, India. *Proc. of International Conference on Advances in Environmental Chemistry, (AEC 2011)* during November 16 – 18, 2011, Mizoram University, Aizawl. **ISBN: 978-93-81361-53-5**, 193 – 195.
- Sadasivan, S., Shukla, V. K., Chinnasaki, S. and Sartandel, S. J. (2003). Natural and Fallout Radioactivity Measurements in Indian Soil. *J. Radio. Anal. And Nucl. Chem.*, 256, 603 – 607.
- Sahoo, B. K., Nathwani, D., Eappen, K, P., Ramachandran, T. V., Gaware, J. J., Mayya, Y. S., (2007). Estimation of Radon Emanation Factor in Indian Building Materials, *Radiat. Meas.*, **42**, 1422 – 1425.
- Sahoo B . K., (2008). Theory of radon emanation and method of source term estimation by flux measurement technique. *Proc. of DAE – BRNS Theme Meeting, Radon – 2008*, 18 – 24, Dated March 11 – 13, 2008.
- Sahoo, B. K. and Mayya, Y. S. (2010). Two Dimensional Diffusion Theory of Trace Gas Emission into Soil Chambers for Flux Measurements. *Agriculture and Forest Meteorology*, **150**, 1211–1224.

- Samiti, J. M., Stolwijk, J., and Rose, S. L., (1991). Summary: International Workshop on Residential Radon Epidemiology, *Health Phys.*, **60**, 223 – 227.
- Sankaran, A. V., Jayaswal, B., Nambi, K. S. V., Sunta, C. M., (1986). U, Th and K distribution inferred from Regional Geology and the Terrestrial Radiation Profiles in India. Technical Report, BARC.
- Sathish, L. A., Sannappa, J., Paramesh, L., Chandrashekara, M. S., and Venkataramaiah, P., (2001). Studies on Indoor Radon/Thoron and Their Progeny Levels at Mysore City, Karnataka State, *Indian Journal of Pure and Applied Physics*, **39**, 738 – 745.
- Shashikumar, T. S., Ragini, N., Chandrashekhar, M. S. and Paramesh, L., (2008). Studies on radon in soil, its concentration in the atmosphere and gamma exposure rate around Mysore city, India. *Current Sci.* **94** (9), 1180 – 1185.
- Shukla, V. K., Ramachandran, T. V., Chinnasakki, S., Sartendal, S. J., and Shanbhag, A. A., (2005). Radiological Impact of Utilization of Phosphogypsum and Fly Ash in Building Materials in India. *Int. Sci. Cong. Series*, **1276**, 339 – 340.
- Singh, B., Singh, S. and Virk, H. S., (1993). Radon Diffusion Studies in Air, Gravel, Sand, Soil and Water, *Nucl. Tracks Radiat. Meas.*, **22**, 455 – 458.
- Singh, Joga., Singh, Harmanjit., Singh, Surinder., and Bajwa, B. S. (2010). Measurement of soil gas radon and its correlation with indoor radon around some areas of Upper Siwaliks, India. *J. Radiol. Prot.*, **30**, 63.
- Srivastava, Alok, Lalramengzami, R., Laldawngliana, C., Sinha, C., Ghosh, S., Dwivedi, K. K., Saxena, A., and Ramachandran, T. V., (1996). Measurement of Potential Alpha Energy Exposure (PAEE) of Radon and its Progenies in Dwellings in the North-Eastern Region of India. *Radiat. Meas.*, **26**, 291 – 295.

- Srivastava, G. K. (2008). Radon and radon daughters measurement with special reference to uranium mining and its environment. *Proc. of DAE – BRNS Theme Meeting, Radon – 2008*, 35 – 40, Dated March 11 – 13, 2008.
- Stranden, E. (1988). Building materials as a source of indoor radon, in Nazaroff, W. W. and Nero, A. V. (eds.), *Radon and its Decay Products in Indoor Air*. Wiley, New York, 113 – 130.
- Subba Ramu, M. C., Muraleedharan, T. S., and Ramachandran, T. V., (1988). Assessment of lung dose from radon daughters in dwellings, *Rad. Prot. Dosim.*, **22**, 187 – 191.
- Subba Ramu, M. C., Ramachandran, T. V., Muraleedharan, T. S., and Shaikh, A. N., (1990). Indoor Levels of Radon Daughters in Some High Background Areas in India. *Radiat. Prot. Dosim.* **30**, 41 – 44.
- Tiwari, R. C., (2006). Analytical Study on Variation of Climatic Parameters at Aizawl, Mizoram (India). *Bull. of Arunachal Forest Research*, **22 (1 & 2)**, 33 – 39.
- Tokonami S. (2005). Summary of dosimetry (Radon and Thoron) studies. *Int. Congress Series* **1276**, 151 – 154.
- UNSCEAR, (1993). United Nations Scientific Committee on the Effects of Atomic Radiation., Sources, Effects and Risks of Ionizing Radiation., Report to the General Assembly, United Nations, New York.
- UNSCEAR., (2000). United Nations Scientific Committee on the Effect of Atomic Radiation, Sources, Effects and Risks of Ionizing Radiation., Report to the General Assembly, United Nations, New York.
- UNSCEAR (2006). United Nations scientific committee on the effects of atomic radiation. Report A/AC.82/-644, Exposures of workers and the public from various sources of radiation, United Nations, New York.
- Vanchhawng, Lalmuanpuia, Rohmingliana, P. C., Thapa, R. K., Sahoo, B. K., Singh, O. P., Zoliana, B., Mayya, Y. S., (2009). To Correlate Radon and Thoron Concentrations

- with Gamma Background Radiation in Mizoram.(Special reference to Aizawl, Champhai and Kolasib districts), *Proc. VI<sup>th</sup> Conference of Physics Academy of North East*, Tripura University, April 3 – 4, 2009.
- Vanchhawng, Lalmuanpuia, Rohmingliana, P.C., Thapa, R.K., Sahoo, B.K., Mishra, Rosaline, Zoliana, B. and Mayya, Y.S., (2011). Study of Population Dosimetry in Middle Part of Mizoram, India. *Proc. of International Conference on Advances in Environmental Chemistry, (AEC 2011)* during November 16 – 18, 2011, Mizoram University, Aizawl. **ISBN: 978-93-81361-53-5**, 97 – 100.
- Vanchhawng, Lalmuanpuia (2012). Measurement of radon, thoron and their progeny concentrations in Mizoram with special reference to Aizawl, Champhai and Kolasib Districts. A Thesis submitted to the Mizoram University for the Degree of Doctor of Philosophy (Physics).
- Vaupotic, J., Sikovec, M., and Kobal, I., (1999). Systematic Indoor  $^{222}\text{Rn}$  and Gamma Ray Measurements in Slovenian Schools, *Health Physics*, **78**, 559 – 562.
- Virk, H. S. (1994). Scope of Radon Monitoring for Earthquake Studies in India. *Bull. Rad. Prot.*, **17**, 53 – 56.
- Virk, H. S., and Sharma, Navjeet., (2000). Indoor  $^{222}\text{Rn}/^{220}\text{Rn}$  Survey Report from Hamirpur and Una Districts, Himachal Pradesh, India, *Applied Radiation and Isotopes*, **52**, 137 – 141.
- Virk, H. S., (2004). Correlation of Radon/Helium Anomalies with Micro-earthquakes in Kangra Valley of N-W Himalaya., Invited talk given during the National Conference Cum Workshop on Solid State Nuclear Track Detectors and Applications., November 1 – 4, Amritsar.
- WHO, (2009). WHO hand book on indoor radon: a public health perspective. Geneva 27, Switzerland: World Health Organisation.

- Wilkening, M. (1986). Seasonal Variation of Indoor  $^{222}\text{Rn}$  at a Location in the Southwestern United States, *Health Physics*, **51**, 427 – 436.
- Zoliana, B., Rohmingliana, P. C., Lalmuanpuia Vanchhawng, Thapa, R. K., Mishra, R., Sahoo, B. K. and Mayya, Y. S. (2011). Measurement of Radon Concentration Inside and Around Dwellings in Fault Regions of Aizawl city, Mizoram, India. *Proc. of International Conference on Advances in Environmental Chemistry, (AEC 2011)* during November 16 – 18, 2011, Mizoram University, Aizawl. **ISBN: 978-93-81361-53-5**, 166 – 169.

## APPENDIX - I (a)

### Calibration experiment for pin-holes dosimeters with fan ON condition using Radon exposure only

#### APPARATUS REQUIRED:

Calibration chamber, dosimeters, LR-115 films, RAD7, Etching bath, Spark counter, Radon source.

#### THEORY:

##### Dosimeter

In this experiment, Twin cup dosimeters are used. In this type of dosimeter, there are three compartments – 1) Filter mode compartment, 2) Membrane/Pinhole mode compartment and 3) Bare mode.

In the filter mode, filter paper is used to cover the entry point of the compartment. This filter paper blocks the entry of the progeny while it allows both Radon and Thoron gas to pass through. So, tracks formed on the film inside this compartment are due to both Radon and Thoron gases and not the progeny. In the membrane mode, semi-permeable membrane is sandwiched between two filter papers which allows Radon gas only to pass through it hence in this compartment tracks on the film are produced due to radon gas only. In case of pinhole, different sizes of pin-holes are used. No membrane is used but filter paper is used to block the progeny. Tracks produced on the film in the pinhole side are due to radon gas only. In the bare mode, as is clear from its name, the film is being exposed openly to the environment and tracks on it are due to Radon gas, Thoron gas and their progeny.



We can calculate the concentration of Radon gas from the Membrane or Pinhole compartment, the concentration of Thoron gas can be calculated by simply subtracting the concentration of Radon gas from the concentration of both Radon and Thoron gases calculated from the Filter compartment. Subtracting the concentration calculated from the Filter compartment from the concentration calculated from the bare mode we can easily obtain the progeny concentration.

Similarly, for calculation of the calibration factor, the same method, i.e. simple subtraction method can be used.

### Calibration Factor

Calibration factors (CFs) are the quantities, which are used for converting the observed track density rates to the activity concentrations of the species of interest. If  $T$  denotes the track densities observed on a SSNTD due to exposure in a given mode to a concentration  $C$  of given species for a time  $t$ , it is obvious that

$$T = kCt \quad (\text{I (a) - 1})$$

where, we define  $k$  as the calibration factor.

In the cup mode, only radon or thoron or both enter the cup and the progeny species from the environment will be filtered out. Hence, the total tracks formed on the SSNTD placed inside the cups will be uniquely dependent on the gas concentrations only.

The corresponding calibration factors may be defined as

$$k_{R(M/F)} = \frac{T_{R(M/F)}}{tC_{R(M/F)}} \quad (\text{I (a) - 2})$$

$$k_{T(F)} = \frac{T_{T(F)}}{tC_{T(F)}} = \frac{T_{R+T(F)} - T_{R(M)}}{tC_{T(F)}} \quad (\text{I (a) - 3})$$

where,  $k_{R(M/F)}$  is the calibration factor of Radon in membrane cup or filter cup and  $k_{T(F)}$  is the calibration factor of Thoron in the filter cup.  $C_R$  is the gas concentration of Radon in  $\text{Bq/m}^3$  and  $C_T$  is the gas concentration of Thoron in  $\text{Bq/m}^3$ .  $T_{R(M)}$  is the tracks recorded for

Radon on the detector in  $\text{tr}/\text{cm}^2$  and  $T_{T(F)}$  is the tracks recorded for Thoron on the detector in  $\text{tr}/\text{cm}^2$ .  $T_{R+T(F)}$  is the tracks recorded for Radon and Thoron in the filter cup. The subscript  $M$  and  $F$  denote the compartments in the dosimeter.  $M$  represents membrane compartment and  $F$  represents the filter compartment.

The activity concentrations of the gases are continuously monitored using RAD-7.

### Calibration Chamber

In this experiment calibration chamber used is a  $1\text{m}^3$  capacity chamber. Inside it there are fan, dosimeter mounting bar, inlets, outlets and a tube light. Radon and Thoron source can be kept inside the chamber while their activity concentrations can be measured continuously using RAD7 as shown in Figure 1 below.

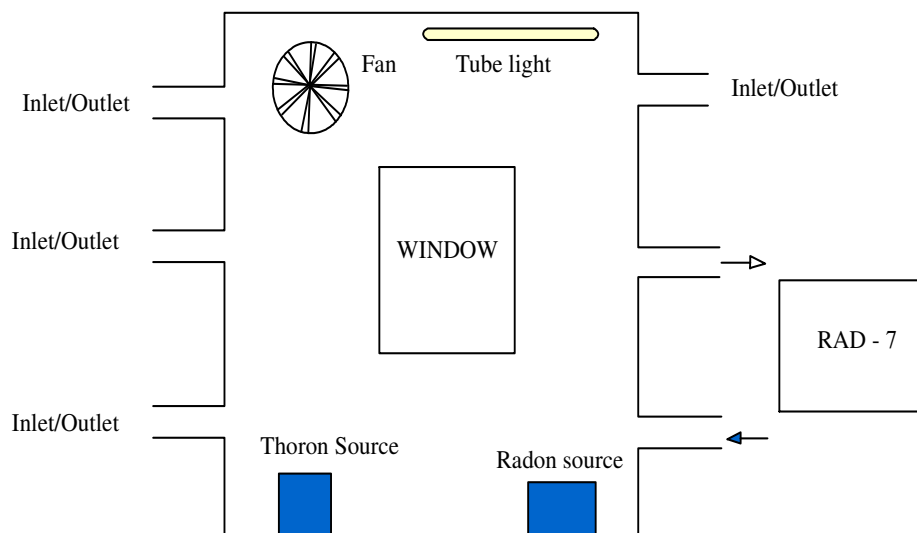


**Figure I (a) – 1** Block diagram of the calibration chamber.

### **PROCEDURE:**

1. Cut the LR-115 film into  $3 \times 3 \text{ cm}^2$  and fix them on the dosimeter, and mount them inside the calibration chamber.
2. Note the exact mounting time.
3. Monitor the activity concentrations of the gases continuously using RAD7.
4. Switch ON the fan which is present inside the calibration chamber.

5. After several hours remove the dosimeters from the calibration chamber and note the time of removal.
6. Etch the films in 2.5N NaOH solution for 60 mins at 60°C with continuous stirring.
7. Count the tracks on each film using Spark counter.
8. Calculate the Calibration factor using Equations (I (a) - 2) and (I (a) - 3).

**OBSERVATION AND RESULTS:**

Starting time : Dt.8<sup>th</sup> July, '08 –18:00 hrs.

Stopping time : Dt.9<sup>th</sup> July, '08 – 09:45 hrs.

Exposure Period : 15 hrs 45 mins.

Average Concentration : 110 kBq/m<sup>3</sup>

Sl No:	Type of Cap				Counts(Tracks/cm <sup>2</sup> )					Calibration (CF)
	Pinhole/ Filter	Diameter (mm)	No. of holes	With/without filter Paper	1	2	3	4	Avg	
1.1	Pinhole	4.0	1	With	1713	1725	1725	1715	1719.5	0.024
1.2	Pinhole	4.0	1	With	1248	1227	1247	1204	1231.5	0.017
1.3	Pinhole	4.0	1	With out	1204	1230	1269	1281	1246.0	0.017
1.4	Pinhole	4.0	1	With out	1127	1121	1160		1136.0	0.016
2.1	Pinhole	3.0	1	With	1024	1041	1042	1048	1038.8	0.014
2.2	Pinhole	3.0	1	With	1239	1279	1258	1264	1260.0	0.017
2.3	Pinhole	3.0	1	With out	1053	1082	1078	1087	1075.0	0.015
2.4	Pinhole	3.0	1	With out	1143	1184	1167	1175	1167.3	0.016
3.1	Pinhole	2.0	1	With	968	959	939	957	955.8	0.013
3.20	Pinhole	2.0	1	With	835	840	831		835.3	0.012
3.3	Pinhole	2.0	1	With out	841	841	832		838.0	0.012
3.4	Pinhole	2.0	1	With out	764	793	779	788	781.0	0.011
4.1	Pinhole	1.0	1	With	834	839	856	848	844.3	0.012
4.2	Pinhole	1.0	1	With	1031	1047	1030	1034	1035.5	0.014

4.3	Pinhole	1.0	1	With out	1278	1284	1301	1310	1293.3	0.018
4.4	Pinhole	1.0	1	With out	1263	1269	1284		1272.0	0.018
5.1	Pinhole	0.4	1	With	962	990	998	1002	988.0	0.014
5.2	Pinhole	04	1	With	1047	1063	1051	1040	1050.3	0.015
5.3	Pinhole	0.4	1	With out	1121	1111	1131	1126	1122.3	0.016
5.4	Pinhole	0.4	1	Without	1088	1102	1126	1125	1110.3	0.015
6.1	Filter				1592	1569	1569	1554	1571.0	0.022
6.2	Filter				1259	1310	1314	1316	1299.8	0.018

### DISCUSSIONS:

The main aim of this experiment is to obtain the calibration factor for Radon using pin-hole type dosimeter with fan OFF condition using Radon source only. From the result, pinhole type dosimeter works well and the value obtained of the calibration factor for Radon is quite good. Also, it does not effect the calibration factor when the fan is in OFF condition.

### PRECAUTIONS:

1. The LR-115 films should be handled carefully and there should be no scratch on it. And the film should not be peeled even on the edge. This will be etched away and may lead to incorrect result.
2. The etching time should be carefully maintained and the etching solution should also be prepared carefully and accurately.
3. The films should be dried completely before counting.
4. Pre-sparking should be done for new films.
5. Each track should be counted at least three times for better result.
6. The films should not be mixed up and should be kept properly and carefully.

## APPENDIX - I (b)

### Calibration experiment for pin-holes dosimeters with fan ON condition using Thoron exposure only

#### APPARATUS REQUIRED:

Calibration chamber, dosimeters, LR-115 films, RAD7, Etching bath, Spark counter, Thoron source.

#### PROCEDURE:

1. Cut the LR-115 film into  $3 \times 3 \text{ cm}^2$  and fix them on the dosimeter, and mount them inside the calibration chamber.
2. Note the exact mounting time.
3. Monitor the activity concentrations of the gases continuously using RAD7.
4. Switch OFF the fan which is present inside the calibration chamber.
5. After several hours remove the dosimeters from the calibration chamber and note the time of removal.
6. Etch the films in 2.5N NaOH solution for 60 mins at  $60^\circ\text{C}$  with continuous stirring.
7. Count the tracks on each film using Spark counter.
8. Calculate the Calibration factor using Equation (I (a) - 3).

#### OBSERVATIONS AND RESULTS:

Starting time	:	Dt. 9 <sup>th</sup> July, '08 –16:15 hrs.
Stopping time	:	Dt. 10 <sup>th</sup> July, '08 – 15:15 hrs.
Exposure Period	:	23 hrs
Average Concentration	:	3699 Bq/m <sup>3</sup> .

Sl.No	Type of cap					Counts(Tracks/cm <sup>2</sup> )					Calibration Factor(CF)
	Pinhole / Filter	Diameter (mm)	No. of holes	Hole Length	With/without filter Paper	1	2	3	4	Avg	
1.1	Pinhole	0.4	1	5mm	With	17	24	20		20.33	0.0057
1.2	Pinhole	0.4	1	5mm	With	48	42	45	64	49.75	0.014
1.3	Pinhole	0.4	1	5mm	With out	23	22	26		23.67	0.0067

### DISCUSSIONS:

In this experiment, there was an unexpected Radon source which result into unsatisfactory result. The main aim of this experiment is to obtain the calibration factor for Thoron using pin-hole type dosimeter with fan ON condition using Thoron source only. But, unfortunately there was a Radon source building up inside the chamber after the source has removed and radon gas was also pumped out from the chamber. The obtained value of the calibration factor for thoron in this experiment was *unacceptably* small.

### PRECAUTIONS:

1. The LR-115 films should be handled carefully and there should be no scratch on it. And the film should not be peeled even on the edge. This will be etched away and may lead to incorrect result.
2. The etching time should be carefully maintained and the etching solution should also be prepared carefully and accurately.
3. The films should be dried completely before counting.
4. Pre-sparking should be done for new films.
5. Each tracks should be counted at least three times for better result.
6. The films should not be mixed up and should be kept properly and carefully.

## APPENDIX - II

### Standardization of etching parameters

**APPARATUS REQUIRED:** LR-115 films, NaOH palettes, Balance, Distilled water, Etching bath etc.

**THEORY:**

A Cellulose Nitrate films (LR-115 type 2) manufactured by Kodak Pathe are used as detectors. The thickness of the sensitive layer of films (Type II) is 12  $\mu\text{m}$ . The choice of the detector LR-115 is made in view of the fact that LR-115 detectors do not develop tracks originating from the progeny alphas deposited on them and therefore are ideally suited for air concentration measurements. The films are not sensitive to electrons and electromagnetic radiations and they can be handled without risk wherever such radiations are present. Nevertheless, care should be taken to avoid any abrasion on the films. LR-115 film when dipped into 2.5N NaOH (Sodium Hydroxide) solution is being chemically etched.

The term Etching means the process of removal of a layer of a substance. Etching of the film is necessary because the tracks produced on the films due to radon, thoron and their progeny are visible for counting only after etching. Etched films are then counted by spark counter. The purpose of this experiment is to standardize the bulk etching rate. Bulk etching rate is the rate of etching of the film (LR-115) per unit time.

Let  $W$  be the weight of the film in grams,  $A$  be the area in  $\text{cm}^2$  and  $\rho$  be the density in  $\text{gram}/\text{cm}^3$ . Then, the thickness of the film can be calculated by using the equation

$$\text{Thickness} = \frac{W}{A \times \rho} \text{ (cm)} \quad (\text{II - 1})$$

If the initial weight be  $w_i$  and final weight be  $w_f$ , then change in weight after etching is given by

$$\Delta W = W_i - W_f \quad (\text{II - 2})$$

Bulk Etching Rate (VB) is given by

$$V_B = \frac{\Delta W}{\Delta t \times \rho \times A} \quad (\text{II - 3})$$

where  $\Delta t$  is the time of etching in seconds.

By using equation (II - 3) the bulk etching rate can be easily calculated.

### PROCEDURE:

1. Take 50g of NaOH palettes by using balance and dissolved completely in 500ml of distilled water. This solution is the 2.5N NaOH solution.
2. Cut the film (LR-115) which is 9cm x 12cm into a smaller pieces ( $3 \times 3 \text{ cm}^2$ ) so that 12 films which are exactly equal in size are cut out. Separate the films into two groups – 6 films each group.
3. Take the weight of each film by using a microbalance and note them carefully.
4. Put the NaOH solution in the beaker of the etching bath and fix the temperature of the thermostat at 60°C.
5. When this temperature is reached dip the weighted films into the 2.5N NaOH solution- one group with stirring and another group without stirring.
6. Note the starting time of the etching.
7. After 60 minutes, take out the films from the solution.
8. Wash the films with running water in order to remove the solution and dry them between filter papers.
9. Take the weight of each film after etching by using microbalance and note them carefully.
10. By using equation (II - 3) the bulk etching rate can be calculated.



**OBSERVATIONS:**

Sl. No.	60 mins with stirring				60 mins without stirring				
	$W_i$ (g)	$W_f$ (g)	$\Delta W = W_i - W_f$ (g)	$v_B = \frac{\Delta W}{\Delta t \times A}$ ( $\mu\text{m/h}$ )	$W_i$ (g)	$W_f$ (g)	$\Delta W = W_i - W_f$ (g)	$v_B = \frac{\Delta W}{\Delta t \times A}$ ( $\mu\text{m/h}$ )	
1	0.1421	0.1368	0.0053	4.176	0.1447	0.1400	0.0047	3.708	
2	0.1345	0.1287	0.0058	4.603	0.1388	0.1339	0.0049	3.888	
3	0.1378	0.1301	0.0077	6.084	0.1533	0.1474	0.0059	4.682	
4	0.1317	0.1256	0.0061	4.824	0.1348	0.1303	0.0045	3.564	
5	0.1357	0.1286	0.0071	5.634	0.1293	0.1235	0.0058	4.603	
6	0.1427	0.1356	0.0071	5.634	0.1434	0.1380	0.0054	4.285	
Average				5.159	Average				4.122

**RESULTS:**

The bulk etching rate calculated for 60 mins with stirring is  $5.159\mu\text{m/h}$  and for 60 mins without stirring is  $4.122\mu\text{m/h}$ .

**DISCUSSION:**

The bulk etching rate calculated for 60 mins with stirring was wrong due to the improper washing of the etched films. The etched film should be thoroughly washed.

**PRECAUTIONS:**

1. Exactly 50g of NaOH palletes should be dissolved into 500ml of distilled water.
2. The etching time should be carefully maintained.
3. The films should be handled with care and scratching should be completely avoided.
4. Etchant temperature should be constant ( $60^\circ\text{C}$ ).
5. The etch films should be wash properly.

## APPENDIX - III

### Experiment to find the operating voltage of a given Spark Counter

**APPARATUS REQUIRED:** Spark Counter, exposed film.

**THEORY:**

Spark counter is an instrument used to count the number of tracks on the films. It works on a simple electronic principle. When the plastic track detector is chemically etched, the through holes are produced along the tracks. The thin detector is placed on top of a thick conductive electrode, commonly made of brass, and covered with an aluminized plastic foil namely a very thin layer of aluminium evaporated onto a Mylar backing. The aluminized side of the plastic foil is in contact with the thin detector. When the high voltage is applied across the capacitor C, an electrical discharge or spark takes place through the track hole. The voltage pulse produced across the resistor R, can easily be counted electronically by a scalar.

The spark passing through a track hole has enough energy to evaporate the thin layer of aluminium coating and produces a much larger hole in the aluminium electrode. After the short circuit and hence the spark is stopped, the capacitor, is charged again but a second spark cannot occur in the same track hole, because of the evaporation of the aluminium in the electrode. The sparks, therefore, jumps randomly from one track hole to another until all track holes are counted. The evaporated spot on the aluminium, which have the diameter of about 100 $\mu$ m are equal to the number of sparks and hence to the number of track holes in the plastic track detector. The aluminium replica can easily be counted by an

optical microscope or a microfiche reader. The schematic diagram of a spark counter is given below.

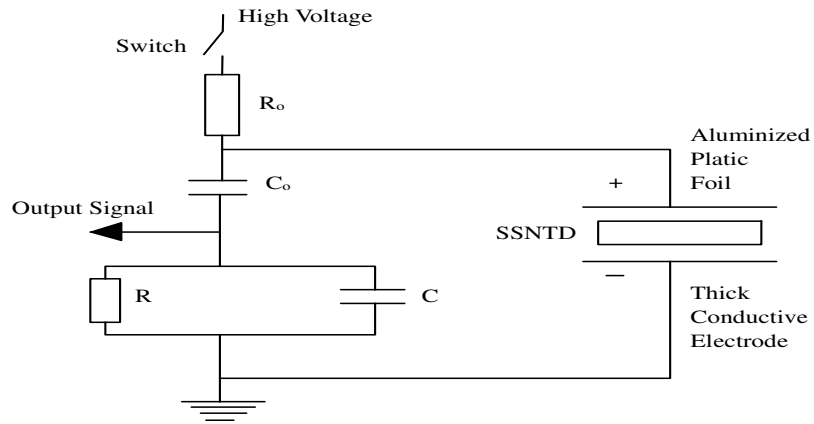


**Figure III – 1** Schematic diagram of a spark counter.

Operating voltage of a Spark counter is that specific voltage by which the counting of tracks should be done. When graph is plot between applied voltages and counts, a plateau region is produced. The corresponding middle voltage of this plateau is taken as the operating voltage for that Spark counter. This plateau region shows that even with a small change in the applied voltage the number of tracks count by the counter remains constant. Hence, with the fluctuation of the applied voltage, the counts will remain the same. The graph plotted between applied voltage and counts is shown in figure III - 2 below.

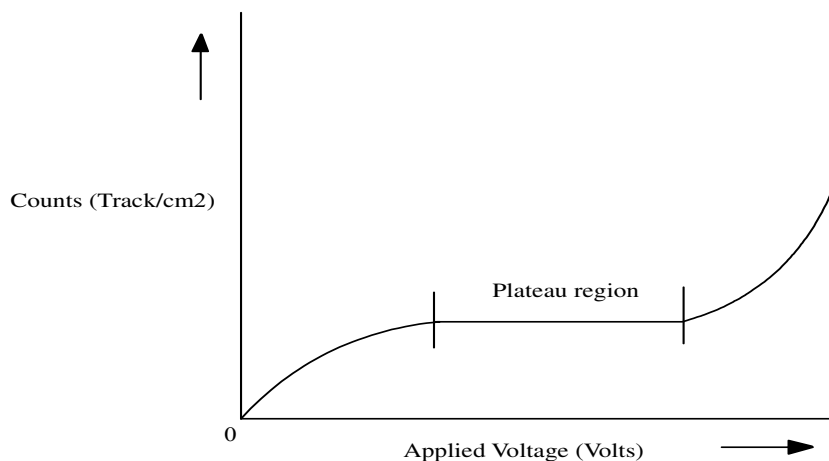


**Figure III – 2** Applied Voltage vrs Count showing the plateau region.**PROCEDURE:**

1. Place the exposed film on the electrode in such a way that the electrode is in contact with the middle portion of the film.
2. Set the voltage at 900 volts for pre-sparking.
3. Pre-spark the exposed film which was already etched in 2.5N NaOH.
4. Set the voltage at 100 volts and count the tracks.
5. Repeat procedure no.4 by increasing the applied voltage by 50V each up to 800V and count the tracks for each applied voltage.
6. Plot a graph between the Applied voltage and Counts, i.e. Applied voltage versus Counts.
7. The plateau of the curve gives the operating voltage of the given Spark Counter.

**OBSERVATIONS:**

Applied Voltage (Volts)	Counts (Tracks/cm <sup>2</sup> )
100	0
200	0
250	0
300	2
350	48
400	132
450	140
500	146
550	200
600	285
650	342
700	518
750	573
800	668

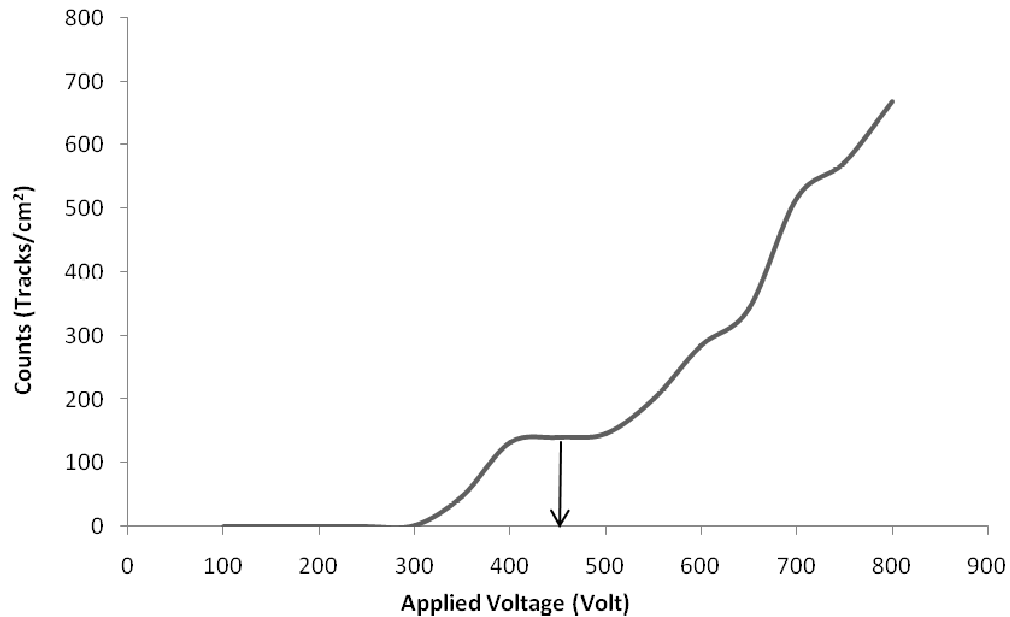


**Figure III – 3** Experimental graph showing the plateau region.

**RESULTS:**

The operating voltage for the given Spark Counter from graph is 450 Volts.

**DISCUSSION:**

When high voltage was applied in the exposed film, holes were produced which leads to an enormous increase in counts and consequently the plateau region cannot be obtained on the graph.

**PRECAUTIONS:**

1. Pre-sparking is always required for newly etched film.
2. Film with less number of tracks should be use because with high number of tracks holes can be formed which will cause error and underestimation.
3. It should be ensured that there are no scratches on the film.
4. Aluminized plastic foil should be changed for each counting.

## APPENDIX - IV (a)

### Energy and Efficiency calibration of NaI(Tl) Spectrometer using Cs<sup>137</sup> & Co<sup>60</sup> Sources

#### APPARATUS REQUIRED:

Cs<sup>137</sup> & Co<sup>60</sup> sources, NaI(Tl) detector, Multichannel analyser.

#### THEORY:

Some detectors do not measure energy. Those which do are referred to as energy spectrometers. The performance of a detector used for energy measurement can be examined by its response to monoenergetic sources of radiation. The distribution is called the response function of the detector for the energy used. The width measured at half of the maximum of the bell shaped curve (response function) is indicated by G or by FWHM (full width at half maximum). Resolution is a measure of detector's capability to distinguish between the closely spaced energies.

In the analyser, channel number Vs energy calibration is representative of pulse height v/s energy distribution. In ideal MCA it is expected to be linear and is represented by

$$\text{Energy} = M * \text{Channel no.} + C \quad (\text{IV (a) - 1})$$

The calibration is done by using spectrum containing known and well-separated energies. Most commonly, spectrum of <sup>137</sup>Cs and <sup>60</sup>Co is used for this purpose. It is possible with a least squares program to compute the slope M (Energy per channel) and intercept C (Energy corresponding to channel zero) from the peak positions in channels and input energy in keV. It is also common to use second order polynomial for energy calibration for analysers of higher memories to account for the possible non linearity in ADC.

## **PROCEDURE:**

### **Setting and putting on the instruments:-**

1. Plug the 3- pin mains connector to mains input socket. It is necessary to have proper grounding from mains.
2. Turn ON the instrument by setting the Mains ON switch on rear panel.
3. LCD graphics display will first display the text message about the instrument and will switch to spectrum display indicating cursor and spectrum data.
4. Contrast Adjust, a screw driver adjustment can be set to get best contrast on the LCD.
5. Ensure that the HV Adjust helipot is turned completely counter clockwise; bring the dial reading to 0.00. Turn HV ON/OFF toggle switch to ON. Adjust the HV supply to 480 volts. The 10.00 dial reading matches to 1500V. Hence, each rotation of the helipot dial will increment the HV by 150V. The typical value of HV is around +750V.
6. The pulse amplitude can be adjusted by setting the Coarse Gain switch to HIGH or LOW. The fine adjustment of output amplitude can be accomplished by setting the Gain Adjust helipot. Set the output peak amplitude to 3V for Cs<sup>137</sup> source.
7. Set the Input Range of ADC to 8V to get an undistorted output pulse of height.
8. Set the ADC IN toggle switch to ON position. As soon as the amplifier output pulses are connected to ADC, the Busy LED will start glowing. The brightness of this LED indicates the 'BUSINESS' of the ADC.

### **Calibration:**

Before starting the analysis of the sample, the spectrometer has to be calibrated for energy using sources of known distinct gamma energies. Most commonly, spectrum of Co<sup>60</sup> and Cs<sup>137</sup> are used for this purpose.

1. Press MODE key till the mode changes to Set Timer. Press ENTER key to start setting the timer.
2. Select Live Time by pressing CURL key.
3. Set the preset time by pressing CURR/CURL to increment/decrement the digits. Press ENTER key to go to next digit.
4. To start acquisition, press MODE key, till Start Timer option is displayed on screen. Press ENTER key to start the acquisition.
5. Acquire the spectrum by keeping the sources ( $\text{Cs}^{137}$  &  $\text{Co}^{60}$ ) for a reasonable time (e.g 500 secs) so that photo peaks have sufficient counts for the analysis.
6. After the acquisition time is over, press MODE key till Stop Timer option is displayed on screen. Press ENTER key to stop the acquisition.
7. To select the region of interest, press MODE key till the LCD shown SET UP ROI under MODE field.
8. Select ROI number first. The arrow appears before ROI numbers. Used CURR/CURL to increment/decrement ROI number. Press ENTER key to confirm the selection. This will make the arrow to jump to next field i.e. Start channel.
9. Set the start channel number. Press ENTER key to confirm the Start channel number. This will make the arrow to jump to the next field i.e. Stop channel number.
10. Set the Stop channel number. Press ENTER key.
11. Repeat the above procedure to set the Start and Stop channel of next ROI.
12. It is essential to have two valid peaks before starting the calibration.
13. Press MODE key till Calibration is displayed on screen under MODE field. Press ENTER.



14. Locate cursor in 1<sup>st</sup> ROI and press ENTER. Enter the energy value of Cs<sup>137</sup> i.e. 662keV and press ENTER. Locate cursor in 2<sup>nd</sup> ROI and press ENTER. Enter the energy value of Co<sup>60</sup> i.e. 1173keV and press ENTER.
15. Calibration is completed at this point.

**To find the Efficiency of a Standard Sources:**

1. Acquire the spectrum by keeping the Standard sources (Potassium, Uranium ore, Thorium) individually in the detector for a reasonable time (around 5000 secs) so that photo peaks have sufficient counts for the analysis.
2. Note the Start and Stop Channel number of each peak.
3. Note the activity of each sources.
4. From the Gamma Library, note the Branching Intensity.
5. From the spectrum obtained, after subtracting the Background counts (Peaks in the background spectrum are due to the presence naturally occurring radionuclides from Uranium and Thorium series and Potassium), find the Net Area.
6. Calculate the Efficiency of each sources by the following relation.

$$\text{Efficiency } (\eta) = [(cps*100) / (dps*BR\%)] \% \quad \text{(IV (a) - 2)}$$

Where,

cps = counts per second or Net Area/Counting Time or Area under the peak

dps = disintegration per second or Activity

BR% = Branching Intensity

7. The calculated Efficiency of each sources should be used for calculating the Activity of unknown soil sample.
8. Once the efficiency for the various energies of interest is calculated, a curve is plotted between energy and efficiency. The photo peak efficiency decreases with gamma photon energy.

**OBSERVATIONS:****Energy Calibration :**

Peak channel No.(x)	Energy (E) in kev	Energy/channel (M)	Energy corresponding to zero channel (C)
197	662	3.4608	-20.644
346	1173		
390	1332		

**Efficiency Calculation:****Cs<sup>137</sup> Source**

Start channel: 177                      End channel: 216              Counting time: 500 secs

Activity: 0.1  $\mu$ Ci at Nov,'99              Time: 10 years              BR = 85%

Half life (T<sub>1/2</sub>): 30.8 years       $\lambda = 0.693/(T_{1/2})$                $A = A_0 * e^{-\lambda t}$

A<sub>0</sub> = 37000 Bq                      Net Area = 93581

$\eta = (\text{cps} * 100) / (\text{Activity (Bq)} * \text{BR}) = 0.475\%$

**Co<sup>60</sup> Source****1<sup>st</sup> peak of 1173 kev:**

Start channel: 322      End channel: 367      Counting time: 500 secs

Activity: 1  $\mu$ Ci at July,2004              Time: 5 years              BR = 100%

Half life (T<sub>1/2</sub>): 5.27 years       $\lambda = 0.693/(T_{1/2})$                $A = A_0 * e^{-\lambda t}$

A<sub>0</sub> = 37000 Bq                      Net Area = 40284

$\eta = (\text{cps} * 100) / (\text{Activity (Bq)} * \text{BR}) = 0.420\%$

**2<sup>nd</sup> peak of 1332 kev:**

Start channel: 370      End channel: 420      Counting time: 500 secs

Activity: 1  $\mu$ Ci at July,2004              Time: 5 years              BR = 100%

Half life (T<sub>1/2</sub>): 5.27 years       $\lambda = 0.693/(T_{1/2})$                $A = A_0 * e^{-\lambda t}$

A<sub>0</sub> = 37000 Bq                      Net Area = 36930

$$\eta = (\text{cps} * 100) / (\text{Activity (Bq)} * \text{BR}) = 0.385\%$$

Sources	Energy (E) in kev	Efficiency ( $\eta$ ) in %
Cs <sup>137</sup>	662	0.475
Co <sup>60</sup>	1173	0.420
	1332	0.385

## RESULTS:

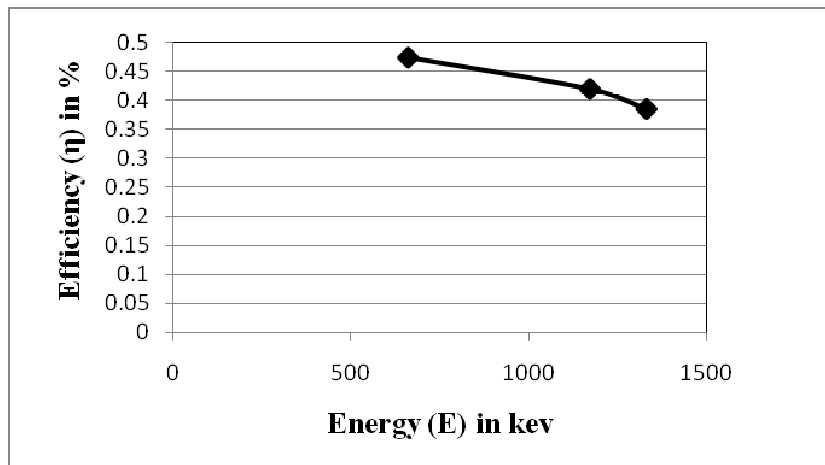
Energy calibration has been done using the Cs<sup>137</sup> & Co<sup>60</sup> sources. The calibration factors obtained are:  $M = 3.4608$ ;  $C = -20.644$

Efficiency calibration has been done and found as:

For Cs<sup>137</sup>:  $\eta$  (662 kev) = 0.475%

For Co<sup>60</sup>: 1<sup>st</sup> peak  $\eta$  (1173 kev) = 0.420%

2<sup>nd</sup> peak  $\eta$  (1332kev) = 0.385%



## DISCUSSION:

The efficiency calculation has been done without subtracting the background counts. The result obtained is not exactly the correct efficiency. A curve is plotted between energy and efficiency. The photo peak efficiency decreases with gamma photon energy, i.e. as the energy increases efficiency decreases.

**PRECAUTIONS:**

1. Good grounding system for mains should be observed for proper functioning of the instrument and to avoid mains noise feed-through through ground loops.
2. Input to the ADC is DC coupled. Care should be taken to ensure that input level does not exceed +10 volts. Higher voltages may permanently damage input stage of the ADC.
3. Care should be taken while handling the HV supply.
4. Do not refer to energy value till the MCA is properly calibrated.

## APPENDIX - IV (b)

### Efficiency calibration using Potassium ( $K^{40}$ ), Uranium ( $U^{238}$ ), Thorium ( $Th^{232}$ ) Sources

#### APPARATUS REQUIRED:

Potassium ( $K^{40}$ ), Uranium ( $U^{238}$ ), Thorium ( $Th^{232}$ ) sources, NaI(Tl) detector, Multichannel analyzer.

#### PROCEDURE:

To find the Efficiency of a Standard Sources:-

1. Press MODE key till the mode changes to **Set Timer**. Press ENTER key to start setting the timer.
2. Select Live Time by pressing CURL key.
3. Set the preset time by pressing CURR/CURL to increment/decrement the digits. Press ENTER key to go to next digit.
4. To start acquisition, press MODE key, till Start Timer option is displayed on screen. Press ENTER key to start the acquisition.
5. Acquire the spectrum by keeping the Standard sources (Potassium, Uranium ore, Thorium) individually in the detector for a reasonable time (around 5000 secs) so that photo peaks have sufficient counts for the analysis.
6. After the acquisition time is over, press MODE key till Stop Timer option is displayed on screen. Press ENTER key to stop the acquisition.
7. To select the region of interest, press MODE key till the LCD shown SET UP ROI under MODE field.

8. Select ROI number first. The arrow appears before ROI numbers. Use CURR/CURL to increment/decrement ROI number. Press ENTER key to confirm the selection. This will make the arrow to jump to next field i.e. Start channel.
9. Set the start channel number. Press ENTER key to confirm the Start channel number. This will make the arrow to jump to the next field i.e. Stop channel number.
10. Set the Stop channel number. Press ENTER key.
11. Repeat the above procedure to set the Start and Stop channel of next ROI.
12. Note the Start and Stop Channel number of each peak.
13. Note the activity of each sources.
14. From the Gamma Library, note the Branching Intensity.
15. From the spectrum obtained, after subtracting the Background counts (Peaks in the background spectrum are due to the presence naturally occurring radionuclides from Uranium and Thorium series and Potassium), find the Net Area.
16. Calculate the Efficiency of each sources by using equation (IV (a) - 2).
17. The calculated Efficiency of each sources should be used for calculating the Activity of unknown soil sample.

**OBSERVATIONS:**

*K<sup>40</sup> Source*

Counting time: 5000 secs    Activity: 3973 Bq    BR = 10.7%    Net Area = 34201

$$\eta = (\text{cps} * 100) / (\text{Activity (Bq)} * \text{BR}) = 1.6 \%$$

*U<sup>238</sup> Source*

Counting time: 5000 secs    Activity: 1914 Bq    BR = 15.9 %    Net Area = 22742

$$\eta = (\text{cps} * 100) / (\text{Activity (Bq)} * \text{BR}) = 1.49 \%$$

*Thorium Source*

Counting time: 5000 secs    Activity: 17374 Bq    BR = 36 % ;    NetArea = 192647

$$\eta = (\text{cps} \cdot 100) / (\text{Activity (Bq)} \cdot \text{BR}) = 0.616 \%$$

Table IV (b) – 1 gives the efficiency of each radionuclides.

**Table IV (b) – 1** Energy and efficiency of radionuclides

Sources	Energy (E) in kev	Efficiency ( $\eta$ ) in %
$K^{40}$	1460	1.6
$U^{238}$	1764	1.49
$Th^{232}$	2614	0.616

## RESULTS:

The Efficiency of three standard sources has been calculated and found out as

$$K^{40} \text{ Source}; \quad \eta = 1.6 \%$$

$$U^{238} \text{ Source}; \quad \eta = 1.49 \%$$

$$Th^{232} \text{ Source}; \quad \eta = 0.616 \%$$

Also, a curve is plotted between Energy and Efficiency as shown in Fig. IV (b) - 1 and found that efficiency decreases with increase in energy.

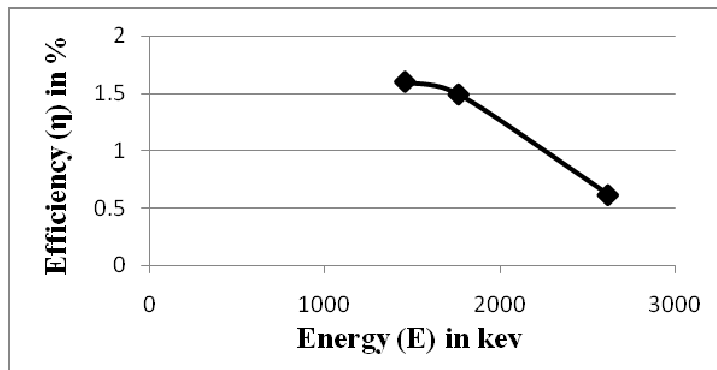


**Figure IV (b) – 1** Graph between energy and efficiency.

## DISCUSSION:

The efficiency calculation has been done without subtracting the background counts. The result obtained is not exactly the correct efficiency. A curve is plotted between energy and efficiency. The photo peak efficiency decreases with gamma photon energy, i.e. as the energy increases efficiency decreases.

**PRECAUTIONS:**

1. Good grounding system for mains should be observed for proper functioning of the instrument and to avoid mains noise feed-through through ground loops.
2. Input to the ADC is DC coupled. Care should be taken to ensure that input level does not exceed +10 volts. Higher voltages may permanently damage input stage of the ADC.
3. Care should be taken while handling the HV supply.
4. Do not refer to energy value till the MCA is properly calibrated.



## APPENDIX – IV (c)

### Experiment to find the Activity of Soil sample

**APPARATUS REQUIRED:** Soil Samples, NaI(Tl) detector, Multichannel analyzer.

**THEORY:**

The fundamental approach in this type of analysis is to fit the response function of the detector for the sources of various energies of which the sample is composed of. This function is then used in the analysis of the spectral data. There are basically three methods commonly used for the analysis of gamma ray spectra obtained from NaI(Tl) detectors.

**1. Method of spectrum stripping**

This method is based on the principle that the gamma ray spectra of multiple radionuclides is due to linear sum of spectrum of individual radionuclides. If the spectrum of single radionuclides is available then, after normalizing they can be subtracted from the composite spectrum one by one. This method is known as spectrum stripping. This method is simple but cannot be effectively used when more than 3 isotopes are present, because of the accumulation of error in the estimation of the peak areas.

**2. Simultaneous Equations Method**

It deploys a mathematical approach for removal of Compton interference from the photopeaks. The only requirement of this method is that

- i. all nuclides present in the sample must be identified
- ii. different photopeak be present for each nuclide

let there be ‘j’ isotopes in the sample and C(1), C(2), ....C(j) be the counts in the ‘j’ photo peak regions of the various isotopes, and P(1), P(2), ....P(j) are the photopeak counts of these isotopes to be determined and f(1,k), f(2,k)...F(j,k) are the Compton fractions of these isotopes P(k) in different regions. The simultaneous equations for j isotopes can be formed like

$$\begin{vmatrix} f(1,1) & f(1,2) & \dots & f(1,j) \\ f(2,1) & f(2,2) & \dots & f(2,j) \\ \dots & \dots & \dots & \dots \\ \dots & \dots & \dots & \dots \\ f(j,1) & f(j,2) & \dots & f(j,j) \end{vmatrix} = \begin{vmatrix} P(1) \\ P(2) \\ \dots \\ \dots \\ P(j) \end{vmatrix} = \begin{vmatrix} C(1) \\ C(2) \\ \dots \\ \dots \\ C(j) \end{vmatrix}$$

or  $[F] [P] = [C]$ ,

Then the solution is  $P = F^{-1} C$  (IV (c) - 1)

The inverted matrix  $F^{-1}$  is obtained by means of computer when order is more than 2. This method can analyse a complex spectra, but since it uses counts in the peak regions only, it is statistically less accurate than the method which uses all the channels.

### 3. *Least Squares Method*

This is the most accurate method compared to the earlier methods for unfolding the complex gamma ray spectra from scintillation detectors. The principle of least squares requires that the sum of the squares of the random errors for the individual channel be a minimum. Initially it is required to generate the response function corresponding to the monoenergetic photons for the nuclides under consideration. The net count after subtraction of background in any channel is the function of activity of each nuclide present in the sample. In the given channel the net counts can be represented as

$$C_i = P_1 f_{i,1} + P_2 f_{i,2} + P_3 f_{i,3} + \dots + P_m f_{i,m} \quad (\text{IV (c) - 2})$$

where  $C_i$  is the net sample counts in the  $i^{\text{th}}$  Channel

$P_1, P_2, \dots, P_m$  = The unknown concentrations of  $m$  nuclides contributing counts to the sample spectrum

$f_{i,1}, f_{i,2}, \dots, f_{i,m}$  = is the fraction of the photopeaks counts of the  $m^{\text{th}}$  isotope in the  $i^{\text{th}}$  channel. Also called Compton fractions calculated from

$$f_{i,m} = N_{i,m} / P_m \quad (\text{IV (c) - 3})$$

where  $N_{i,m}$  and  $P_m$  are the counts due to isotope in channel '  $i$  ' and photo peak respectively. These fractions are determined by counting standards of each nuclide separately.

In a multilinear regression model, the  $C$ 's (the observed counts in each channel) are dependent variables and known  $f$ 's are the independent variables. Even though some of the ' $m$ ' nuclides may not contribute counts to all the channels, the model is valid because the channel efficiencies will merely be zero for those channels in which no counts appear from a particular nuclide.

Applying the theory of weightage least squares we can get a set of equations

$$P = (F^T W F)^{-1} (F^T W C) \quad (\text{IV (c) - 4})$$

where  $W$  is the weighing matrix. The variance of each value is calculated by the diagonal elements of the inverted matrix. Unfolding of the NaI(Tl) spectrum is achieved in two steps. In the first step the program generates the response functions for the individual

isotopes from the separately counted spectral data of individual isotope standards. The second step the program calculates the energy and intensity of the individual gamma energies peaks based on least squares method.

The advantages of least square method

1. This method provides greatest accuracy in the determination of individual nuclide activity content of the complex sample. The method utilises data in all the channels to estimate the nuclide concentrations.
2. The error associated with the measurement of each nuclide is readily obtained
3. Well suited for the automated data processing of large number of samples
4. Qualitative identification of sample content can be avoided.
5. Decay and counting corrections can be made automatically.

Disadvantages of least square method

1. Well calibrated standards for all nuclides to be analysed is required to generate the accurate response functions of individual nuclides.
2. Computer is required to process the spectral data
3. Spectrometry system should be stable and yield reproducible performance.

In the case of natural activity measurements it is required to have standard sources for uranium, thorium and potassium which is contributing to natural activity in the environment. Well separated high energy photo peaks of 1460 keV, 1764 keV and 2614 keV for  $^{40}\text{K}$ ,  $^{214}\text{Pb}$  and  $^{208}\text{Tl}$  are used for this analysis.

#### **PROCEDURE:**

1. Put the sample in the detector.
2. Press MODE key till the mode changes to **Set Timer**. Press ENTER key to start setting the timer.
3. Select Live Time by pressing CURL key.
4. Set the preset time by pressing CURR/CURL to increment/decrement the digits. Press ENTER key to go to next digit.
5. To start acquisition, press MODE key, till Start Timer option is displayed on screen. Press ENTER key to start the acquisition.
6. Acquire the spectrum by keeping the unknown sources for a reasonable time (e.g 50,000 secs. The sample is a natural activity, it may not be a high activity. So, it has to be kept for longer period) so that photo peaks have sufficient counts for the analysis.

7. After the acquisition time is over, press MODE key till Stop Timer option is displayed on screen. Press ENTER key to stop the acquisition.
8. To select the region of interest, press MODE key till the LCD shown SET UP ROI under MODE field.
9. Select ROI number first. The arrow appears before ROI numbers. Used CURR/CURL to increment/decrement ROI number. Press ENTER key to confirm the selection. This will make the arrow to jump to next field i.e. Start channel.
10. Set the start channel number. Press ENTER key to confirm the Start channel number. This will make the arrow to jump to the next field i.e. Stop channel number.
11. Set the Stop channel number. Press ENTER key.
12. Repeat the above procedure to set the Start and Stop channel of next ROI.
13. Note the counting time, Start and Stop channel and the peak energy value and the weight of the sample.
14. From the peak energy, we can know whether it is Potassium, Uranium series and Thorium series.
15. From the spectrum obtained, after subtracting the Background counts, find the Net Area.
16. Calculate the Activity of Unknown sources by the following relation.

$$\text{Activity (Bq)} = [\text{cps} / (\eta * \text{BR})] \quad \text{(IV (c) - 5)}$$

Where,

cps = counts per second or Net Area/Counting Time or Area under the peak

$\eta$  = Efficiency calculated from standard sources

BR% = Branching Intensity

17. If least square method is used to subtract Background counts for getting Net peak area, Branching Intensity should be excluded for calculation of Activity.

*The operating procedures for Least Square Fitting program*

A. *NETSWIN:*

- 1 Load the spectrum in memory.
- 2 Spectrum is normally stored in binary format.

B. *Spectral data collection:*

1. Acquire spectra of background, K-40 std. U-std., Th-std. and the sample for suitable counting time and save these spectra.
2. Note the Region of Interest (ROI) of K-40 (1460 keV), Bi-214 (1764 keV) and Tl-208 (2614 keV) from the spectra of K-40 std. U-std. and Th-std. respectively.
3. Convert the above spectra to ASCII format which can be made readable to the program. For that we can use the program DATAFORMAT or T-Aptec.
4. Click F4 or PRINT button. Next, click CNTRPT button. Enter Header and Sample specification.
5. Store the spectrum in ASCII format with 10 column representation.

C. *Compton Fraction Generation and Spectrum Analysis:*

1. For making the Compton fraction library of the standard sources it is required to make an input file containing spectral data of individual isotopes, background spectra with details of counting time and region of interest for the analysis to be carried out. The sample format for the input file is given (COMPINP.TXT). Now run the program COMP2008.EXE and give the name of the input file you created. The program will calculate the Compton fractions and save the data in a Compton library file COMP.TXT.
2. For the analysis of activity in the sample it is required to run the program NAI2008.EXE. The spectral data of the sample along with background, ROI details and counting time have to be incorporated in an input file. The format of the sample input file is given (RADM2008.TXT). While running the NAI2008.EXE program it is

required to give the Compton library file (COMP.TXT) and the sample input file as inputs and to name of the file to which the analysis results are to be stored as output file. The output file contains the net counts of the isotopes (in ROI) and the details of the analysis.

3. The sensitivity or efficiency (Cps/Bq) of the detector system for the particular geometry and for the energy can be calculated from the net count rate obtained from the least squares analysis for the standard spectra. The factors can be directly applied to the net counts obtained from the sample analysis to estimate the respective activity in the sample. The original spectral data and the fitted spectral data from the analysis will be stored in a DATAFILE.TXT which can be plotted to see the accuracy of the least squares analysis.

### **OBSERVATIONS:**

For this experiment, the efficiency of each standard sources are calculated as:

Sources	Activity in Bq/kg	Net Area	Counting time(secs)	Counts per second(cps)	Branching intensity in %	Efficiency ( $\eta$ ) in %
Potassium std.	3973	34900	5000	6.98	10.7	0.175
Uranium std.	1914	38500	5000	7.7	15.9	0.402
Thorium std.	17374	271000	5000	54.2	36	0.312

#### For Soil Sample No.:- M-14

Weight of soil sample is 280 grams.

#### K-40 Nuclide

Counting time : 50000 secs ; BR = 10.7% ; Net Area = 11300  $\eta$  = 0.175 %

Activity (Bq) = [cps / ( $\eta$  \* BR)] = 129.14 Bq

296 gm of soil sample = 129.14 Bq of K-40 nuclide.

1000 gm or 1 kg of soil sample = 436.28 Bq/kg

#### U-238 Nuclide

Counting time : 50000 secs ; BR = 15.9 % ; Net Area = 1570;  $\eta$  = 0.402 %

Activity (Bq) = [cps / ( $\eta$  \* BR)] = 7.81 Bq

296 gm of soil sample = 7.81 Bq of U-238 nuclide.

1000 gm or 1 kg of soil sample = 26.39 Bq/kg

#### Thorium Nuclide

Counting time : 50000 secs ; BR = 36 % ; NetArea = 1560;  $\eta = 0.312 \%$

Activity (Bq) =  $[\text{cps} / (\eta * \text{BR})] = 10.00 \text{ Bq}$

296 gm of soil sample = 10.00 Bq of Thorium nuclide.

1000 gm or 1 kg of soil sample = 33.78 Bq/kg

For Soil Sample No.:- M-8

Weight of soil sample is 296 grams.

K-40 Nuclide

Counting time : 50000 secs ; BR = 10.7% ; Net Area = 12300  $\eta = 0.175 \%$

Activity (Bq) =  $[\text{cps} / (\eta * \text{BR})] = 140.57 \text{ Bq}$

280 gm of soil sample = 140.57 Bq of K-40 nuclide.

1000 gm or 1 kg of soil sample = 502.04 Bq/kg

U-238 Nuclide

Counting time : 50000 secs ; BR = 15.9 % ; Net Area = 3470;  $\eta = 0.402 \%$

Activity (Bq) =  $[\text{cps} / (\eta * \text{BR})] = 17.26 \text{ Bq}$

280 gm of soil sample = 17.26 Bq of U-238 nuclide.

1000 gm or 1 kg of soil sample = 61.64 Bq/kg

Thorium Nuclide

Counting time : 50000 secs ; BR = 36 % ; NetArea = 3180;  $\eta = 0.312 \%$

Activity (Bq) =  $[\text{cps} / (\eta * \text{BR})] = 20.38 \text{ Bq}$

280 gm of soil sample = 20.38 Bq of Thorium nuclide.

1000 gm or 1 kg of soil sample = 72.79 Bq/kg

For Soil Sample No.:- M-18

Weight of soil sample is 320.3 grams.

K-40 Nuclide

Counting time : 50000 secs ; BR = 10.7% ; Net Area = 5710  $\eta = 0.175 \%$

Activity (Bq) =  $[\text{cps} / (\eta * \text{BR})] = 65.26 \text{ Bq}$

320.3 gm of soil sample = 65.26 Bq of K-40 nuclide.

1000 gm or 1 kg of soil sample = 203.75 Bq/kg

U-238 Nuclide

Counting time : 50000 secs ; BR = 15.9 % ; Net Area = 2100;  $\eta = 0.402 \%$

Activity (Bq) =  $[\text{cps} / (\eta * \text{BR})] = 10.45 \text{ Bq}$

320.3 gm of soil sample = 10.45 Bq of U-238 nuclide.

1000 gm or 1 kg of soil sample = 32.63 Bq/kg

Thorium Nuclide

Counting time : 50000 secs ; BR = 36 % ; NetArea = 2060;  $\eta = 0.312 \%$

Activity (Bq) =  $[\text{cps} / (\eta * \text{BR})] = 13.21 \text{ Bq}$

320.3 gm of soil sample = 13.21 Bq of Thorium nuclide.

1000 gm or 1 kg of soil sample = 41.24 Bq/kg

### **RESULTS:**

The three soil samples contains three nuclides each - Potassium, Uranium and Thorium.

In soil sample No: M-14, the activity of Potassium nuclide is highest (436.28 Bq/kg) followed by Thorium nuclide (33.78 Bq/kg) and Uranium nuclide has the lowest activity (26.39 Bq/kg).

In soil sample No: M-8, the activity of Potassium nuclide is highest (502.04 Bq/kg) followed by Thorium nuclide (72.79 Bq/kg) and Uranium nuclide has the lowest activity (61.64 Bq/kg).

In soil sample No: M-18, the activity of Potassium nuclide is highest (203.75 Bq/kg) followed by Thorium nuclide (41.24 Bq/kg) and Uranium nuclide has the lowest activity (32.63 Bq/kg).

### **DISCUSSIONS:**

The Activity calculation has been done with subtracting the background counts. The result obtained is exactly the correct activity. From the results, we can see that the activity of Potassium nuclide is highest in all the three soil samples followed by Thorium nuclide and Uranium nuclide has the lowest activity.

### **PRECAUTIONS:**

- (1) Good grounding system for mains should be observed for proper functioning of the instrument and to avoid mains noise feed-through through ground loops.
- (2) Input to the ADC is DC coupled. Care should be taken to ensure that input level does not exceed +10 volts. Higher voltages may permanently damage input stage of the ADC.
- (3) Care should be taken while handling the HV supply.



- (4) Do not refer to energy value till the MCA is properly calibrated.
- (5) The sample is a natural activity, it may not be a high activity. So, it has to be kept for longer period.

## LISTS OF RESEARCH PUBLICATIONS

### (I) Journals:

#### (a) National:

- (1) Measurement of indoor concentrations of radon and thoron in Mizoram, India, **P.C.Rohmingliana**, Lalmuanpuia Vanchhawng, R.K.Thapa, B.K.Sahoo, R.Mishra, B.Zoliana and Y.S.Maya, *Sci. Vis.* **10** (4) 148 – 152 (2010).
- (2) Radon and the risk of lung cancer in Aizawl district, Mizoram, India, B.Zoliana, Lalmuanpuia Vanchhawng, **P.C.Rohmingliana** and R.K.Thapa, *Sci. Vis.* **10** (2) 66 – 72 (2010).
- (3) Measurements of the equilibrium factor of radon in Aizawl, Mizoram, India Lalmuanpuia Vanchhawng, **P.C.Rohmingliana**, R.K.Thapa, R.Mishra, B.K.Sahoo, B.Zoliana and Y.S.Mayya, *Sci. Vis.* **11** (2) 102 – 105 (2011).
- (4) Measurement of radon concentration in dwellings from the affected landslide area of Mamit town, Mizoram, India, **P.C. Rohmingliana**, L. Vanchhawng, R. K. Thapa, M. Lalthansangi, Lalrintluangi, Laltlanchhungi, Lalremruati Hmar, Lalnunthara, B. K. Sahoo, Y. S. Mayya and B. Zoliana, *Sci. Vis.* **12** (3) 92 – 96 (2012).

**(II) Conferences:**

**(a) International:**

- (1) Measurement of Equilibrium Factors and Inhalation dose for radon/thoron in dwellings using Direct Progeny Sensors in North-Eastern region of India, B.Zoliana, Lalmuanpuia Vanchhawng, **P.C.Rohmingliana**, R.K.Thapa, B.K.Sahoo, Rosaline Mishra, and Y.S.Mayya, *Proceedings of 7<sup>th</sup> International Conference on High Levels of Natural Radiation and Radon Areas (7HLNRRRA)* during November 24 – 26, 2010, The Park Hotel, Navi Mumbai.
- (2) Seasonal Variations of Radon/Thoron and Their Progeny Concentrations in Saiha District, Mizoram, India, **P.C.Rohmingliana**, Lalmuanpuia Vanchhawng, R.K.Thapa, B.K.Sahoo, R. Mishra, Y.S.Mayya and B.Zoliana, *Proc. of International Conference on Advances in Environmental Chemistry (AEC)*, Excel India Publisher, **ISBN: 978-93-81361-53-5**, 193 – 195 (2011).
- (3) Study of Population Dosimetry in Middle Part of Mizoram, India, Lalmuanpuia Vanchhawng, **P.C.Rohmingliana**, R.K.Thapa, B.K.Sahoo, Rosaline Mishra, B.Zoliana and Y.S.Mayya, *Proc. of International Conference on Advances in Environmental Chemistry (AEC)*, Excel India Publisher, **ISBN: 978-93-81361-53-5**, 97 – 100 (2011).
- (4) Measurement of Radon Concentration Inside and Around Dwellings in Fault Regions of Aizawl city, Mizoram, India, B.Zoliana, **P.C.Rohmingliana**, Lalmuanpuia Vanchhawng, R.K.Thapa, R.Mishra, B.K.Sahoo and Y.S.Mayya, *Proc. of International Conference on Advances in*

*Environmental Chemistry (AEC)*, Excel India Publisher, ISBN: 978-93-81361-53-5, 166 – 169 (2011).

- (5) The study of Population Dosimetry in North East India. B.Zoliana, **P.C.Rohmingliana**, Lalmuanpuia Vanchhawng, R.K.Thapa, R.Mishra, B.K.Sahoo and Y.S.Mayya, *International Symposium on Natural Radiation Exposures and Low Dose Radiation Epidemiological Studies (NARE 2012)* at Hirosaki University, Japan during 29.2.2012 – 3.3.2012.
- (6) Measurement of Equilibrium Factor for Indoor Radon/Thoron Using Direct Progeny Sensor in North Eastern India. B.Zoliana, **P.C.Rohmingliana**, Lalmuanpuia Vanchhawng, R.K.Thapa, R.Mishra, B.K.Sahoo and Y.S.Mayya, *Symposium on Radiation Measurements and Applications at City Center Marriott*, Oakland California, USA , organized by Department of Nuclear Engineering, University of California, Berkeley and Lawrence Berkeley laboratory, Berkeley, California during 14 – 17 May 2012.

**(b) National:**

- (1) Measurement of Indoor Radon and Thoron concentrations in correlation to Geographical Location and Construction types of buildings in Mizoram, **P.C.Rohmingliana**, Lalmuanpuia Vanchhawng, R.K.Thapa, B.K.Sahoo, Y.S.Mayya, O.P. Singh and B.Zoliana, *VI National Conference of PANE*, Tripura University, 2 – 4 April, 2009.
- (2) To Correlate Radon and Thoron concentrations with Gamma Background Radiation in Mizoram. (Special reference to Aizawl, Champhai and Kolasib districts), Lalmuanpuia Vanchhawng, **P.C. Rohmingliana**, R.K.Thapa,

B.K.Sahoo, O.P. Singh, B.Zoliana and Y.S. Mayya, *VI National Conference of PANE*, Tripura University, 2 – 4 April, 2009.

- (3) Study of Radon concentration in the landslide area of Mamit Town in Mizoram, India. **P.C.Rohmingliana**, Lalmuanpuia Vanchhawng, R.K.Thapa, B. Zoliana, B.K. Sahoo, R. Mishra, Y.S. Mayya, *One Day State Level Seminar on Recent Advances in Radiation Physics* on 15<sup>th</sup> April, 2011, Mizoram University, Aizawl.
- (4) Study of radon flux from soil surface in middle part of Mizoram, India, **P.C.Rohmingliana**, Lalmuanpuia Vanchhawng, R.K.Thapa, B.Zoliana, B.K.Sahoo, R.Mishra, and Y.S.Mayya, *National Symposium on Solid State Nuclear Track Detectors and Their Applications (SSNTDs-17)*, 2011.
- (5) Study of radon concentrations in relation with radioactivity content of building materials in Aizawl District, Mizoram, India, Lalmuanpuia Vanchhawng, **P.C.Rohmingliana**, R.K.Thapa, B.K.Sahoo, Rosaline Mishra, B.Zoliana and Y.S.Mayya, *National Symposium on Solid State Nuclear Track Detectors and Their Applications (SSNTDs-17)*, 2011.

**(III) Workshops/ Training Programmes attended:**

- (1) VI<sup>th</sup> National Conference of the Physics Academy of North East on '*Physics Research in Nort East (PANE)*', organized by Department of Physics, Tripura University, Suryamaninagar – 799130, Tripura, India. 2<sup>nd</sup> – 4<sup>th</sup> April, 2009.
- (2) State Level Seminar on '*Climate Change and Biodiversity*', Organized by Mizo Post-Graduate Science Society (MIPOGRASS), Aizawl in

collaboration with Mizoram Council of Science, Technology & Environment, 20<sup>th</sup> August, 2010.

- (3) 10<sup>th</sup> North East Workshop on Computational Information Processing, Organized by Electronics & Communication Sciences Unit, Indian Statistical Institute Kolkata and Govt. Zirtiri Residential Science College, Aizawl, Mizoram, 10<sup>th</sup> – 12<sup>th</sup> November, 2010.
- (4) One day State Level Seminar on '*Recent Advances in Radiation Physics*', organized by Department of Physics, Mizoram University and UGC – DAE Centre for Scientific Research (CSR), Indore, 15<sup>th</sup> April, 2011.
- (5) One Day State Level Symposium on "*Chemistry – our life, our future*", jointly organized by Mizo Post-Graduate Science Society (MIPOGRASS), Aizawl, with Mizoram Council of Science, Technology and Environment, Government of Mizoram catalysed and supported by National Council for Science & Technology Communication, Department of Science and Technology, 31<sup>st</sup> August, 2011.
- (6) National Symposium on '*Solid State Nuclear Track Detectors and Their Applications (SSNTD - 17)*', organized by Nuclear Track Society of India (NTSI), c/o Radiochemistry Division, Bhabha Atomic Research Center, Mumbai – 400085 and Department of Physics, Faculty of Science, The M.S. University of Baroda, Vadodara, Gujarat, India. 17<sup>th</sup> – 19<sup>th</sup> October, 2011.
- (7) International Conference on '*Advances in Environmental Chemistry (AEC - 2011)*', organized by Department of Chemistry, Mizoram University, Aizawl – 796004, Mizoram, India. 16<sup>th</sup> – 18<sup>th</sup> November, 2011.

## BRIEF BIODATA OF P.C. ROHMINGLIANA

<b>Name</b>	:	P.C. ROHMINGLIANA
<b>Father's name</b>	:	P.C. Neihkima
<b>Date of birth</b>	:	17 - 02 - 1981
<b>Address</b>	:	H/No. M-131, Mualpui, Chhingchhip, Serchhip District, Mizoram, India. PIN 796161
<b>Subject of Specialization</b>	:	Computer Application in Physics.
<b>Educational Qualifications</b>	:	
• H. S. L. C	1996 (Dec)	First Division.
• H. S. S .L. C. (Sc)	2001	Third Division.
• B. Sc (Physics Honours)	2004	Second Division.
• M. Sc. (Physics)	2007	Second Division.
• Pre-Ph. D. Course	2010	Grade 'B'

### **Research Experience:**

- Completed M. Sc. Project work (on Computer Application in Physics) entitled "Calculation of Chaos in Environment using Logistic Equation" at Department of Physics, Mizoram University, Aizawl 2007.
- Started research works in Project on Measurement of radon and thoron Research group under the guidance of Prof. R. K. Thapa, Department of Physics, Mizoram University, Aizawl, Mizoram and co-guidance of Prof. B. Zoliana, Project Principal Investigator, Department of Physics, Govt. Zirtiri Residential Science College, Aizawl since March 2008.
- Completed one week training course for the Project on Measurement of radon and thoron in Environment Assessment Division (EAD), BARC, Mumbai in July 2008.
- Calculations of radon, thoron and their progeny concentration, Equilibrium factors and Inhalation dose rate.

- Completed one week training course for measurement of radioactivity content using  $\gamma$ -spectrometer (NaI (Tl) Scintillation Detector).
- Measurement of surface flux and radon content in soil gas using RAD7.
- Measurement of Background gamma radiation level using Micro-R Survey Meter.
- Preparation of DRPS and DTPS using LR-115 films.
- Working knowledge of operating systems DOS/WINDOWS XP and FORTRAN.

**Teaching experience:**

- Part-time Lecturer in Department of Electronics at Govt. Zirtiri Residential Science College, Aizawl, under the Directorate of Higher and Technical Education, Govt. of Mizoram from June, 2011 to March, 2012.